MB 2020-02

Structural interpretation of enhanced high-resolution aeromagnetic depth slices of the Eeyou Istchee Baie-James region, Québec Superior province

Documents complémentaires

Additional Files

Licence

License

Cette première page a été ajoutée au document et ne fait pas partie du rapport tel que soumis par les auteurs.

Énergie et Ressources naturelles
Québec

Structural interpretation of enhanced high-resolution aeromagnetic depth slices of the Eeyou Istchee Baie-James region, Québec Superior province

Nathan R. Cleven, Lyal B. Harris et Carl Guilmette

MB 2020-02

Énergie et Ressources naturelles
Québec

Structural interpretation of enhanced high-resolution aeromagnetic depth slices of the Eeyou Istchee Baie-James region, Québec Superior province

Ministère de l'Énergie et des Ressources naturelles, Québec

by

Nathan R. Cleven[1], Lyal B. Harris[2], Carl Guilmette[1]

[1]Université Laval, Département de géologie et de génie géologique

[2]Institut National de la Recherche Scientifique (INRS)

Abstract

This report provides a structural analysis of the high-resolution MERN aeromagnetic survey of the Eeyou Istchee Baie-James region in Québec focusing on the La Grande and Opinaca subprovinces of the Archean Superior province. Structural domains interpreted from deformation patterns in enhanced aeromagnetic images that highlight upper crustal structures show deformation is partitioned into areas dominated by (i) zones dominated by dextral E-W striking shear structures, with discrete synthetic dextral NW-SE shear zones, (ii) conjugate NW-SE dextral, NE-SW sinistral ductile shear, and (iii) zones of N-S convergent structures consistent with prolonged ductile shearing in a thrust sense. These structures are interpreted as having formed during a single, prolonged, pervasive dextral transpressional episode. Regional-scale deep crustal domains from analysis of long wavelength components of aeromagnetic data indicate that conjugate shear systems accommodated lateral extrusion of large-scale tectonic blocks and the formation of mega-boudinage structures, defining a contemporaneous to late-stage component of E-W oriented regional extension. Convergent deformation structures in the Opinaca, in conjunction with the general low angle northward dip of many major structures in the La Grande are consistent with a North over South sense of regional tectonic transport. Regional structural datasets collected through cartographic efforts of Géologie Québec provide outcrop-based supporting evidence for these interpretations of upper crustal deformation.

Résumé

Ce rapport présente une analyse structurale du levé aéromagnétique à haute résolution du MERN dans la région d'Eeyou Istchee Baie-James au Québec touchant particulièrement les sous-provinces de La Grande et d'Opinaca de la Province archéenne du Supérieur. Des domaines structuraux interprétés à partir des patrons de déformation observés sur les cartes aéromagnétiques montrent que la déformation a été répartie dans des régions dominées par (i) des zones de cisaillement dextres E-W, avec des zones de cisaillement synthétiques dextres NW-SE, (ii) des zones de cisaillement conjuguées NW-SE dextres et NE-SW senestres, et (iii) des zones caractérisées par des structures convergentes N-S, compatibles avec un cisaillement ductile prolongé associé à un mouvement de chevauchement. Ces observations favorisent un modèle impliquant une seule phase importante de déformation en transpression dextre. L'analyse de la composante de grande longueur d'onde du même ensemble de données permet de mettre en évidence des domaines de croûte profonde d'importance régionale et la présence de structures tectoniques profondes. Ces observations indiquent que les systèmes de cisaillement conjugués ont permis l'extrusion latérale de blocs tectoniques à grande échelle et la formation de mégaboudins qui mettent en évidence l'existence d'une composante d'extension régionale E-W contemporaine ou tardive. Les structures de convergence dans l'Opinaca, de même que le pendage généralement faible de nombreuses structures majeures dans le La Grande, indiquent un transport tectonique régional du nord vers le sud. Les données structurales régionales recueillies sur le terrain lors des travaux de cartographie de Géologie Québec sont compatibles avec ces interprétations.

Table of contents

List of Figures

1. Introduction

The main goal of this report is to provide a large-scale structural interpretation of the map pattern in the Eeyou Istchee Baie-James region of the Northeast Superior Province, Québec, which was produced during a major and protracted Neoarchean tectonic event that spanned the entire Superior Province (Card, 1990; Poulsen et al., 1992; Percival et al., 2012). The study area has been affected by widespread ductile deformation during high-grade metamorphism; the scale of the resulting structures creates limitations for interpreting outcrop geology and can even provide difficulties for interpreting map-scale geology into a regional context, e.g. broad shear zones may not be recognized in the field, especially where there is limited outcrop. Regional-scale syntheses of surface bedrock geology, lithostratigraphic analysis, geochronology and structural data have previously established limits for somewhat homogeneous lithotectonic domains within the Superior, called subprovinces (Card and Ciesielski, 1986; Percival et al., 2012). Further integration with the results of various large-scale geophysical analyses, such as from seismic and gravity surveys, has refined tectonic models of Superior province formation (Calvert et al., 1995; Percival et al., 2006; Frederiksen et al., 2007). Drastic rheological differences between some subprovinces has created boundary regions that can be structurally complicated and have unevenly distributed strain. Different structural levels of crust are exposed amongst the subprovinces, and yet subprovinces of dominantly supracrustal rocks are thought to be relatively thin veneers overlying thick Archean sialic basement. It is possible that the surface or shallow expressions of deformation may relate to deep seated features in the lower crust or upper mantle.

Aeromagnetic geophysical surveys have provided a dependable tool for geological mappers for many decades. They yield images with details of the surface and subsurface variations in magnetic susceptibility that, when used in conjunction with geo-located lithological and structural observations, aid mapping of major structures, lithological contacts, metamorphic facies changes, alteration zones, etc. With a substantial extent of bedrock covered in overburden or wetlands throughout Canada, aeromagnetic maps can drastically increase mapping efficiency. These maps have been worked into the standard operational procedures of surveys and industry for geological mapping at both large-scale and small-scale. As aeromagnetic surveys provide detailed data directly based on the extent of units and structures, they have been used as a definitive method for delineating subprovince boundaries (Stott et al., 2010). However, it must always be taken into consideration that they represent an integration of the magnetic signal over a certain depth of the crust. Untreated images may be dominated by long wavelength signals that reflect deeper crustal levels (i.e. arising from sources to the Curie depth at which rocks lose their magnetic signature) and require enhancement to highlight near surface features. Whilst vertical derivatives are commonly used in North America to highlight upper crustal structures, their calculation from horizontal gradients in regional total field surveys frequently introduces noise (Naidu and Mathew, 1998) and provides no control on source depths. Frequency domain analysis (Spector and Grant, 1970; Cooper and Cowan, 2006), also known as (pseudo-)depth slicing, is a geophysical analysis tool performed in the frequency domain that separates different wavelength components of the total magnetic field, related to different source depths based on the slope of the power spectrum. Thus, separate images based on the signal from shallow geology, irrespective of deeper variations, and on the deep pattern, more representative of overall units, deep structures, and large-scale crustal blocks, can be analyzed. For enhancement of the images, the tilt angle calculation (Miller and Singh, 1994; Salem et al., 2007) is applied to both long and short wavelength component data, as it more accurately places and visually displays dipping structures in their correct map position irrespective of signal magnitude and dip. This treatment is effective for regions exhibiting complex, pervasive ductile deformation, such as the Northeast Superior province.

Our strategy to approach this problem is to examine first the short wavelength component of the aeromagnetic data (representing shallow geology) to break the large-scale lithotectonic domains into subdomains exhibiting similar or consistent styles of apparent deformation. From this we can identify the relative degrees of strain between regions, shear kinematics, and overprinting relationships. Secondly, we examine the long wavelength component of the aeromagnetic survey (representing the deep geology) to establish the location of major structures that separate large-scale, structurally bound crustal blocks, and to determine the final, post-deformation orientation and shape of these crustal blocks. This allows us to evaluate similarities and differences of deformation at different exposed structural levels, and establish the relative timing of observed deformation structures and patterns. Synthesis of the geophysical interpretation with known surface geology and analysis of existing structural data provides a robust methodology for defining regional deformation and tectonic events and has extensive implications for mineral exploration.

2. Tectonics of the Superior province

Models of Superior province (Figure 1A) formation and assembly have largely developed out of studies of its western and southern regions that have been interpreted as representing a collage of sequentially accreted terranes, now preserved as alternating, east-west oriented, southward-younging volcano-plutonic and metasedimentary belts that include limited domains of gneissic-plutonic rocks (Percival et al., 2012). While little can be determined of pre-2.8 Ga events from very limited regions of preserved Paleo- to Mesoarchean crust, two distinct models of Neoarchean development and tectonic assembly of the Superior have evolved. The first model synthesizes lithostratigraphy, structural analysis, and geochronology into a uniformitarian model of arc accretion where metasedimentary domains are interpreted as syn-orogenic flysch basins that formed during sequential north to south accretion of terranes (Polat et al., 1998; Percival et al., 2012, and references therein). In contrast, non-uniformitarian tectonic models (Bédard et al., 2003; Bédard and Harris, 2014; Harris and Bédard, 2014) explain the formation of the Superior through a catastrophic mantle overturn event causing wholesale disaggregation of pre-existing continental crust overlying a vast upwelling zone. A transition to reassembly follows through cascading collision and imbrication of large crustal blocks and slivers, with motion driven by traction of the mantle against deep cratonic keels. While each model has different explanations for each phase of the Superior provinces development, both are constrained by the timing of phases of volcanism, metamorphism and deformation: 2780-2695 Ma is a phase of mafic and ultramafic volcanism, as well as localized crustal recycling at concentrations of TTG suite intrusions (Percival et al., 2012); 2720-2680 Ma is a phase of more widespread TTG plutonism, accompanied by collision, convergent deformation (Benn et al., 1994); 2705-2685 Ma saw the development of large basins (metasedimentary subprovinces; Corfu et al., 1995; Davis, 2002); the period 2680-2620 Ma includes phases of regional metamorphism and transpressional deformation, with metasedimentary subprovinces as loci of high-grade, low-pressure, high-temperature metamorphism (Corfu et al., 1995; Côté-Roberge, 2018; Piette-Lauzière et al. 2019) and penetrative ductile deformation. Deformation has been characterized as broadly dextral transpressional, with a strong north-south oriented component of convergent deformation (Kerrich and Feng, 1992; Polat et al., 1998). This may have included late-phase, orogen-parallel, E-W oriented extension (Moser et al., 1996). Epigenetic mineralization is widely associated with late-phase deformation and the general transition towards cooler crustal conditions with more localized deformation in discrete shear zones (Kerrich and Feng, 1992; Gauthier et al., 2007; Aucoin et al., 2012; Mercier-Langevin et al., 2012).

3. Geological background of the Eeyou Istchee Baie-James region

The Eeyou Istchee Baie-James region is situated in the Archean Northeastern Superior province in northern Québec (Figure 1A), and comprises gneissic-plutonic, volcano-plutonic, and metasedimentary domains constituting five subprovinces (from North to South): the Minto, the La Grande, the Opinaca, the Nemiscau, and the Opatica. The Ashuanipi Subprovince, which lies to the east of the area covered by the interpreted aeromagnetic data, is not discussed in this report. Archean rocks have been intruded by Paleoproterozoic mafic dyke swarms (Buchan et al., 2007; Maurice et al., 2009), and are locally overlain by Paleoproterozoic sediments, such as the Sakami basin.

3.1 Minto and Opatica subprovinces

The Minto gneissic-plutonic subprovince is the largest of its kind, occupying a vast region north of the study area. The smaller Opatica gneissic-plutonic subprovince is situated in the south of study area (Figure 1B). These gneissic-plutonic subprovinces comprise strongly deformed and foliated deep crustal plutonic rocks (Bédard et al., 2003; Simard et al., 2003; Bédard, 2006; Percival et al., 2012); only the nature of their boundaries with the intervening La Grande and Opinaca subprovinces are included in the analysis.

3.2 The La Grande subprovince

The La Grande volcano-plutonic subprovince comprises four major lithologic assemblages (Figure 1B). The oldest units are 3.45- 2.9 Ga orthogneiss, including the Langelier complex which is locally preserved throughout the subprovince (Goutier et al., 2000). Two distinct phases of mafic to bimodal volcanic rocks are the ca. 2820 Ma Guyer Group and the ca. 2730 Ma Yasinski Group (Goutier et al., 2000; Goutier et al., 2001, 2002; Bandyayera et al., 2011, 2014; Sappin et al., 2018). The voluminous ca. 2719-2709 Ma Duncan TTG suite was emplaced throughout the La Grande subprovince during a widespread magmatic event (Goutier et al., 1998, 1999a, 2002), similar in timing to the latest stages of formation of the Minto subprovince. The youngest lithological assemblage comprises terrestrial to nearshore coarse clastic sedimentary rock sequences which overlie the Yasinski and Guyer Groups. They are locally sourced (Duparc et al., 2016), resemble Timiskaming-style sediments of the Abitibi subprovince, and deposition has been constrained to younger than ca. 2710 Ma (Davis et al., 2014). The Langelier Complex exhibits complex deformation patterns that imply it experienced earlier deformation events (Goutier et al., 2000). However, the volcanic sequences and their overlying sedimentary rocks consistently form linear belts and are commonly folded into tight synclinal structures, commonly located between and enveloping Duncan suite plutonic bodies. Plutonic bodies are irregularly shaped, to round or oblate, and can contain complex internal foliation patterns.

Volcano-sedimentary sequences in the La Grande subprovince exhibit a metamorphic gradient, from greenschist and lower amphibolite in the west, to granulite in the east (Goutier et al., 1999a, 1999b; Cadéron, 2003; Gauthier et al., 2007; Gigon and Goutier, 2017). However, the timing of regional metamorphism is poorly constrained to within the age span of numerous intrusions dated between ca. 2700 and 2600 Ma. The Langelier complex may have experienced a previous phase of metamorphism, prior to deposition of the Guyer group (Goutier et al., 1999b).

Extensive mineral showings occur in the La Grande subprovince, especially along its boundary region with the Opinaca subprovince (Card and Poulsen, 1998; Gauthier et al., 2007; Ravenelle et al., 2010;

Aucoin et al., 2012; Mercier-Langevin et al., 2012; Fontaine et al., 2015; Hanes et al., 2017; SIGÉOM, 2018). These include orogenic vein hosted gold (lode gold) and other base metal occurrences, as well as ultramafic rock hosted Ni-Cu-PGE occurrences (Houlé et al., 2015). Due to the relationships between structures and mineralization, a robust regional interpretation and characterization of deformation events may provide context and further insight for exploration.

3.3 The Opinaca and Nemiscau subprovinces

The Opinaca and Nemiscau metasedimentary subprovinces both comprise high-grade metasedimentary rocks with numerous syn- to post-tectonic intrusions. The metasediments have protoliths of wacke with a minor constituent of pelite. Rare conglomerate, iron formation, tuffs, and mafic volcanic rocks are present, commonly in regions close to its boundary (Bandyayera et al., 2010). Depositional constraints for the Opinaca subprovince have been interpreted from intrusions within its metasediments, such as the Marjoulet tonalitic gneiss (2702 ± 6 Ma; SIGÉOM, 2018, data unpublished) and the Féron suite tonalite (2710 ± 2 Ma; Augland et al., 2016). The basement onto which the Opinaca and Nemiscau sediments were deposited remains undetermined, as does the general tectonic setting of the basin.

Granulite grade metamorphism affected the south, central and east Opinaca subprovince, amphibolite grade in the north, and greenschist in a small region in the northwest. Peak metamorphism occurred between ca. 2665-2635 Ma and included migmatization of the granulite metasediments as well as injections of leucocratic material from deeper sources (Morfin et al., 2013; Côté -Roberge et al., 2016). Within this “injection complex” (Morfin et al., 2013) a large amount of anatectic melt accumulated at and percolated through the currently exposed structural level. Opinaca metasedimentary rocks, including stromatic migmatite layering (Bandyayera et al., 2010), has been pervasively folded and exhibits widespread, penetrative ductile deformation. The early stage of metamorphism, pre-deformation, was likely high-temperature, low-pressure (Côté -Roberge, 2018), a characteristic common to other metasedimentary subprovinces (Harris and Goodwin, 1976; Kehlenbeck, 1976; Percival, 1989).

The Opinaca hosts deformed ultramafic intrusions. The intrusions have very limited areal extent, and commonly form bead-like strings of occurrences situated generally along major structural features. Individual outcrops are commonly separated by several kilometres. Their exact timing and tectonic nature is uncertain, and it is unclear whether they have been boudinaged by late deformation, or if intrusions were sporadically intruded along major structures formed.

3.3.1 Transitional metasedimentary domains

Metasedimentary domains that resemble metasedimentary subprovinces exist within bounds of what is traditionally labeled as the La Grande subprovince. These include regions contiguous to the Opinaca (and possibly the Nemiscau; Fig. 1) and contain a mixture of the common La Grande and Opinaca lithologies, including stratiform amphibolite, exhalative iron formations, and conglomerates within the extensive units of high grade and locally migmatized metasedimentary rocks (SIGÉOM, 2018). Orthogneiss is also present, commonly migmatized, and may be present as early sills intruded within the sediment pile, or as basement to the sediments (Cadéron, 2003). These domains have been labeled transitional metasedimentary domains (TMDs) in Figure 1. These TMDs complicate the definition of subprovince boundaries, due to their similarity to both subprovince types. Their definition as individual domains stems from analysis below in this report, as we have noted that they are separated from the main metasedimentary subprovince domain

by major tectonic boundaries. Therefore, in this report we will try to better define their role in subprovince development and how they may be defined through the application of our geophysical methods and analysis.

4. Methodology

All aeromagnetic map images produced for this report were generated from Québec Ministère de l'Énergie et des Ressources naturelles aeromagnetic data (D'Amours, 2011) by Lyal Harris of the Institut National de la Recherche Scientifique (INRS), Québec City, using Geosoft's Oasis Montaj software, with the participation of the first author. This section includes descriptions of the purpose, effects and uses of the aeromagnetic treatments. However, explanations of the geophysical concepts behind the treatments are simplified.

4.1 The base aeromagnetic data set

The high-resolution (60 m grid) MERN Baie-James aeromagnetic survey used for analysis in this report (Figure 2) was compiled from numerous aeromagnetic surveys performed at a 80-100 m flight height, 250 m line spacing between 2007-2011 (D'Amours, 2011). The outline of this data set is irregular, yet it covers the major units and subprovinces in the region. Each region has a fairly unique signature in the total magnetic field image (Figure 2). For example, the Opinaca shows fairly consistent high total field magnetic signature, whereas large portions of the La Grande show a moderate to low magnetic signature. The Minto subprovince shows large regions of high magnetic signature with intervening portions of very low magnetic signature. The relative differences between these domains is important to note for regional comparisons, however, finer detail of structures may be implicit in regions that exhibit only a small range of the overall magnitude of the magnetic signature. We wish to highlight local differences in the magnetic signature irrespective of the magnitude of the magnetic signature to accentuate structures. For this we employ the tilt angle treatment, which is explained in detail below. In some images presented, we also examine the large-scale variation magnetic signature through filtering out the high-frequency portion of the signal. These two techniques provide us with more effective maps of both regional and local structure.

4.2 Treatments of the aeromagnetic data

4.2.1 Frequency domain analysis (depth slicing)

The long wavelength and short wavelength components identified (Figure 3) based on changes in slope of the radially averaged power spectrum (Spector and Grant, 1970) were separated. A long wavelength component representative of depths between 8 km and 35 km is identified. The Oasis Montaj software was used to isolate this long wavelength component and separate it from the residuals (short wavelength component) that represent signal from less than ca. 8 km depth using a Butterworth filter (so as not to introduce ringing effects that a sharp bandpass filter may introduce). These long and short wavelength components were analyzed and treated separately to provide a view of their respective depth range (Figure 4). The tilt angle treatment is applied to each component (Figure 5). Visually, the long wavelength component aeromagnetic map shows the regional variation without the fine details from the short

wavelength component. The short wavelength component aeromagnetic map shows the fine details, without the regional differences in base magnetic signal created by the long wavelength component.

4.2.2 Tilt angle treatment

The tilt angle is defined as the arctangent of the ratio of the 1st vertical derivative to the total horizontal gradient. This local phase edge enhancement provides a visually accentuated map of all structures and contacts that are defined by abrupt changes in magnetic susceptibility. Dipping or folded layered lithologies with varying degrees of magnetism between layers are common features best accentuated by the tilt angle treatment (or by other local phase filters such as the theta angle; Wijns et al., 2005). Faults and shear zones can be channels or conduits for fluid flow (Kerrich and Feng, 1992), a characteristic that typically results in the removal or addition of magnetic minerals. The resulting abrupt changes in magnetic susceptibility are also well accentuated by the tilt angle treatment. The result is that structures of various dips in any orientation are accentuated. Being a ratio of magnitudes provides a secondary effect in that variations within narrower bands of the scale of signal are displayed within a higher band of contrast. For example, within the treated data set regions such as the western Opinaca, which shows little detail in the total magnetic intensity map, exhibit much more detailed structures (Figure 5). The tilt angle treatment was applied to both the short wavelength and long wavelength component aeromagnetic maps.

4.2.3 Pseudogravity Transformation

Using assumptions of density for magnetized bodies pseudogravity can be calculated from its relationship with magnetic potential (Baranov, 1957; Jekeli et al., 2010). The aeromagnetic survey data was transformed into pseudogravity images to accentuate deep crustal features, the differences between individual domains or terrains (Figure 4 and 5), and deep intrusions.

4.3 Aeromagnetic processing

A typical workflow is depicted in Figure 5, showing how the total magnetic intensity map is split into long and short wavelength components, or transformed into pseudogravity, then a treatment such as the tilt angle is subsequently applied. Other treatments similar to the tilt angle, such as the first vertical derivative, and the theta angle, have been used in the creation of some maps in this report. Composites of different images are also presented to provide a unique view, often to show both deep and shallow structures within the same image.

Figure 6 shows the five maps used for the figures in this report, as well as the total magnetic intensity base map for comparison. The short wavelength component tilt angle image and the ternary gradient image are both used to analyze shallow, detailed structures. Each of the two treatments provide specific benefits. The tilt angle image in grayscale provides an excellent depiction of folds, faults and the trends of regional foliations. The ternary gradient image, a composite image with each of the 1st vertical derivative, tilt angle, and analytic signal images representing a separate colour component (Harris and Bédard, 2014), provides excellent delineation of structures and units in volcano-plutonic complexes, as well as late crosscutting plutons. The long wavelength component tilt angle image and the pseudogravity ternary gradient image each delineate major structures and the general bounds of tectonic blocks. The

pseudogravity with the superimposed pseudogravity theta angle image is used to delineate major regional differences in structures as well as subtle north-south oriented features.

5. Regional structural and kinematic analysis

This section describes specific, recurring large-scale structures in key areas of the Eeyou Istchee Baie-James region (Figure 7). Common structures include faults, folds and shear zones, yet in the relatively high-grade rocks of this region, and with the high resolution of the aeromagnetic images, many structures are observed at an uncommonly large scale. Shear zones, fold patterns, and boudinage structures have been identified in the deca-kilometer scale. At such a scale, lithological variation defined competency contrasts, and resulted in different modes of deformation between units. Examples below include instances where plutonic bodies appear to have acted like porphyroclasts in a mylonite, and coherent volcano-sedimentary successions like anisotropic fabric elements defining a tectonic foliation wrapped around the plutonic bodies. While the concept of scale-independence is a topic of debate for shear zone structures, we note many instances of kinematic consistency between such structures and discrete shear zones or faults in synthetic orientations that recur throughout the region, with identifiable senses of motion between offset blocks. All observations and interpretations of structures from the various aeromagnetic treatment images are collated into a regional-scale map of structural domains to best illustrate the consistency within the regional structural pattern. These observations provide an idea of the scale of deformation during Neoarchean tectonic events, the implications for which are discussed below. The locations within the region of Figures 8-15, which detail the structural and kinematic analysis, are provided in Figure 7.

Within this report the La Grande has been subdivided into its domain north of the Opinaca (referred to as the La Grande), and the Eastmain domain, south of the Opinaca. This distinction is drawn from nomenclature found within some literature (e.g. Ciesielski, 1991), as it is unclear whether the Eastmain domain is directly related to the remainder of the La Grande. This distinction will be further discussed below.

5.1 Structures and kinematic analysis by region

5.1.1 Shear structures in the western La Grande

The internal structures of plutonic and volcanic units in the western La Grande (Figure 8) are well delineated by the ternary gradient image. The plutonic bodies in red and orange display mottled, linear and concentric foliation patterns. Volcanic lithologies, in blue, black and yellow, show alternating planar fabrics attributed to primary volcanic stratigraphic layering. This layering in many instances is wrapped and warped around plutonic bodies. Many of these volcanic horizons form tight to isoclinal synclinal folds along the margins of these plutonic bodies (c.f. Goutier et al., 2002). These synclines are commonly tight when between two closely spaced plutons (dome and keel structures), however, some open more broadly, facing towards the centre of plutonic bodies. The schematic diagram in Figure 8 depicts the general outline of deformed plutons within this region. The plutons have irregular shapes, although many are ovoid to sigmoidal in shape (e.g. Figure 8, structure i). They generally have a longer aspect ratio in the E-W orientation. In some cases, narrowed, stubby terminations of the plutons appear deformed into “tails”, such as those commonly observed in sheared microstructural porphyroblasts found in mylonites.

The deformation of both pluton terminations (e.g. Figure 8, structure ii), and some close folded volcanic horizons (e.g. Figure 8, structure iii), into tails are interpreted to be strain shadows of the pluton (Figure 8). Axes of rotational symmetry are indicated on the plutonic bodies in Figure 8, as central divisions between upper and lower strain shadows. In most cases tails within the strain shadows do no cross the axes of rotational symmetry, and therefore the deformed plutons form σ-type structures. The axes of rotational symmetry for all plutons in this region trend generally E-W, however there is some local variation towards NW-SE and NE-SW. Median lines of the strain shadow tail structures are also indicated in Figure 8, and their approximate 30° inclinations from the axes of rotational symmetry indicate dextral shearing. Therefore, the dominant orientation of shearing is E-W, parallel to the axes of rotational symmetry. Within the western La Grande all strain shadows observed consistently indicate dextral shearing. The moderate to high aspect ratio of the plutonic bodies may be an indication of a component of north-south flattening, which considered in conjunction with dextral shearing implies transpression.

Some regions with strong magnetic gradients, and that exhibit extreme deflection of structural lineaments, are indicators of major discrete shear surfaces (Figure 8). Some discrete shears are oriented E-W and traverse the region. There is an additional discontinuous shear that is oriented NW-SE (Figure 8). These shears in different orientations intersect, but instead of cross cutting, mutually interfinger. This is an indication that they have been active contemporaneously. The overall E-W shear orientation indicates that the discrete NW-SE ductile shear is synthetic to the principal broad E-W shear zones.

5.1.2 Shear and extension structures in the western Eastmain domain

Figure 9 depicts a region of the Eastmain domain, where it is in contact with the Nemiscau subprovince. Similar to the western La Grande, plutonic bodies deformed into sigmoidal shapes have asymmetrical tails, or tails of deformed volcanic rocks, which we interpret to be strain shadows indicating dextral shear. These form σ-type structures. Their axes of rotational symmetry are oriented E-W, and their median lines are inclined, consistent with dextral shear. However, some plutons exhibit a higher aspect ratio than plutons in the western La Grande, with longer E-W axes.

This region includes a large plutonic body in the west with an irregular internal pattern that exhibits little organization (Figure 9, structure i). Its northern boundary exhibits a deflection of the tectonic foliation along its margins consistent with dextral deformation in a NW-SE orientation (Figure 9, structure ii). To the contrary, it southern boundary exhibits sinistral deformation within volcanic stratigraphy. This volcanic layering (Figure 9, structure iii) exhibits a progressive rotation and smearing towards parallelism with the boundary with the pluton, and similar rotation in the opposite direction on its southeast side. This is consistent with a large-scale sinistral C-S fabric with the C-surface (shear surface) oriented NE-SW, parallel to the boundary of the pluton. These opposing kinematic senses on the north and south boundary imply a relative westward motion of the main, undeformed plutonic body. This relative motion is a likely indication of E-W extension in the region.

The schematic diagram in Figure 9 depicts an angular, irregularly shaped plutonic body (Figure 9, structure iv) that shows no internal deformation textures, which, together with the large plutonic body described above (Figure 9, structure i), may have formed an early continental block that became disaggregated during E-W extension. The two blocks are now separated by volcanic rocks, therefore its (structure iv) path of transport, relative to the main block (structure i) in the west, is eastward. It can be observed to impinge severely on volcanic stratigraphy to its south, having caused the tectonic foliation and volcanic stratigraphy to wrap around its southern point, therefore it remained relatively undeformed and rigid with respect to the surrounding rocks. It may have deformed along its margins to pinch towards the

west or may have rotated to find a stable orientation with its long axis oriented north-south (Figure 8). Above, we establish that the main pluton (structure i) has opposing kinematics of the north and south shear zones, and considered in conjunction with the symmetric, inward deflection of the tectonic foliation between the main pluton and the segregated block, these structures are consistent with boudinage during north-south shortening and E-W extension. Additionally, fragments of the main plutonic body (structure i) appear to have been transported dextrally over the north side of the boudin neck. This may post-date formation of the boudin, or alternatively may have translated to fill the developing boudin neck. Dextral deformation appears to have been generally concurrent with the boudinage and is the dominant sense of shear in the region. Therefore, the local deformation regime may be described as dextral transpression, including a strong E-W extension component. The NE-SW sinistral shears are in an antithetic orientation and developed locally for the accommodation of the E-W extension component, and its associated translation of rigid blocks.

5.1.3 Shear structures at the Eastmain domain and Opinaca boundary

Figure 10 depicts a region of the Eastmain domain in contact with the Opinaca subprovince. Similar to Figure 8, sigmoidal shaped plutonic bodies are present, formed with stubby tails or tails of deformed volcanic rocks which we interpret to be asymmetric strain shadows. These form σ-type structures (e.g. Figure 10, structure i). Their axes of rotational symmetry are oriented E-W, and their median lines are respectively inclined, consistent with dextral shear. However, one large pluton (Figure 10, structure i) exhibits a retort shape where abutted against the Opinaca subprovince (Figure 10, structure ii). A large appendage of the plutonic body appears to be progressively rotated and elongated towards the southeast, crossing the original axis of rotational symmetry for the plutonic body. This form may be a δ-type structure, formed during syn-tectonic intrusion, or may be two individual plutons amalgamated due to convergent deformation and shearing. Along the Opinaca side of the boundary, the regional foliation shows a deflection consistent with a relative southeastward motion of the Opinaca. These structures indicate prolonged NW-SE oriented dextral deformation along the subprovince boundary. In the southeast corner of the sketch diagram in Figure 10 symmetric shading in the geophysical image is consistent with a set of folds. Their apparent E-W axial traces interrupt the NW-SE oriented dextral deformation zone and may be consistent with transpressive folding. Alternatively, they may be due to north-south convergence.

5.1.4 Shear structures at the Nemiscau and Opatica boundary

Figure 11 depicts a region of the Nemiscau subprovince and Eastmain domain in contact with the Opatica subprovince, or the Opatica TMD (Figure 7). This region exhibits a broad zone of pervasive penetrative ductile deformation with numerous sharp gradients between high and low signals. This zone is largely metasedimentary, however, the sharp gradients defining the foliation traces are likely deformation related and not primary bedding. Few sigmoidal shaped deformed plutonic bodies exhibit stubby to elongate tails, interpreted to be asymmetric strain shadows. However, these consistently indicate a sinistral sense of shearing (Figure 11, structures i and ii).

The metasedimentary rocks also exhibit a foliation trace that varies between E-W and NW-SE. Multiple traces oriented NW-SE progressively curve into the E-W orientation, coalescing into a single trace. These dominant E-W traces have long strike lengths, are very pronounced features in the aeromagnetic image, and are interpreted to be traces of faults or shear zones. This deflection of the NW-SE traces towards

dominant E-W traces is consistent with a sinistral C-S structure at a large-scale (Figure 11), with E-W being the dominant shear direction.

The foliation traces exhibit large-scale isoclinal folds with axial surface traces generally oriented E-W to NW-SE. Some are rootless, and their limbs terminate against interpreted shear surfaces (Figure 11). Their morphology and orientation may be consistent with sinistral shearing; however, this is not a robust interpretation without an understanding of the orientation of their fold axes. Their morphologies could be consistent with oblique slip or shearing in a thrust sense. Closely associated with folds, the region also exhibits nested, concentric, elliptical foliation traces, with a longer aspect ratio in an E-W orientation. These structures may be explained by different phenomenon, including the foliation wrapping around an oblate pluton, or doming of the rocks above an intrusion. However, in regions with a high magnitude of shear strain sheath folds and non-cylindrical folds are common. The proximity to isoclinal folds, the high aspect ratio of their elliptical shape, and the nested, concentric structure could be consistent with either sheath folds formed at high-grade conditions (Alsop and Holdsworth, 2006) or doubly plunging shear-related folds. Both are reasonably expected to be found at this scale, in high strain zones of this magnitude (Carreras et al., 2005; Alsop et al., 2007). The presence of such folds and isoclinal folds together, within the plan view, indicate a high magnitude of shear strain, possibly with kinematics that have a thrust sense dominating the effects of sinistral shearing.

While the sinistral component appears to have a dominant E-W shear orientation, the NE-SW oriented boundary between the Nemiscau and Eastmain domains also exhibits deflected foliation traces consistent with sinistral C′ (Figure 11, structure iii) and C-S fabrics (Figure 11, structure iv). The major E-W oriented shear zone and the NE-SW oriented boundary zone merge, and do not cross-cut one another, therefore it is apparent they formed contemporaneously. The NE-SW orientation is synthetic to the dominant E-W orientation, and if the structures described above are correctly identified as thrust-related, this region underwent sinistral transpression.

5.1.5 Convergence structures in the southern Opinaca

Figure 12 depicts a region of the Opinaca subprovince along its southern boundary with the Eastmain domain. The shaded region in the schematic diagram presents a region with a specific set of likely convergent-related structures interpreted from foliation traces within high-grade metasediments of the Opinaca, dominantly oriented NW-SE. The foliation traces exhibit long sweeping isoclinal folds, most of them rootless; the traces of their limbs terminate against pronounced black lineaments in the aeromagnetic image, which we interpret to be high strain ductile shear zones or slip surfaces. This relationship is consistent with the isoclinal folding having progressively developed and further deformed during shearing. The interpreted slip surfaces form a complex network, and some of their traces appear either folded or enveloping existing folds, which illustrates the progressive development of these structures. Slip surfaces themselves are folded, an example of cascading folds and thrusts commonly found in ductile convergent or extensional regimes (Harris et al., 2002; Harris and Koyi, 2003).

Within sections of metasedimentary rocks between slip zones, some locations exhibit nested concentric elliptical folds and mushroom folds. As explained in section 5.1.4, there are many possible interpretations of these structures; however, the presence of both concentric elliptical folds and mushroom folds together, spanning the entire width between slip surface traces, in proximity to rootless isoclinal folds, leads us to believe that these structures are shear-related and likely sheath folds, or partially developed sheath folds in the case of mushroom folds (Carreras et al., 2005). Their aspect ratio in plan view is consistent with a thrust sense of motion, or possibly the opposing sense. Therefore, convergent deformation

that involves local north-over-south thrusting is suggested but is inherently difficult to confirm from the map view of aeromagnetic images; the absence of kinematic indicators is consistent with this interpretation.

5.1.6 Concentric fold patterns, extrusion, or doming structures in the central Opinaca

Figure 13 depicts a region in the central eastern Opinaca that exhibits a very large, approximately 50 km diameter zone of a concentric, near circular, pattern in the tectonic foliation, traced in blue on the tilt angle image. The centre-most circular traces remain round with a very even aspect ratio. Portions of the concentric foliation show irregular traces and fold patterns; however, the concentric pattern is generally retained across the width depicted by the shaded region. This concentric pattern does not have an aspect ratio that is consistent with sheath folding (Whitney et al., 2004; Alsop and Holdsworth, 2006), nor is there an intrusion identified at the core of the structure to explain its pattern. We interpret that the most likely explanation is doming deformation related to either a metamorphic core complex (Whitney et al., 2004), or possibly extrusion of a channelized flow of high-grade rocks, partially molten rocks, or immediately underlying anatectic magmas (Schulmann et al., 2008). The implications of a dome or core complex style of deformation, versus a flowing ductile channel may be as different as an extensional environment versus forced channel flow of material during convergence, respectively. This domain of "doming" deformation abuts the convergence zone depicted in Figure 12 to its south, and a similar zone to the north which exhibits isoclinal and nested elliptic folds separated by interpreted slip surfaces (Figure 13), which we interpret to be convergent deformation. Further study of the tectono-metamorphic conditions of the "doming" deformation, and the kinematics of deformation in the convergent zones surrounding it, would be required to further develop an understanding of this structure. The fact that the centre of the concentric rings remain circular implies that no subsequent deformation altered its organization from its original state.

The long wavelength component tilt angle map (Figure 13 top) depicts minor curvilinear structures in similar orientations to the short wavelength tilt angle map circular patterns. More significantly, the map depicts a series of evenly spaced northwest trending deep linear structures that are unique to the region. These may be consistent with a series of deep faults that created with an even spacing due to the consistent rheology throughout the underlying crust beneath the Opinaca. This would be consistent with NE-SW oriented extension or upwelling related faulting in basement beneath the Opinaca metasediments.

5.1.7 Conjugate shear zones in the Opinaca

Figure 14 depicts a region of the central Opinaca and the boundary zones at its north and south. The northern boundary exhibits long sweeping drag folds of the tectonic foliation in both Opinaca and La Grande lithologies. The drag of the foliations depicts a dextral sense of shear along a shear zone oriented NW-SE (Figure 14, structure i). Within the Opinaca sinistral deflections of the tectonic foliation coalesce along a lineament oriented ENE-WSW (Figure 14, structure ii). The degree of strain is not high enough to have formed a single shear plane, rather the deformation appears to be distributed throughout a series of smaller shear zones deflected into a near-consistent orientation. The NE-SW sinistral and NW-SE dextral shearing do not cross cut each other, instead they appear to merge at the eastern edge of the diagram. This is an indication that both sinistral and dextral deformation were active contemporaneously. Their orientations are conjugate, and the NE-SW sinistral shear zone is antithetic to the dominant NW-SE dextral shear zone. Within the Opinaca, where the conjugate shear zones merge there are irregular deformation patterns with foliations traces generally oriented north-south, and the lithologies are largely plutonic rocks (Figure 14, structure iii). This may be explained as a zone of low-pressure, intruded by plutons, due to extension at the

locus of the conjugate system. Alternatively, it may be an extensional zone of upwelling (a horst), thus exposing of deeper sections of the Opinaca near the intersection of the conjugate shear zones. This explanation may be more viable, considering that the Frégate pluton exists in this zone and has been dated at 2710 Ma (Augland et al., 2016), placing it as a likely early intrusion into the Opinaca metasediments. Additionally, the general NE trend of the axial traces of apparent folds in the Opinaca (Figure 14) appear cross-cut by the irregular N-S foliation traces, and separated by the extensional zone, although they are not deviated in any fashion. Dextral back-rotational folding of the NW-SE dextral shear zone (Figure 14, structure iv) accommodated the impingement of the translating block of folded paragneiss, indicating the structures extension and shearing occurred contemporaneously.

At the regional scale, the conjugate shear zone system implies that there was a relative westward motion of the western Opinaca with respect to the eastern Opinaca and the contiguous La Grande. This lateral protrusion (Leonov, 2008) is consistent with regional scale E-W extension due to bulk N-S shortening (Taylor et al., 2003). This deformation may be a relatively late phase, considering that it deflects previously established tectonic foliations. However, this region's mode of deformation fits within the previously established structural regime of regional dextral transpression with E-W extension, with partitioned zones of N-S convergent deformation and E-W dextral shearing (Figures 9-12), and therefore would be a late phase of the same event.

5.1.8 Fold superposition in the La Grande

Figure 15 depicts a region of the southeastern La Grande subprovince labeled as the Boisbriand TMD in Figure 7. This region of metasedimentary and orthogneiss rocks exhibits elliptical concentric visual patterns and gradations in the tilt angle image interpreted to be folds. The complexity of the patterns indicates at least two generations of fold interference. These differ from previously described elliptical concentric fold patterns as their pattern is highly repetitive throughout the region, is consistent across multiple lithologies, individual structures are not consistently separated by slip surfaces, and they exhibit folded axial surface traces and classic shapes consistent with doubly plunging folds. Antiform and synform shapes were estimated from the visible gradation patterns seen within the tilt angle image, and these structures are interpreted to be a dome and basin style of fold interference pattern. The fold pattern appears to have a first generation of E-W axial traces. Second generation folds have a near N-S axial surface trace which are approximated in the Figure 15 sketch diagram. The folded region is limited by a slip surface to the South and the border with the Ashuanipi to the East. The northern border is ambiguous, where deformation appears to fade or become irregular. The first generation E-W oriented fold axes may be associated with convergence-related flattening, however, the localization of the secondary E-W shortening (N-S fold axes) is unique to the region, and may be attributable to relative westward convergence of the Ashuanipi (Cadéron, 2003).

5.2 Structural domains for the Eeyou Istchee Baie-James region

In the previous section (5.1), detailed examples of structures observed in aeromagnetic images were described to provide explicit examples of the structural characteristics of the Eeyou Istchee Baie-James region. Examples of each type of structure observed, and each phase of deformation were provided. In this section we extrapolate from these detailed examples to the remainder of the map area, where the structural characteristics may not be so ideal. Throughout the region there exist many further examples of similar structures to those outlined in section 5.1 and Figures 8-15, in similar orientations, providing similar

kinematic indicators. Figure 16 presents the entire map region, subdivided into domains such that each has a recognizable, consistent structure, set of structures, or structural pattern according to one of nine types that we establish out of the analysis and interpretation in section 5.1. We call these structural domains, and generalized definitions of the nine domain types are outlined below, with discussion of the overall pattern and its implications following.

East-west dextral transpressive shearing

These domains dominantly comprise volcano-plutonic lithologies with the associated structures of deformed plutonic bodies mantled by folded volcanic stratigraphy. The deformed plutonic bodies commonly exhibit dextral σ-type structures with stubby to elongate tails, or tails of deformed volcanic rocks, forming strain shadows. The axes of rotational symmetry of these structures are generally oriented E-W, parallel to their shear direction, and the median lines of their strain shadows are inclined to the axes of symmetry by roughly 30° (e.g. Figures 8-10). These structures are similar in concept to sheared rigid porphyroclast microstructures. Many occurrences of these structures, commonly in clusters, exist in the Eeyou Istchee Baie-James region, most significantly in the western La Grande domain (section 5.1.1, Figure 8). The asymmetric, oblate, sigmoidal pluton shapes identify these structures as transpressional.

Northwest-southeast dextral transpressive shearing

These domains encompass regions surrounding significant NW-SE striking shear zones. Many of the NW-SE shear zones are not laterally continuous and do not traverse the entire region. Most notably, they comprise the northern and southern boundaries of the Opinaca, where in contact with the La Grande and Eastmain domains respectively. Structures within these domains include progressive rotation of the principal E-W tectonic foliation towards the NW-SE shear direction (e.g. Figure 14). They also include folds with axial surface traces oriented NE-SW, perpendicular to shear. Plutonic rocks within these domains exhibit flattening in a NW-SE direction, as well as δ-type structures (e.g. Figure 10).

Sinistral shearing

Domains exhibiting sinistral shear structures have limited occurrences, both along the western boundary between the Opatica and the Nemiscau as well as internal to the Opinaca. In proximity to the Opatica, the structures are well formed and include strong sinistral C-S structures, sinistral σ-type structures in deformed plutons, all with a dominant shear orientation E-W (e.g. Figure 11). It also includes a synthetic NE-SW shear orientation that exhibits progressive rotation of bands of the tectonic foliation towards a NE-SW orientation. Internal to the Opinaca there is a linear band of deformation, oriented NE-SW, that shows a sinistral deflection of the tectonic foliation (section 5.1.7, Figure 14). This band of deformation did not accumulate enough strain to coalesce into one consistent shear surface. This orientation of is also present in minor zones in the western Eastmain domain, within sinistral C-S structures (section 5.1.2, Figure 9).

E-W extension with an irregular N-S pattern

One limited domain within the central Opinaca exhibits irregular tectonic foliation trajectories, with an overall north-south orientation. This domain lies in this zone of intersection between the dextral shear zone bounding the Opinaca at the North, and the sinistral shear zone internal to the Opinaca, which we have interpreted to be a zone of extension (section 5.1.7, Figure 14). A second limited zone within the Eastmain domain also exhibits irregular foliation trajectories, with an overall north-south orientation. This domain lies in a zone of E-W extension that we interpret to be associated with crustal-scale boudinage (section 5.1.2, Figure 9).

Convergent deformation

These domains are mostly metasedimentary sections of the Opinaca and Nemiscau domains. They are defined by regions exhibiting tight to isoclinal folds with dominantly E-W axial surface traces that are closely associated with local nested eye fold and mushroom fold patterns (e.g. Figures 12 and 13). Isoclinal folds are commonly rootless, where their limbs terminate against slip or shear surfaces. These are typical shear zone structures; however, their orientations are more consistent with north-south shortening, accommodated by north-over-south shearing (thrusting) with a component of bulk north-south flattening strain during regional convergence. We have interpreted the nested elliptical folds and mushroom patterns to be related to large-scale sheath fold development during high-magnitude dip-slip shearing or displacement. Many such structures are up to 5 km along their long axes. Regions of the La Grande major domain exhibits E-W oriented linear-shaped structural domains. Their boundaries are very straight and generally oriented E-W. These are suggestive of thrust sheets (Cadéron, 2003) and could represent crustal blocks or slivers imbricated through convergent tectonism.

Rigid bodies

Many dominantly plutonic or gneissic units appear to have behaved as rigid bodies set in a more deformable matrix during the deformation events that characterize the region. Their domains are defined by their internal foliation trace patterns that are not consistent with the observed patterns in the surrounding domains. Some of these domains may exhibit limited deformation along their boundaries, but the core that remains appears well defined. An example of this is a large pluton in the western Eastmain domain (section 5.1.2, Figure 9) whose boundaries are deformed parallel to the local foliation, yet the deformation rapidly fades towards the irregular nature internal to the block. The term ‘rigid bodies’ refers to the observation that these blocks remaining relatively undeformed by the dominant deformation event that defined the map pattern. Some may have undergone a degree of flattening, but this is difficult to establish considering the relatively high degree of strain in the rocks surrounding them.

Concentric folding, extrusion, or doming pattern

This domain type is restricted to the core of the southeastern Opinaca, where the foliation traces appear as a near circular concentric pattern around a central point (section 5.1.6, Figure 13). This style of concentric pattern is unique to the region. These domains transition into convergent deformation domains to the north and south. Above, we interpret that these domains may be associated with extension as an upwelled or domed region of high-grade metamorphic rocks, and thus the concentric foliation traces would depict the contours of the dome. The circularity of the central region suggests that it was not subjected to any subsequent flattening.

Necking and flattening deformation

These domains include a variety of structures associated E-W stretching and N-S flattening of units. They most commonly comprise volcano-plutonic lithologies and exhibit large-scale necking structures, as well as thinned, symmetric tails organized into strain shadows along a central axis of symmetry. In some cases, symmetric mantles of the tectonic foliation around plutonic bodies demonstrates flattening in the absence of shearing. Stretching appears to be in an overall E-W orientation (with N-S shortening), and created long, ribbon like domains with tapered terminations. Local conjugate shear systems appear to have accommodated some crustal motions, and aided the deformation of thinned, necked and boudinaged units, which are included in these domains.

Folded superposition with a second-generation north-south fold axis

These domains are spatially limited to the eastern La Grande deep crustal domain. They comprise a region of folded metasediments, with a first generation of folds that have E-W axial surface traces, likely due to initial north-south convergence. A second generation of folds with north-south axial surface traces overprints the region, creating dome and basin fold interference patterns (section 5.1.8, Figure 15). This secondary deformation event may be due to collision with the Ashuanipi (Cadéron, 2003).

5.3 Common structural orientations

With the observations made for Figures 8-14 it is apparent that there are recurring, consistent orientations of structures throughout the region. Established throughout the structural domain map (Figure 16) fault and shear structures dominate the map pattern in NW-SE, NE-SW, and E-W orientations. From the extensive detail in the short wavelength component maps it is difficult to establish the relative importance or degree of different fault and shear systems. A composite image of the long wavelength component tilt angle map and the pseudogravity ternary provides a gauge of where certain structures have strong signatures at depth. The same three major orientations are present in these maps (Figure 17). An additional orientation of structures, north-south, are subtle in the composite long wavelength component tilt angle map and pseudogravity ternary map, and very subtle in the short wavelength component maps. Figure 17 shows that the deep expressions of many structures may not be continuous, or that their continuity may not be well represented by the aeromagnetic survey. However, many major important structural features such as the boundary of the Opinaca, boundaries of the Opatica, and significant structures within the La Grande, exhibit lateral continuity over hundreds of kilometres.

The existing mapped subprovince boundary between the Minto and La Grande is not prominent (Figure 17). However, a lineament 20 to 30 km south is laterally continuous and traverses nearly the entire northern La Grande subprovince. This fault zone is associated with the localization of Proterozoic basins such as the Sakami. Its strong signature in the deep components of the aeromagnetic survey may imply that Proterozoic deformation affected the signal. However, such a deep signature could represent a more significant tectonic boundary reactivated during minor Proterozoic extension. The orientation of this major fault also recurs throughout the eastern La Grande, implying that is a very significant fault orientation for the region.

Deep structures bounding the Opinaca to its north and south have consistent NW-SE orientations but are difficult to trace laterally for long distances (Figure 17). This may be due to the metasedimentary nature of the Opinaca or the high grade, ductile deformation that it underwent. It is possible that some of these boundaries are not significant deformation zones and may have originally had a primary contact relationship. However, this is not explicitly determinable through analysis of the aeromagnetic maps. The NE-SW striking sinistral shear zone that traverses the Opinaca (Figure 14) has a more distinct signature in the deep aeromagnetic map (Figure 17), showing a segmented but near continuous and linear structure traversing the entire map region. It is interrupted only around the segregated rigid block within the Eastmain domain, as depicted in Figure 9.

E-W structural lineaments appear to be concentrated in both the eastern La Grande as well as the central Eastmain domain (Figure 17). In this region segments of E-W structures span the north boundary of the Nemiscau subprovince and form an intermittent band through the Eastmain and the Eastmain TMD (Figure 7). This orientation of structure is rarely seen in the Opinaca, the northern Eastmain, and the western La Grande.

Subtle linear north-south structures are observable, creating discontinuous arrays largely in the western portion of the map area (Figure 17). They appear as truncations of units or the tectonic grain, discontinuities, and magnetic lows. Some of these structures appear concentrated within previously described extensional zones (e.g. Figures 9 and 14), whereas others appear associated with regions of extensive Neoarchean plutonic rocks. Within the Opinaca many of these north-south lineaments terminate at the subprovince boundary yet have further associated lineaments along strike. The role of these features with respect to mineralization will be discussed below.

5.4 Kinematics, convergence, and extension summary

The observations of large-scale kinematic indicators, shearing, convergent and extensional structures described and interpreted in sections 5.1-5.2 are summarized in Figure 18. The interpreted deep structures from section 5.3 (Figure 17) are overlain on the short wavelength component ternary gradient map, with additional interpreted structural continuations observed within the fine detailed patterns of the underlain map. These define the largest structural breaks (discrete fault and shear zones) that are interpretable from the aeromagnetic maps. With the respective kinematic indicators outlined in the map, it is apparent that many regions exhibit broad zones of dextral ductile deformation. There are fewer observations of sinistral ductile deformation than dextral.

In this map (Figure 17) the relationship between shearing patterns and flattening deformation is apparent, as many extensional zones appear to have accommodated deformation through shearing along the boundaries of major units or bodies. This is most apparent in the Eastmain domain where, beyond the examples outlined in Figure 9, the opposing kinematics of the North and South boundaries of the Nemiscau

subprovince indicate a relative westward motion of the Nemiscau. The region North of the Opatica, within the Eastmain TMD (Figure 7), appears to be both a large-scale flattening and convergent zone that may have accommodated large-scale E-W extension and boudinage of the Eastmain by flow of the Opinaca southward (convergence) and relative northward impingement of the Opatica block into the boudin neck.

The dominantly convergent and flattening deformation that we previously interpreted to have affected the eastern La Grande may have defined the array of linear E-W (to NE-SW) structures that traverse it. They are relatively evenly spaced and contain only isolated domains of shearing. Their traces are sheared at their western contact with the Opinaca, a possible indication that these could be some of the earliest structures in the region, representing the effects of early convergent deformation in the La Grande. This style of very linear, repetitive structure is not observed elsewhere, possibly due to the subsequent Neoarchean overprinting deformation that affected the more competent eastern La Grande domain to a lesser degree.

6. Deep crustal domains

Analysis of the composite long wavelength component tilt angle map and pseudogravity ternary map provides judgment of which structures may bound individual crustal blocks, which we term “deep crustal domains” (Figure 19). These delineate domains that appear to have deformed or rheologically behaved self-consistently throughout the deformation, similar in concept to the structural domains we outline above, but are bounded by major structures that are continuous or penetrative to depth. In this map, as well as the base long wavelength components tilt angle map (Figure 19), the fine detail representative of shallow geology is absent and therefore lithological contacts between individual units are no longer apparent. The deep crustal domain boundaries can be recognized in the long wavelength component image as regions with a transition from a relative high to low value over a significant gradient. The boundaries are not meant to represent subprovince boundaries, as subprovince boundaries are defined by more specific features such as lithologies. However, the major structures constituting deep crustal domain boundaries may be separating crustal blocks with identifiably different histories and therefore could be taken into consideration when defining subprovince boundaries.

6.1 Deep crustal domains of the Eeyou Istchee Baie-James region

In the Eeyou Istchee Baie-James region six regional deep crustal domains are recognized in the map (Figure 19). Subdomains are interpreted within these deep crustal domains, as implied by observed internal major structures. Below we describe the domains, their boundaries, and their internal structure.

The Minto domain

The Minto domain lies at the North of the map area and is separated from the La Grande domain by a major fault structure that does not match with the existing Minto-La Grande subprovince boundaries based on lithologies (Figure 7). The major fault structure is observed as a generally E-W trending strong magnetic low that is laterally continuous and fairly linear for a long strike length. It has a wide low to high signal gradient on the southern side, within the La Grande domain, and a sharp gradient from the northern (Minto) side. This may suggest that the La Grande dips underneath the Minto. North of the boundary, La Grande

subprovince units create a more irregular contact shape than its respective deep crustal domain boundary. If this contact is a thrust, the bounding structure may be straight at depth and represented at surface by the structure bounding the deep crustal domain boundary (Figure 19). However, fragments of La Grande lithologies may have been intercalated or included into the Minto block along the boundary during thrust transport. This may explain the more irregular boundary at surface than at depth. The internal structure of the Minto domain shows fairly consistent high signals with irregular linear structural elements as low signals. This may be related to internal folding, plutonic boundaries, or internal tectonism due to prolonged or previous deformation.

The La Grande and Opinaca domains

The La Grande and Opinaca domains have only apparently minor deep crustal structures separating them. The northern and southern boundaries of the Opinaca are minor to major fault or shear zone structures. The structure bounding the westernmost tip of the Opinaca from the La Grande is not pronounced in the composite aeromagnetic image (Figure 19). While this region is still deformed, the boundary may not be a major fault or shear zone, and therefore is the only region that could potentially be evaluated for a relict primary boundary.

The La Grande is subdivided into nine significant subdomains. The five subdomains along the northeast boundary of the Opinaca are generally oriented E-W and have high aspect ratios. They are separated by minor structures that generally trend E-W, and the domains are lenticular to lozenge shaped. The one La Grande subdomain along the western boundary of the Opinaca does not share this orientation or shape. It has a different internal structure that includes a series of Northeast trending evenly spaced linear structures. The structures may be separating specific volcano-plutonic complexes, or be deep structures related to their formation.

Internally the Opinaca is divided into six subdomains along NE-SW, and NW-SE trending continuous linear structures that are prominent in the long wavelength component image. These subdomains are lenticular to lensoidal in shape and each have differently oriented internal structural features. The northern-most contains one discontinuous linear structural feature along its long axis. The central domain contains a series of irregular structural elements, including two north-south structures that terminate at its subdomain boundaries. The Southeast domain contains a set of linear structural elements that are loosely parallel, and oriented NW-SE.

The Eastmain domain

The Eastmain domain is defined here as the region between the southern boundary of the Opinaca, and the northern boundary of the Opatica (Figure 19). This delineates a deep crustal domain that includes volcano-plutonic complexes typically associated with the La Grande subprovince. It also includes the Nemiscau subprovince, and the Eastmain transitional metasedimentary domain (Figure 7) that is traditionally included in the Opinaca subprovince.

The Eastmain domain comprises one large central domain that resembles an E-W linear belt exhibiting thinning or necking deformation in a region central to the map area. This appears as two large lenticular blocks joined by a central region (the Eastmain TMD) connecting their thinned terminations. Subdomains of the western Eastmain domain also appear lensoidal to lenticular in shape, with stubby thinned terminations. The Eastmain domain also contains the Nemiscau basin/subprovince. While the

Nemiscau is readily delineated on the long wavelength component aeromagnetic map, however, some portions of its boundaries exhibit only minor structures. This may indicate that the Nemiscau has some relict primary depositional relationships with the surrounding volcano-plutonic complexes.

The Opatica domain

The Opatica domain lies at the south of the map region and its northern domain boundary closely follows the known lithology-based subprovince boundary. Its main plutonic core forms the central subdomain and exhibits irregular internal structure. The western Opatica domain includes the subdomain that lithologically comprises mostly metasedimentary rocks. It forms a linear belt that is delineated from the central Opatica domain by a minor structure.

7. Structural data analysis and synthesis

7.1 Strategy and initial observations

Many years of cartographic efforts by MERN in the Eeyou Istchee Baie-James region provide a large database of structural information (SIGÉOM, 2018). We analyze their compiled database of outcrop measurements for interpretations that correlate to our structural analysis of the aeromagnetic images. Our initial strategy is to examine patterns in ductile stretching lineation measurements (the subset of available SIGÉOM (2018) lineation data that was compiled is defined in the appendix, along with a location map of all data points; Figure A1). It is common for transpressional regimes to have ductile stretching lineation patterns that are difficult to interpret with respect to the direction of tectonic transport (Passchier et al., 1997; Tikoff and Greene, 1997). However, with further context for interpretation including the general shape, orientation, and rheology of units and deformation zones, the types, conditions and kinematics of deformation, and an idea of the relative magnitudes of strain, lineation patterns may provide a regional sense of stretching or transport directions (Jiang, 2014). The above analysis of aeromagnetic images provides, in part, this context and illustrates many examples of strain localization and partitioning. Sites of partitioning mark phases of development in collisional orogens (Gapais et al., 2009), and within a regional transpression regime they can provide information on the progressive accumulation of individual strain components with respectively simpler lineation patterns.

Preliminary analysis of the nearly 5000 ductile stretching lineation measurements (Figure 20) within the entire map region indicate that there is a general concentration of steeply plunging lineations (within the region outlined in red, Figure 20), and a second concentration plunging moderately to shallowly eastward (within the region outlined in blue, Figure 20). In the context of the dominantly E-W tectonic grain, the population of shallowly eastward plunging stretching lineations is likely associated with strike-slip shearing, or E-W extension. The population of steeply plunging stretching lineations is likely indicative of vertical stretching, or possibly normal-sense or imbrication-related thrust-sense shearing. Many regions exhibit lineations from both populations in close proximity; however, other regions indicate a distinct spatial distribution of the two lineation populations (Figure 21): steeply plunging stretching lineations are concentrated within volcano-plutonic complexes, and along boundary structures, whereas they are not common in metasedimentary subprovinces; shallowly eastward plunging stretching lineations are consistently found throughout the Opinaca and Nemiscau domains, as well as transitional metasedimentary domains in the La Grande; regions of local necking and flattening deformation, such as in the western

Eastmain domain (Figures 9, 20) also have high concentrations of shallowly eastward plunging lineations. These distributions support our interpretations that: 1) transpressive deformation was occurring in regions exhibiting both populations of lineations, and 2) strain partitioning occurred at a large scale, producing similar structures between related or rheologically similar units. With these preliminary observations confirming the efficacy of our strategy, we present the results of more detailed analysis by deep crustal domain.

7.2 Analysis by deep crustal domain

Figures 22-25 provide a breakdown of ductile stretching lineation measurements and fold axis measurements by each deep crustal domain displayed in equal area stereonets. Each figure portrays irregular outlines of the regions represented by the displayed data. Within the La Grande and Eastmain domains structural data is concentrated within volcanic units. These lithologies represent a small fraction of the areal extent of the map, however they disproportionately represent the majority of data. This may be sampling bias due to many factors including the presence of mineralization, outcrop exposure, the nature of deformation, and the presence of measurable folds and stretching lineations. In many cases, the intervening plutons do not exhibit measureable deformation. Analysis of the data therefore is partially limited to comparison between greenstone belts and to a degree, the plutonic bodies between them.

7.2.1 Western La Grande

Within the western La Grande fold axis and hinge measurements are generally parallel to stretching lineation orientations while exhibiting moderate variability in orientation (Figure 22). As well, lineations are generally sub-vertical to steeply plunging North. Domains in the north of this region display a more consistent steep plunge towards the North. Three regions exhibit steeply west plunging clusters (Figure 22, stereonets LGW-A, B, G), located in the southwest and southeast of the domain. One volcano plutonic complex was spatially divided into four sectors, into north, east, south and west sectors, according to the plutonic body's asymmetric axes. While the west and east sectors exhibit comparable lineation patterns the north and south sector stretching lineations plunge steeply towards the north and south respectively, depicting a possible domed nature of the plutonic body.

7.2.2 Eastern La Grande

The eastern La Grande exhibits some significant variation between regions, some with patterns that appear inconsistent or random at a large scale that may reflect local variations (Figure 23, stereonets LGE-A, K, L). Similar to the western La Grande, fold axis and hinge measurements in most regions are generally parallel to stretching lineation measurements. A significant observation is that numerous domains exhibit shallow west to northwest plunging stretching lineations (Figure 23, stereonets LGE-C, D, E, F, I). This includes regions delineated as flattening deformation zones in Figure 16. As these lineations are not only concentrated along boundaries, this lineation pattern supports the interpretation that flattening domains include a strong E-W component of extension in the eastern La Grande. Other volcano-plutonic domains exhibit moderate to steeply plunging lineation concentrations towards the south (stereonet LGE-B), the southeast (stereonet LGE-D), and the north (stereonets LGE-J, K). Lineation clusters plunging north are located in the southern eastern La Grande, and lineation clusters plunging south and southeast are located along strike from each other in the central eastern La Grande.

The boundary between the Opinaca and La Grande exhibits different patterns of stretching lineations in the west versus the east. In the west, where the boundary is oriented NW-SE, ductile stretching lineation orientations are spread from moderately plunging towards the north to shallowly plunging towards the west (Figure 23, stereonet LGE-G). There is a concentration of measurements plunging moderately towards the north. This may indicate that there are components of convergent deformation that dominated stretching lineation development over the dextral shearing depicted in Figure 14. The contact is oriented north-south the lineations plunging moderately to shallowly towards the North (stereonet LGE-H). In the east, the boundary generally trends E-W and the lineation orientations plunge sub-horizontally towards the west to southwest (stereonet LGE-I).

7.2.3 Eastmain and Nemiscau

Almost all regions of the Eastmain domain exhibit stretching lineations plunging sub-vertically to very steeply towards the east (Figure 24, stereonets EM-C, D, I, J, K, L, M). Exceptions lie in the northwest, in the zone of extension and necking deformation with the disaggregated plutonic body depicted in Figure 9. The lineations in this region plunge shallowly (stereonet EM-G) to moderately (stereonet EM-A) towards the west to southwest (stereonet EM-H). Stretching lineations in proximity to the Opinaca boundary also exhibit shallow westward plunging orientations (stereonet EM-F), however it is possible these are related to shearing along the boundary. Stretching lineation orientations within the Nemiscau have a large dispersion in their orientations, however, there is a strong concentration plunging moderately towards the west-northwest (stereonet NEM-A). Few fold axis or hinge measurements exist for this region, though for regions with measurements they are generally parallel to ductile stretching lineation orientations.

7.2.4 Opinaca

Structural data in the Opinaca subprovince is largely restricted to the West and is not as numerous as other domains. Some domains exhibit highly irregular random patterns (Figure 25, stereonets OP-B, F) or provide too little data on which to base a solid interpretation. In general stretching lineation measurements plunge shallowly towards the east (stereonet OP-D, J), northeast (stereonet OP-I), or southeast (stereonet OP-E, G). Many fold axis and hinge measurements are generally parallel to the stretching lineation orientations and their respective domain, and axes plunging shallowly towards the east are most common (stereonets OP-D, E, F, G, I). However, some domains show a wider spread of axis measurements. One example is stereonet OP-H, which provides measurements within the large-scale mushroom fold depicted in Figure 12. Fold axis measurements are distributed around a great circle in the stereonet. This is consistent with the rotation of local or parasitic fold axes during shearing and sheath fold (or mushroom fold) development.

7.3 Data summary

Point maxima of contoured structural data were compiled for each significant data cluster in the stereonets of Figures 22-25, for both ductile stretching lineation data and fold axis data. In addition, averaged foliation measurements for consistent clusters of data in forty-five locations around the map were compiled. The subset of available SIGÉOM (2018) foliation data that was compiled is defined in the appendix, along with a location map of all data points (Figure A2). Stereonets of these foliation data can be found as poles to foliations in the appendix (Figures A6-9). These compiled data points are each representative of many data, some with significant spread to their range of orientations, and therefore must be considered with due care.

The compiled data points are displayed as structural symbols in Figure 26, geolocated in a representative location within their respective domain. Figure 26 displays structural domains, with the major structures interpreted from the long wavelength images, and their continuations interpreted from short wavelength images. These are superimposed on a composite image of both the long and short wavelength tilt angle maps. This map provides a comprehensive compilation of our structural interpretations from aeromagnetic images with added context of structural data distilled from outcrop observations.

The averaged ductile stretching lineation compilation points can also be compared to each other, by the associated lithotectonic assemblage of their representative location, by the structural domain type, or by region. Figure 27 provides an equal area stereonet plot of all compilation lineation points coloured by structural domain with different symbols for lithotectonic assemblage type (metasedimentary, volcanic, or plutonic). The major clusters associated with each region are also schematically shown. Volcanic assemblage compilation points exhibit a significant cluster of sub-vertical measurements, with an average of the cluster plunging roughly 80° towards the northwest. This cluster includes volcanic assemblages within dominantly dextral transpressive shearing structural domains, with a lower proportion of multiple other structural domain types. This cluster is directly associated with the western La Grande and Eastmain regions. A secondary cluster of volcanic assemblage lineations compilation points plunge moderately to shallowly towards slightly north of east, and these are dominantly associated with necking and flattening deformation domains, and some NW-SE dextral transpressive shearing domains in the eastern La Grande region and along its boundary with the Opinaca. Plutonic assemblage compilation points exhibit a wider variety of orientations plunging steeply south to shallowly north to shallowly east. Their average can be loosely interpreted as plunging moderately towards the east. They represent a wide variety of structural domain types, with no apparent relationship between structural domain type and orientation. Metasedimentary assemblage compiled lineations exhibit a cluster with an average plunging shallowly towards the east approximately 30°. These lineations dominantly correlate to convergent deformation structural domains. From the perspective of structural domain types, E-W oriented dextral transpressive shear domains consistently exhibit steep to subvertical compilation point orientations. However, NW-SE oriented dextral transpressive shear domains vary from steep to moderately east plunging. Necking and flattening deformation compilation points vary from steep to a concentration that plunge moderately to shallowly eastward. Convergent deformation domain compilation points dominantly plunge shallowly east, however two points are subvertical and two points plunge moderately north to northeast. Rigid body domain compilation points relatively consistently plunge moderately north. The patterns in ductile stretching lineation compilation point stereonet (Fig. 27) provide a more detailed, yet similar, interpretation to the initial observations put forth in Figures 20-21. In general, stretching, shearing and transport directions in metasedimentary subprovinces plunge shallowly towards the east. Stretching, shearing and transport directions within the volcanic assemblages are generally sub-vertical with the noted exceptions in the eastern La Grande.

8. Discussion and application to mineral exploration

8.1 Deformation events interpreted from the map pattern

Analysis of the map pattern in terms of the relationships between lithotectonic assemblages, types of structures, recurring orientations of structures, overprinting relationships and interpreted strain partitioning, can establish a sequence and characteristics of regional deformation events. This sequence of events is limited to the large regional scale of observation defined within our above analysis, yet may provide a

contextual framework for local studies. As with all scales of shear and ductile deformation, the interpretation of sequential events may be hampered by progressive strain accumulation in some types of structural domains.

With the oldest units in the region, the La Grande may exhibit evidence of early deformation. Paleo- to Mesoarchean gneisses may have been deformed in Mesoarchean events, yet the preserved remnants do not appear to have influenced the map-scale deformation pattern or large-scale structures that have recurring orientations. Therefore, Neoarchean deformation likely defined the map pattern. Neoarchean deformation is evident in both orientations of dextral transpressive shearing domains, sinistral transpressive shearing domains, necking and flattening domains, and convergent deformation domains, which together constitute the majority of the map (Figure 26) and define the major recurring orientations of structures (Figure 18). Much of the transpressive shear deformation is temporally constrained by the intrusive suites of Neoarchean TTGs, which together with older volcanic successions comprise the dome and keel structures in both the western and eastern La Grande. The isoclinally folded volcanic successions forming the keels of the dome and keel structures formed pre- or syn-shearing and post-pluton emplacement. As most plutons within dome and keel structures are similar in age to the Duncan suite, isoclinal fold development is constrained to being younger than ca. 2719-2705 Ma (Goutier et al., 1998, 1999a, 2002). The eastern and western La Grande regions have starkly different styles of unit shapes, types and orientations. The eastern La Grande comprises linear to lenticular E-W oriented deep crustal domains (Figure 19), separated by a roughly parallel, E-W oriented series of moderately to shallowly northward dipping, discrete linear structures that have deep and shallow expressions (Figure 26). It is possible that these are early structures that were subsequently modified during Neoarchean TTG emplacement and transpressive shearing. They are deflected by shearing along the boundary of the Opinaca, indicating they pre-date NW-SE oriented dextral shearing. E-W dextrally sheared plutons abut E-W linear structures, which may indicate they formed as partitioned N-S convergent or flattening strain during transpression. Neoarchean plutons in the eastern La Grande (ca. 2698-2693 Ma Richardie suite; Gigon and Goutier, 2017) constrain shearing, or continued shearing, along these structures to younger than 2693 Ma. Deformation remained active for an extended period, as they exhibit deformation through to late brittle-ductile, and brittle conditions (Gigon and Goutier, 2017). East-west extension within the eastern La Grande, as a partitioned component of the flattening deformation structural domains (Figure 26) include units wrapped around the 2704 Ma Polaris batholith (Augland et al., 2016). This may be interpreted as constraining E-W extension to younger, however, this could alternatively be interpreted as a late syn-tectonic pluton that intruded into a developing necking zone. In either case, orogen-parallel extension likely occurred syn- to post- formation of the E-W discrete linear structures discussed above, considering that some flattening structural domains bound by the linear structures exhibit an overprint of necking deformation.

The Eastmain domain is a linear belt that is continuous across the map area and exhibits a strongly necked central region. This may have been controlled or influenced by the shape of the Opatica domain, whose greater competency appears to have allowed it to act as an indenter at the southern boundary of the necking site. In contrast, the less competent metasedimentary rocks of the Opinaca appear to have flowed, during convergent deformation, to occupy the necked region along its northern boundary. The Opinaca sediments may also be a thin veneer, with the necking deformation controlled by the rheology of underlying crust. Internally, the Eastmain domain comprises a complex array of disaggregated and deformed plutonic bodies, localized shear structures, the Nemiscau subprovince, and expansive intervening volcanic domains. As a set, these features are generally consistent with flattening deformation that includes a north-south

oriented convergent component and a contemporaneous E-W oriented extension component. Structural domains (Figure 16) of conjugate NW-SE dextral shear and NE-SW sinistral shear indicate that strain localized on opposing sides of necking zones to accommodate large-scale boudinage. Other regions underwent pervasive ductile shearing; E-W to NW-SE dextral deformation structures are more widespread and are hosted in a wider variety of lithologies. These structures may have formed contemporaneously and are compatible with a dextral transpressional deformation event with a dominant north-south convergent component, and an E-W extension component. Dome and keel structures are similarly constrained as with the La Grande, to being younger than adjacent plutons (e.g. the 2709 Ma Opinaca Reservoir pluton; David et al., 2011). Additionally, Timiskaming-type sediments within folded volcano-sedimentary sequences defining keel structures associated with the Roberto deposit locally constrain the structures to <2675 Ma (Ravenelle et al., 2010; Fontaine et al., 2015). Other than 2616-2600 Ma undeformed pegmatite dykes (Ravenelle et al., 2010) in the region of the Roberto deposit that constrain the end of deformation, no further geochronological constraints are apparent.

Deformation in the Opinaca contrasts sharply with the simpler necking and boudinage of the stiffer rheology in the La Grande and Eastmain N-S convergence, E-W extension structures, which formed at shallower structural levels. The Opinaca exhibits localized convergent structures along its southern and northeastern boundaries, indicating intense N-S shortening that was likely accommodated through thrusting and imbrication or through ductile extrusion. The associated structures differ from folds within the interior of the Opinaca, which exhibit NE-SW axial traces consistent with regional-scale E-W dextral transpression. Folded stromatic leucosome within the Opinaca indicate deformation affected the Opinaca syn- to post-peak metamorphism, through ca. 2665-2635 Ma (Morfin et al., 2013) Localized NW-SE dextral shear zones formed along its north and south boundary, which may be a synthetic orientation to E-W dextral shear. However, NW-SE dextral shearing has modified the existing E-W foliation, and therefore may have increasingly localized through to late stages of deformation (<2614 Ma sheared pegmatite dyke; Bogatu, 2017). It was active contemporaneously with N-S shortening and deformed in conjunction with NE-SW sinistral shearing to accommodate E-W extension and the relative westward lateral protrusion (c.f. Leonov, 2008; Chardon et al., 2009) of the western Opinaca. It is likely that the entire Eeyou Istchee Baie-James region was in motion, and the different portions may have been extending or translating eastward at a faster rate than the western Opinaca to create the apparent westward extrusion structures. Gneissic doming (Figure 13) and E-W extensional (Figure 14) structural domains in the central to eastern Opinaca give the appearance of post-dating other deformation. However, the N-S orientation of the foliation within the E-W extensional domain indicates it formed concurrently with the conjugate shear zones and the relative westward protrusion of the Opinaca, which in turn is concurrent with N-S convergence. Subtle N-S oriented deep structures (Figure 17) throughout the region are likely associated with this phase of deformation, representing distributed strain related to E-W extension. They are likely brittle-ductile faults within dry granulitic basement underlying the Opinaca, as they have exceptionally linear traces. Their only expression in the shallow aeromagnetic images are local fold interference patterns caused by monoclinal folding within the rheologically softer sediments directly above the discrete basement structures. The N-S deep structures thus post-date the first generation folds internal to the Opinaca. Similarly, the gneissic dome likely formed during E-W extension, illustrating how relative motions may be complex in convergent and transpressional regimes; the local flow of deep structural levels of Opinaca paragneiss into the Eastmain necking zone may have exceeded the southward convergent transport rate, thus permitting extrusion of the dome during convergence. This forced accommodation of space defined the fan-like pattern of regularly spaced discrete

deep basement structures observed in the deep aeromagnetic images (Figure 13), consistent with local, average NE-SW oriented extension within and beneath the gneissic dome domain.

The structures and relationships described above are consistent with a prolonged deformation event that:

1. Initiated with N-S convergence, thus creating E-W oriented structures and foliations that remain preserved in the eastern La Grande.
2. Phased in dextral shearing to a regime of transpression, thus forming fold and localized convergence structures in the Opinaca, E-W oriented transpressional σ- and δ-type shear structures in the western and eastern La Grande, and the Eastmain domains.
3. Transitioned into a dextral transpression regime with a stronger N-S flattening component with diametrically opposed E-W extension that disaggregated and boudinaged the Eastmain domain, stretched and flattened the La Grande, and formed conjugate shear zones, and gneissic dome and extensional structures in the Opinaca.
4. Continued in the same regime through to higher crustal conditions, with shear deformation localizing into discrete shear zones, and distributed arrays of discrete, deep cryptic N-S oriented brittle-ductile basement faults forming to accommodate extension.

The continuous transitions in relative magnitudes of suggested strain components (shearing, N-S flattening, E-W extension) between phases provide for difficult interpretation of overprinting relationships. Some features, such as the gneissic dome in the eastern Opinaca (Figure 13), are clearly late features, however, there are examples of more ambiguous timing and overprint relationships. An example is the σ-type pluton structures in the western La Grande that show a consistent E-W shear orientation (Figure 8), despite synthetic displacement along NW-SE dextral shear zones that transported the Minto block southeastward towards or over the La Grande. This synthetic shear does not indicate any sort of overprint or effects on the E-W dextral shearing, and, apart from a brief stepover, it continues along the north boundary of the Opinaca where it records late dextral shearing associated with the phase of conjugate shearing and extension. Therefore, if transpression had ever transitioned into single-component NW-SE shearing, E-W shear structures would have been overprinted.

8.1.1 Correlations between structural data and geophysical interpretation

Analysis of the lineation patterns by deep crustal domains (Figures 22-25) supports interpretation that strain partitioned differently into different structural domain types, although the associated lithotectonic assemblage appears to be a large factor as well (Figure 27). Most averaged lineation orientations (Section 7.3, Figure 27) from volcanic assemblages cluster around subvertical, trending slightly towards a steep north-northwest plunge, regardless of structural domain type. Many of these structural domain types are E-W oriented dextral transpressive shear domains, and this subvertical stretching, transport or shear is consistent with transpression. We interpret that within these domains the convergent component of transpression partitioned strain into vertical extrusion, to a higher magnitude than dextral shear strain. Thus, shear indicators are visible in the map, yet lineation orientations are steep. The fewer moderately to shallowly eastward plunging average lineation orientations within volcanic assemblages are the opposing example of strain partitioning, as they are within necking and flattening, and NW-SE dextral transpressive domains. Localized E-W stretching, transport, or shear must have exceeded the magnitude of vertical extrusion, and dextral shear, to provide shallow lineation orientations within these domains. Therefore, the

averaged outcrop structural data is in general agreement with our interpretation of structural domains for volcanic assemblages.

Convergent deformation domains correlate largely to metasedimentary assemblages, and their averaged lineation measurements trend dominantly towards a moderate to shallow eastward plunge. Two exceptions of subvertical averaged lineations within convergent deformation domains exist, both of which are from regions located along major structures (Figure 26). They would be consistent with lineations occurring along the structures from thrusting and imbrication, reverse-oriented shearing, or vertical extrusion. Otherwise, the trend of shallowly eastward plunging lineations in metasedimentary rocks indicates that E-W extension localized strain in the metasedimentary subprovinces and may have succeeded convergence. Many individual outcrop lineation measurements from metasedimentary subprovinces are in late plutonic rocks as part of granitoid injection complexes, in which case extension likely post-dated, or continued through, anataxis. Thus, extension either rotated existing, or created new, linear structural elements at a late phase of deformation. The high-grade nature of the majority of the Opinaca metasediments dictates a weak rheology, with little preservation potential for lineations until late phases of deformation. This line of evidence supports interpretation that convergence occurred initially, and a component of E-W extension progressively phased in.

Plutonic lithotectonic assemblages exhibit averaged lineation orientations that moderately plunge eastward in general, but spread towards north, northeast, and southeast. These appear to be in an intermediate orientation between the volcanic and metasedimentary assemblages. However, there are fewer average lineation points from this lithotype, and they have a high variation in structural domain type and no apparent correlation between type and orientation. The wider spread is difficult to interpret, it may suggest that the relatively more rigid plutonic domains provided a median degree of stretching between the differing deformation between volcanic and metasedimentary domains. As with some plutonic lithotectonic assemblage averaged lineations, the averaged lineations from rigid body structural domains plunge moderately northward. Their moderately shallow orientations are the most consistent with north-over-south transport, and may represent a more homogenous, early response to convergence.

Regionally, the western La Grande shows consistency amongst averaged lineation orientations, all steeply plunging (Fig 27, schematic). It is also fairly consistently one structural domain type. The eastern La Grande exhibits two distinct lineation clusters, one plunging steeply north, overlapping with the extent of western La Grande orientations, and one plunging shallowly east-northeast, illustrating the partitioning of strain into extrusion, or north-over-south transport, and extension. The shallow orientations are similar to the plunge and orientation of Opinaca lineations, supporting interpretation that extensional deformation in the eastern La Grande was contemporaneous with E-W extension in the Opinaca. Their boundary region averaged lineations are spread between the steep and the shallow clusters, which suggests the localization of transpressional deformation along the boundary. Averaged lineation orientations within the Eastmain domain are spread from subvertical, through moderately northeast, and through to shallowly eastward in overlap with the Opinaca. This spread illustrates the wider variety of structural domain types in the Eastmain, that in some domains deformation localized as vertical extrusion similar to the western La Grande but in others transpression and extension varied the stretching, transport or shearing towards shallower orientations. The orientations are consistent with deformation in the Eastmain domain following a similar regime to all other regions in this study.

8.1.2 Tectonic event timeline

The relative sequence of deformation phases in at least one, prolonged, multi-phase tectonic event can be loosely placed on an absolute timescale. Various radiometric dates from literature are referenced to build a timeline of these phases:

- 2716-2709 Ma Duncan suite (Goutier et al., 1998, 1999a, 2002) and similar plutonic rocks – all structures in volcano-plutonic sequences, including the dome and keel structures, and σ- and δ-type plutonic structures in western La Grande, post-date the formation of this suite. All volcanic suites pre-date the Duncan suite.
- 2710 Ma, Pluton de la Frégate (Augland et al., 2016) – tonalite pluton located within the E-W extension structural domain in the Opinaca. This may be exposed basement exhumed during extensional deformation, or exposed deeper, older levels of the basin that were intruded by tonalite plutons.
- 2704 Ma Polaris batholith (Augland et al., 2016) – large, round intrusion (in map view) within the eastern La Grande domain. The surrounding domains wrap around this pluton which hence acted as a rigid body. This implies that convergent deformation and E-W extension post-date Polaris batholith emplacement.
- 2666 – 2636 Ma Leucosome zircon age (Morfin et al., 2013; Côté-Roberge, 2018) Metamorphic peak and leucosome injection in the Opinaca – deposition of the Opinaca pre-dates this. This is the likely period for convergent deformation and dextral transpression. Regional E-W extension may have been synchronous or initiated late within this period (Moser et al., 1996).
- 2618 Ma Granite du Vieux-Comptoir (Goutier et al., 1999b) – undeformed granites of this suite are found within the Opinaca, and this date constrains the age of bulk, regional deformation (folding and penetrative strain).
- 2614 Ma Pegmatite (Bogatu, 2017) – Localized deformation in discrete dextral shear zones along the north boundary of the Opinaca post-dates this age, as recorded in deformed pegmatite dykes. This is the approximate timing of local second generation folds along the boundary between the La Grande and Ashuanipi.

Deformation processes were active throughout, at least, an approximately 100 m.y. timescale. Early phases may have been limited to deformation within volcano-plutonic subprovinces and may have been associated with the emplacement of regional plutonic suites. Based on the loose constraints stated above, we estimate that formation of structures defining the map pattern, and analyzed within this work, occurred between 2680-2600 Ma.

8.2 The nature of tectonic boundaries

8.2.1 Transitional metasedimentary domains

Some high metamorphic grade domains are difficult to classify as part of either a metasedimentary subprovince or an adjacent volcano-plutonic subprovince. These domains are indicated in Figure 1 and 7 as transitional metasedimentary domains (TMDs). These domains include coherent units and fragments of lithologies that are typically associated with volcano-plutonic subprovinces, including stratiform mafic volcanic units, conglomerate, iron formation, amphibolite, and orthogneiss. However, they are dominantly metasedimentary rocks that exhibit high-grade metamorphism, migmatization, and leucocratic injections, similar to those developed in a metasedimentary subprovince. In the example of the Boisbriand TMD at the eastern edge of the La Grande, migmatization and the metamorphic grade diminishes rapidly northward.

Such domains may be relict margins of the same extensional basin that developed into a metasedimentary subprovince (Kehlenbeck, 1976). In the Eeyou Istchee Baie-James region, they lie across tectonic boundaries that, elsewhere, clearly delineate the Opinaca from the La Grande. In this study, structural domains of the Opinaca (Figure 26) lie across deep crustal domain boundaries (Figure 19) from structural domains of the contiguous Eastmain and Boisbriand TMDs (Figure 7), where along strike the same bounding structure separates the Opinaca from the La Grande proper. The choice to include the TMDs as part of either the La Grande or Opinaca subprovince is somewhat ambiguous, based on current definitions of a subprovince, which can include tectonic, intrusive, or depositional boundaries. Therefore, this point of debate requires further study and discussion to resolve, such as comparing ages, sedimentological, and metamorphic characteristics between the Opinaca and the TMDs. Analysis and comparison of the volcanic and amphibolite lithologies within the TMDs to the surrounding volcano-plutonic subprovinces may also provide useful relationships. However, a structural basis for delineating these subprovinces and differentiating the TMDs, an example of which could be how we define our deep crustal domains, could be less ambiguous. Problematically, this would resemble a terrane definition.

8.2.2 Subprovince versus terrane terminology

The deep crustal domains that we outline in Figure 19 are, in a limited extent, similar to terrane boundaries. Common usage of the term terrane refers to a crustal block or domain that is fault bound and has an internally coherent set of lithologies from the same, linear geologic history which differs from adjacent terranes. This is different from subprovince terminology in that subprovince boundaries delineate distinct lithotectonic assemblages, and the type of boundary may be intrusive, depositional, or structural, thus creating some ambiguity about where and why specific boundary points are chosen. Additionally, the units within a subprovince may not share the same linear geologic or tectonic history. The ambiguity of subprovince boundaries becomes more apparent where primary boundaries, either intrusive or depositional, were subsequently deformed by late structures. The deep crustal domains we have established (Figure 19) are likely individual fault bound crustal blocks. However, analysis of the nature of the bounding structures would be required to confirm that faults or shear zones are present in each case of interpretation made from the aeromagnetic maps. The analysis in this work is largely structural, and does not include the complete history of each deep crustal domain, which would be required to identify or group domains into terranes. The most extreme reinterpretation we present for the region is our separation of the Eastmain domain from the La Grande domain. This suggests that, as different crustal blocks, they may not have consistent geological histories between the domains, and that deformation may have juxtaposed them into contact. Applying terrane terminology to the Eeyou Istchee Baie-James region, or refining subprovince boundaries through applying some terrane analysis concepts, may be beneficial as it would highlight these potential incongruities. However, considerable further study would be required to confirm such hypotheses. This may include detailed compilations of ages and unit assemblages, as well as further, various isotopic works to establish the nature of the early histories of each domain. The decision to apply terrane concepts would require extensive debate amongst the community but is worth exploring. If so, four potential major terrane boundaries or relationships are recognized in the work from this report:

1. The current Minto-La Grande boundary is interpreted as intrusive, yet the La Grande is exposed at a lower metamorphic grade than the bulk of the Minto. The boundary region between the Minto and the La Grande may include a significant structure that we delineate in our deep crustal domain map (Figure 19). The structure resides in the northern La Grande but is fairly linear and deep seated in rocks with a moderate to shallow northward dip (Figure 26), meaning that it may be the surface expression of a bounding structure between two subprovinces that are irregularly shaped at depth.

Volcano-plutonic units north of this structure, but south of the current Minto-La Grande boundary (Figure 7), could be examined for any true relationship to the La Grande; they may have been thrust upon it, or imbricated as slivers of La Grande into the Minto hangingwall.

2. The division of the La Grande into the La Grande (north and northwest of the Opinaca) and the Eastmain is a potential terrane division. It is uncertain if the two domains share a complete history. The western Eastmain domain (as delineated in this report, Figure 19) has a strongly deformed northern boundary, and unfortunately the aeromagnetic survey does not depict where it is in contact with the La Grande. This contact region may be entirely tectonic, deformed during N-S shortening of the Opinaca, in which case the two domains would have unique histories.
3. The western and eastern portions of the Eastmain domain (Figure 19) are interpreted to be separated by a tectonic scale boudin neck. This interpretation could be explored further to establish whether or not the east and west subdomains have in fact been segregated by deformation, and therefore represent a singular domain, or terrane.
4. The boundary between both the Opatica and the Opatica TMD (Figure 7), and the Eastmain domain, may be a continuous tectonic boundary. The Opatica and Opatica TMD may have a separate geological history from the Eastmain domain and the Nemiscau subprovince prior to their tectonic amalgamation. Establishing this history would require extensive analysis of sediment age and source differences between the Nemiscau and the Opatica TMD.

8.3 Correlations between structures and metamorphism

The Eeyou Istchee Baie-James region exhibits complex patterns of metamorphic isograds. The extreme difference between the granulite in the central Opinaca and greenschist facies rocks in the La Grande and Eastmain represents approximate difference in exposed structural level of up to 20 km, which cannot be accounted for only through differential erosion. The very strong “metamorphic gradient” established from aeromagnetic interpretation, which is considered prospective for mineral exploration (Gauthier et al., 2007), has a strong relationship to structure. Previous workers have extrapolated regions of granulite, amphibolite, and greenschist rocks in the Eeyou Istchee Baie-James region (Figure 28) based on the observed textures of the aeromagnetic map, in correlation with compiled metamorphic geology from regional reports (Gauthier et al., 2007 and references therein). These respective regions of differing extremes in metamorphic grade correlate well with specific types of structural domains outlined in this work.

The granulite facies domain of Figure 28, outlined in red, within the Opinaca correlate to the E-W extension and gneissic doming domains, the sinistral NE-SW shear zone domains that separate them, and the series of adjacent convergent domains that occupy the boudin neck of the Eastmain domain. This is consistent with our interpretation that local doming and lower crustal flow occurred within the Opinaca related to syn-convergent extension. The sinistral shear zone appears to be a significant tectono-metamorphic boundary between granulite and amphibolite facies regions, a further indication that it is contemporaneous to doming and extension structures. This further supports our interpretation that the E-W extension domain in the Opinaca is a horst structure that exposes deeper sections of the basin, and possibly the basement.

Sinistral deformation zones along the Nemiscau to Opatica TMD boundary (Figures 7 and 11) are also associated with granulite facies metamorphism (Figure 28). The isograd crosses the middle of the Nemiscau, parallel to the northern boundary, suggesting that southern regions of the Nemiscau may have been extruding southwestwards parallel to local moderately northeast plunging lineations (Figure 26). The

Opatica TMD occupies what may be the necked westward termination of the Opatica domain, however, the aeromagnetic survey does not extend far enough south to confirm this.

The delineated greenschist facies domains of Figure 28, outlined in green, correlate to volcanic plutonic complexes that are within E-W oriented dextral shear, or necking and flattening deformation structural domains. The concentration of dextral deformation into zones of greenschist facies rocks is an indication that transpression localized the dextral shear component into the most rigid and competent (coolest) lithotectonic domains. Not all regions that we categorized as E-W dextral shearing were interpreted as greenschist by Gauthier et al. (2007), however, their work was done at a large-scale and is approximate. Within the Eastmain domain dextral and flattening domains along the axis of the tectonic-scale boudin were delineated as greenschist. This boundary is also the boundary with the Nemiscau along its western extent. This may be an indication that a continuous significant structure trends along the axis of the Eastmain domain 'boudin'.

8.4 Application to mineral exploration

The maps supplied in this report provide tools applicable to mineral exploration, including the identification of prospective local and regional, both deep and shallow, fluid and magma pathways. Some structures depicted in long wavelength component aeromagnetic or gravity data may exist at depth, yet have no, or insignificant, surface expression (Dufréchou et al., 2014 and references therein). Situations such as this may have created structural traps for percolating metal-laden fluids. Correlations between gravity maps (Figure 29; see Cleven, 2017) and the structures observed in the deep geophysical maps (Figure 17) indicate that north-south structures may exist at depth and do not have consistent or easily recognizable shallow or surface expressions.

Figure 29 (from Cleven, 2017) depicts traces of north-south lineaments in a theta angle short wavelength component gravity map. These north-south structures form large networks spanning the Minto block, through the Eeyou Istchee Baie-James region, towards the Abitibi. Within the Eeyou Istchee Baie-James region they are concentrated in the west and are located similarly to interpreted N-S structures we provide in this report (Figure 17). Such structures are difficult to identify in the short wavelength component maps; however, they are more readily discernible in pseudogravity maps. Figure 30 is a composite pseudogravity (colour) and short wavelength pseudogravity theta angle (greyscale shading) image that provides enough detail to identify collections of individual structures, including series of fold axes, or what appear to be detachment faults dipping towards the west, in alignment over the N-S structures interpreted previously (Figure 17). Figure 30 also includes locations of base metal mineralization in the Eeyou Istchee Baie-James region. Mineralization appears to correlate to boundary regions around the Opinaca where N-S structures terminate against the boundary. Throughout the region mineralization correlates to intersections of major structures and N-S structures. Ultramafic intrusions within the Opinaca are concentrated between the N-S structures, which may be an indication these deep structures are trans-crustal and allowed upward percolation of deep magmas. Above, we associate formation of the N-S structures with late-phase regional syn-convergence E-W extension, therefore the motions of underlying stiff, dry granulitic basement blocks beneath of the Opinaca metasediments may have been a causal factor in mineralization, as they could feasibly have transferred heat through percolation of ultramafic intrusions, broken stratigraphic or structural caps, created dilation, channels and new pathways, and generally instigated a major fluid mobilization event.

Our analysis of the regional map pattern, and the characterization of the deformation event that created it, provides a template for establishing the context of local mineralized sites. The breakdown of the region into specific structural domains provides establishes the respective structural nature of specific mineralized sites (Figure 31). The boundaries of many of the structural domains also host mineralization, commonly above major deep structures. E-W extension related structures, including conjugate shear zones, north-south oriented linear structural elements, and necked or flattened regions, may be dilation sites prospective for vein-hosted mineralization (Leclerc et al., 2012). Boundary regions between the Opinaca and La Grande that include dilation sites, in proximity to the E-W extensional domain or north-south structures, do exist in the region.

Gold and silver occurrences (Figure 32) provide a more specific view of sites of structurally controlled epigenetic mineralization. The most significant, the Roberto deposit (Ravenelle et al., 2010; Fontaine et al., 2015) provides a template for examining the regional structural controls that could provide concentrated mineral wealth. In the context of the structural domains defined here, and the major structures at depth (Figure 32), the Roberto deposit lies:

- in an E-W extensional zone, in proximity to a major NW-SE structure that roughly delineates the Opinaca from the La Grande subprovince
- in proximity to deep N-S structures
- where a major NE-SW sinistral shear zone intersects the boundary (and takes a stepover)
- where NW-SE dextral deformation localized along the subprovince boundary
- where metasediments of the Opinaca comprise convergent structural domains
- within the necked region along the margin of a deep crustal domain (the Eastmain)

Other occurrences are present in the immediate vicinity of the Roberto deposit; however, the region does not have any other sites that have the same confluence of structural criteria. Many sites have subsets of the criteria (indicated in Figure 32), and some have different criteria that are noted to be suitable in other works. These include, but are not limited to, being in dextral transpressional zones and flattening deformation zones. These criteria are strictly based on the observations in this report and are not exhaustive for the general criteria required for hosting mineralization.

9. Conclusions

Aeromagnetic images indicate that Archean rocks of the Eeyou Istchee Baie-James region exhibit deformation patterns consistent with a prolonged period of penetrative ductile deformation that transitioned towards strain localization into discrete structures. The multi-phase event that defined the regional pattern spanned ca. 2720 Ma to 2600 Ma. East-west dextral transpression within broad ductile shear corridors is interpreted from σ- and δ-type foliation trajectories around volcano-plutonic assemblages, terrane-scale wide synthetic and antithetic shear zones, and non-cylindrical folds in the Opinaca subprovince, pre- to syn-peak metamorphism ca. 2665-2635 Ma. N-S shortening and concomitant E-W extension appears to have increased with time, leading to boudinage and disaggregation of the Eastmain domain of the La Grande subprovince, partitioning flattening into volcanic assemblages in the eastern La Grande and overprinting the Opinaca with a shallowly east plunging lineation. We speculate that the rate of flow of material from the southeast Opinaca into the Eastmain domain boudin neck locally exceeded convergence rates and thus formed extension structures including a horst that exposes deep, early levels of the Opinaca, and a gneissic dome. This late, largely extensional phase was likely responsible for fluid mobilization and regional

epigenetic mineralization. By ca. 2620-2600 Ma regional penetrative ductile deformation had ceased, yet dextral shear zones were still actively localizing strain.

References

ALSOP, G.I. – HOLDSWORTH, R.E., 2006 – Sheath folds as discriminators of bulk strain type. Journal of Structural Geology, 28(9), pages 1588-1606.

ALSOP, G.I. – HOLDSWORTH, R.E. – MCCAFFREY, K.J.W., 2007 – Scale invariant sheath folds in salt, sediments and shear zones. Journal of Structural Geology, 29(10), pages 1585-1604.

AUCOIN, M. – BEAUDOIN, G. – CREASER, R. A. – ARCHER, P. – HANLEY, J., 2012 – Metallogeny of the Marco zone, Corvet Est, disseminated gold deposit, Baie-James, Quebec, Canada. Canadian Journal of Earth Sciences, 49 (10), pages 1154–1176.

AUGLAND, L. – DAVID, J. – PILOTE, P. – LECLERC, F. – GOUTIER, J. – HAMMOUCHE, H. – LAFRANCE, I. – TALLA TAKAM, F. – DESCHENES, P. – GUEMACHE, M., 2016 – Datations U-Pb dans les provinces de Churchill et du Superieur effectuees au GEOTOP en 2012-2013. Report RP 2015-01, Ministère des Ressources naturelles du Québec, 42 pp.

BANDYAYERA, D. – BURNIAUX, P. – MORFIN, S., 2011 – Geology of the Lac Brune (33G07) and Baie Gavaudan region (33G10). Report RP 2011-01 (A), Ministère des Ressources naturelles du Québec, 24 pp.

BANDYAYERA, D. – GOUTIER, J. – BURNIAUX, P., 2014 – Géochimie des roches volcaniques et intrusives de la région des lacs Guyer et Nochet, Baie-James. Report RP-2014-03, Ministère des Ressources naturelles du Québec, 29 pp.

BANDYAYERA, D. – RHÉAUME, P. – MAURICE, C. – BÉDARD, E. – MORFIN, S. – SAWYER, E. W. 2010 – Synthèse géologique du secteur du Réservoir Opinaca, Baie-James. Report RG 2010-02, Ministère des Ressources naturelles du Québec, 44 pp.

BARANOV, V., 1957 – A new method for interpretation of aeromagnetic maps: pseudogravimetric anomalies. Geophysics, 22 (2), pages 359–382.

BÉDARD, J.H., 2006 – A catalytic delamination-driven model for coupled genesis of Archaean crust and sub-continental lithospheric mantle. Geochimica et Cosmochimica Acta, 70(5), pages 1188-1214.

BÉDARD, J.H. – BROUILLETTE, P. – MADORE, L. – BERCLAZ, A., 2003 – Archaean cratonization and deformation in the northern Superior Province, Canada: an evaluation of plate tectonic versus vertical tectonic models. Precambrian Research, 127(1-3), pages 61-87.

BÉDARD, J.H. – HARRIS, L.B., 2014 – Neoarchean disaggregation and reassembly of the Superior craton. Geology, 42(11), pages 951-954.

BENN, K. – MILES, W. – GHASSEMI, M.R. – GILLETT, J., 1994 – Crustal structure and kinematic framework of the northwestern Pontiac Subprovince, Quebec: an integrated structural and geophysical study. Canadian Journal of Earth Sciences, 31(2), pages 271-281.

BOGATU, A., 2017 – The Orfée prospect: a Neoarchean orogenic gold occurrence along the contact between the La Grande and Opinaca subprovinces (Eeyou Istchee Baie-James, Québec). Masters thesis, Université Laval, Québec, Canada, 205 pp.

BUCHAN, K.L. – GOUTIER, J. – HAMILTON, M.A. – ERNST, R.E. – MATTHEWS, W.A., 2007 – Paleomagnetism, U–Pb geochronology, and geochemistry of Lac Esprit and other dyke swarms, James Bay area, Quebec, and implications for Paleoproterozoic deformation of the Superior Province. Canadian Journal of Earth Sciences, 44 (5), pages 643-664.

CADÉRON, S., 2003 – Interprétation tectonometamorphique du nord de la province du Supérieur, Québec, Canada. PhD thesis, Université du Québec à Montréal, Montréal, and Université du Québec à Chicoutimi, Canada; 314 pp.

CALVERT, A. – SAWYER, E. – DAVIS, W. – LUDDEN, J., 1995 – Archean subduction inferred from seismic images of a mantle suture in the Superior Province. Nature, 375 (6533), pages 670-674.

CARD, K., 1990 – A review of the Superior Province of the Canadian Shield, a product of Archean accretion. Precambrian Research, 48 (1), pages 99-156.

CARD, K. – CIESIELSKI, A., 1986 – DNAG# 1. Subdivisions of the Superior Province of the Canadian shield. Geoscience Canada, 13 (1), pages 5-13.

CARD, K. – POULSEN, K., 1998 – Geology and mineral deposits of the Superior Province of the Canadian Shield. Geology of the Precambrian Superior and Grenville Provinces and Precambrian Fossils in North America, Geological Survey of Canada, Geology of Canada, 7, pages 13-194.

CARRERAS, J. – DRUGUET, E. – GRIERA, A., 2005 – Shear zone-related folds. Journal of Structural Geology, 27 (7), pages 1229-1251.

CHARDON, D. – GAPAIS, D. – CAGNARD, F., 2009 – Flow of ultra-hot orogens: a view from the Precambrian, clues for the Phanerozoic. Tectonophysics, 477 (3-4), pages 105-118.

CIESIELSKI, A., 1991 – Geology of the eastern Superior Province, Baie-James and Bienville subprovinces. Geological Survey of Canada, open file 2398, 9 pp.

CLEVEN, N., 2017 – Application of gravity and pseudogravity geophysical treatments to structural targeting in the Eeyou Istchee Baie-James region, Québec Superior Province: Preliminary interpretations. Report MB 2017-14, Ministère de l'Énergie et des Ressources naturelles du Québec, 30 pp.

COOPER, G. – COWAN, D., 2006 – Enhancing potential field data using filters based on the local phase. Computers & Geosciences, 32 (10), pages 1585–1591.

CORFU, F. – STOTT, G.M. – BREAKS, F.W., 1995 – U Pb geochronology and evolution of the English River Subprovince, an Archean low P high T metasedimentary belt in the Superior Province. Tectonics, 14(5), pages 1220-1233.

CÔTÉ-ROBERGE, M., 2018 – Contexte tectonométamorphique du nord-ouest du complexe de Laguiche, sous-province d'Opinaca, Eeyou Itschee Baie-James. Masters thesis, Université Laval, Québec, Canada; 201 pp.

CÔTÉ-ROBERGE, M. – GUILMETTE, C. – GOUTIER, J., 2016 – Étude du contexte tectono-métamorphique du Complexe de Laguiche, Sous-province d'Opinaca, Eeyou Istchee Baie-James, Québec. Ministère des ressources naturelles, Québec, Report MB 2016-13, 27 pp.

D'AMOURS, I., 2011 – Synthèse des levés magnétiques de la Baie-James. Report DP-2011-08, Ministère des Ressources naturelles et de la Faune, Québec, 4 pp.

DAVID, J. – DAVIS, W.D. – BANDYAYERA, D. – PILOTE, P. – DION, C., 2009 – Datations U-Pb effectuées dans les sous-provinces de l'Abitibi et de La Grande en 2006-2007. Report RP 2009-02, Ministère des Ressources naturelles et de la Faune, Québec, 17 pp.

DAVIS, D. W., 2002 – U-Pb geochronology of Archean metasedimentary rocks in the Pontiac and Abitibi subprovinces, Quebec, constraints on timing, provenance and regional tectonics. Precambrian Research, 115 (1), pages 97-117.

DAVIS, D.W. – SIMARD, M. – HAMMOUCHE, H. – BANDYAYERA, D. – GOUTIER, J. – PILOTE, P. – LECLERC, F. – DION, C., 2014 – Datations U-Pb dans les provinces du Supérieur et de Churchill en 2011-2012. Ministère de l'Énergie et des Ressources naturelles, Québec; RP 2014-05, 62 pages.

DUFRÉCHOU, G. – HARRIS, L. B. – CORRIVEAU, L., 2014 – Tectonic reactivation of transverse basement structures in the Grenville orogen of SW Quebec, Canada: Insights from gravity and aeromagnetic data. Precambrian Research, 241, pages 61–84.

DUPARC, Q. – DARE, S.A. – COUSINEAU, P.A. – GOUTIER, J., 2016 – Magnetite chemistry as a provenance indicator in Archean metamorphosed sedimentary rocks. Journal of Sedimentary Research, 86 (5), pages 542-563.

EATON, D. W. – DARBYSHIRE, F., 2010 – Lithospheric architecture and tectonic evolution of the Hudson Bay region. Tectonophysics, 480 (1), pages 1–22.

FONTAINE, A. – DUBÉ, B. – MALO, M. – MCNICOLL, V. – BRISSON, T. – DOUCET, D. – GOUTIER, J., 2015 – Geology of the metamorphosed Roberto gold deposit (Éléonore Mine), Baie-James region, Québec: diversity of mineralization styles in a polyphase tectono-metamorphic setting. *In:* Targeted Geoscience Initiative 4: Contributions to the Understanding of Precambrian Lode Gold Deposits and Implications for Exploration, Editors: B. Dubé and P. Mercier-Langevin, Geological Survey of Canada, Open File 7852, pages 209–225.

FREDERIKSEN, A. – MIONG, S.-K. – DARBYSHIRE, F. – EATON, D. – RONDENAY, S. – SOL, S., 2007 – Lithospheric variations across the Superior Province, Ontario, Canada: Evidence from tomography and shear wave splitting. Journal of Geophysical Research: Solid Earth, 112 (B7), 20 pp.

GAPAIS, D. – CAGNARD, F. – GUEYDAN, F. – BARBEY, P. – BALLEVRE, M., 2009 – Mountain building and exhumation processes through time: inferences from nature and models. Terra Nova, 21 (3), pages 188-194.

GAUTHIER, M. – TRÉPANIER, S. – GARDOLL, S., 2007 – Metamorphic gradient: a Regional-Scale Area Selection Criterion for Gold in the Northeastern Superior Province, Eastern Canadian Shield. Society of Economic Geologists Newsletter, 69, pages 10-15.

GIGON, J. – GOUTIER, J., 2017 – Géologie de la région du lac Richardie, municipalité d'Eeyou Istchee Baie-James. Report RG 2016-04, Ministère des Ressources naturelles du Québec, 43 pp.

GOUTIER, J. – DOUCET, P. – DION, C. – BEAUSOLEIL, C. – DAVID, J. – PARENT, M. – DION, D.-J., 1998 – Géologie de la région du lac Kowskatehkakmow (33F/06). Ministère des Ressources naturelles, Québec, RG 98-16, 48 pp.

GOUTIER, J. – DION, C. – DAVID., J. – DION, D.-J., 1999a – Géologie de la région de la passe Shimusuminu et du lac Vion (33F/11 et 33F/12). Ministère des Ressources naturelles, Québec, RG 98-17, 41 pp.

GOUTIER, J. – DION, C. – LAFRANCE, I. – DAVID, J. – PARENT, M. – DION, D., 1999b – Géologie de la région des lacs Langelier et Threefold (SNRC 33F/03 et 33F/04) - RG 98-18, Ministère des Ressources naturelles et de la Faune, Québec, 52 pp.

GOUTIER, J. – DION, C. – OUELLET, M.-C. – DAVID, J. – PARENT, M., 2000 – Géologie de la région des lacs Guillaumat et Sakami (SRNC 33F/02 et 33F/07). Report RG 99-15, Ministère des Ressources naturelles du Québec, 37 pp.

GOUTIER, J. – DION, C. – OUELLET, M.-C. – DAVIS, D. W. –DAVID, J. – PARENT, M., 2002 – Géologie de la région du lac Guyer (33G/05, 33G/06 et 33G/11). Report RG 2001-15, Ministère des Ressources naturelles du Québec, 54 pp.

GOUTIER, J. – DION, C. – OUELLET, M.-C. – MERCIER-LANGEVIN, P. – DAVIS, D. W., 2001 – Géologie de la Colline Masson, de la passe Awapakamich, de la Baie Carbillet et de la passe Pikwahipanan (SRNC 33F/09, 33F/10, 33F/15 et 33F/16). Report RG 2000-10, Ministère des Ressources naturelles du Québec, 67 pp.

HAMMOUCHE, H. – BURNIAUX, P. – KHARIS, A.-A., 2017 – Géologie de la région du lac des Vœux (SNRC 33H10, 33H15 et 33H16), Eeyou Istchee Baie-James. Report RG 2016-01, Ministère des Ressources naturelles du Québec, 37 pp.

HANES, R. – HUOT, F. – CLEVEN, N.R – GOUTIER, J. – BEAUDOIN, G. – GUILMETTE C., 2017 – Orogenic gold veins related to transpressional shear zones along the north-western contact of the La Grande and Opinaca subprovinces, Eeyou Istchee James Bay, Québec, Canada. Proceedings of the 14th SGA Biennal Meeting, 20-23 August 2017, Québec City, Canada. pages 39-42.

HARRIS, L.B. – BÉDARD, J.H., 2014 – Crustal evolution and deformation in a non-plate-tectonic Archaean Earth: Comparisons with Venus. *In*: Evolution of Archean Crust and Early Life. Editors: Y Dilek and H. Furnes; Modern Approaches in Solid Earth Sciences volume 7, Springer, Dordrecht, pages 215-291.

HARRIS, L.B. – KOYI, H.A., 2003 – Centrifuge modelling of folding in high-grade rocks during rifting. Journal of Structural Geology, 25 (2), pages 291-305.

HARRIS, L.B. – KOYI, H.A. – FOSSEN, H., 2002 – Mechanisms for folding of high-grade rocks in extensional tectonic settings. Earth-Science Reviews, 59 (1-4), pages 163-210.

HARRIS, N.B.W. – GOODWIN, A.M., 1976 – Archean rocks from the eastern Lac Seul region of the English River Gneiss Belt, northwestern Ontario, part 1. Petrology, chemistry, and metamorphism. Canadian Journal of Earth Sciences, 13 (9), pages 1201-1211.

HOULÉ, M.G. – GOUTIER, J. – SAPPIN, A.-A. – MCNICOLL, V.J., 2015 – Regional characterization of ultramafic to mafic intrusions in the La Grande Riviére and Eastmain domains, Superior Province, Quebec. Targeted Geoscience Initiative 4: Canadian nickel-copper-platinum group elements-chromium ore systems – fertility, pathfinders, new and revised models, Geological Survey of Canada, Open File 7856, pages 125–137.

JEKELI, C. – ERKAN, K. – HUANG, O., 2010 – Gravity vs pseudo-Gravity: a comparison based on magnetic and gravity gradient measurements. Gravity, Geoid and Earth Observation. Editor: S.P. Mertikas, Springer, International Association of Geodesy Symposia, volume 135, pages 123-127.

JIANG, D., 2014 – Structural geology meets micromechanics: A self-consistent model for the multiscale deformation and fabric development in Earth's ductile lithosphere. Journal of Structural Geology, 68, pages 247-272.

KERRICH, R. – FENG, R., 1992 – Archean geodynamics and the Abitibi-Pontiac collision: implications for advection of fluids at transpressive collisional boundaries and the origin of giant quartz vein systems. Earth-Science Reviews, 32 (1-2), pages 33-60.

KEHLENBECK, M.M., 1976 – Nature of the Quetico–Wabigoon boundary in the de Courcey–Smiley Lakes area, northwestern Ontario. Canadian Journal of Earth Sciences, 13 (6), pages 737-748.

LECLERC, F. – HARRIS, L.B. – BÉDARD, J.H. – VAN BREEMEN, O. – GOULET, N., 2012 – Structural and stratigraphic controls on magmatic, volcanogenic, and shear zone-hosted mineralization in the Chapais-Chibougamau Mining Camp, Northeastern Abitibi, Canada. Economic Geology, 107 (5), pages 963–989.

LEONOV, M.G., 2008 – Lateral Protrusions in the Structure of the Earth's Lithosphere. Geotectonics, 42 (5), pages 327-356.

MAURICE, C. – DAVID, J. – O'NEIL, J. – FRANCIS, D., 2009 – Age and tectonic implications of Paleoproterozoic mafic dyke swarms for the origin of 2.2 Ga enriched lithosphere beneath the Ungava Peninsula, Canada. Precambrian Research, 174 (1-2), pages 163-180.

MERCIER-LANGEVIN, P. – DAIGNEAULT, R. – GOUTIER, J. – DION, C. – ARCHER, P., 2012 – Geology of the Archean Intrusion-Hosted La-Grande-Sud Au-Cu Prospect, La Grande Subprovince, Eeyou Istchee Baie-James region, Québec. Economic Geology, 107 (5), pages 935–962.

MILLER, H.G. – SINGH, V., 1994 – Potential field tilt – A new concept for location of potential field sources. Journal of Applied Geophysics, 32 (2-3), pages 213-217.

MORFIN, S. – SAWYER, E. W. – BANDYAYERA, D., 2013 – Large volumes of anatectic melt retained in granulite facies migmatites: An injection complex in northern Quebec. Lithos, 168, pages 200-218.

MOSER, D.E. – HEAMAN, L.M. – KROGH, T.E. – HANES, J.A., 1996 – Intracrustal extension of an Archean orogen revealed using single grain U Pb zircon geochronology. Tectonics, 15 (5), pages 1093-1109.

NAIDU, P.S. – MATHEW, M.P., 1998 – Digital analysis of aeromagnetic maps: Detection of a fault. Journal of applied geophysics, 38 (3), pages 169-179.

PASSCHIER, C.W. – BROK, S.W.I. – GOOL, J.A.M. – MARKER, M. – MANATSCHAL, G., 1997 – A laterally constricted shear zone system—the Nordre Strømfjord steep belt, Nagssugtoqidian Orogen, W. Greenland. Terra Nova, 9 (5 6), pages 199-202.

PERCIVAL, J. A., 1989 – A regional perspective of the Quetico metasedimentary belt, Superior Province, Canada. Canadian Journal of Earth Sciences, 26 (4), pages 677-693.

PERCIVAL, J. – SANBORN-BARRIE, M. – SKULSKI, T. – STOTT, G. – HELMSTAEDT, H. – WHITE, D., 2006 – Tectonic evolution of the western Superior Province from NATMAP and Lithoprobe studies. Canadian Journal of Earth Sciences, 43 (7), pages 1085–1117.

PERCIVAL, J. A. – SKULSKI, T. – SANBORN-BARRIE, M. – STOTT, G. M. – LECLAIR, A. D. – CORKERY, M. T. – BOILY, M., 2012 – Geology and tectonic evolution of the Superior Province, Canada. Tectonic Styles in Canada: The Lithoprobe Perspective, Special Paper, 49, pages 321–378.

PIETTE-LAUZIÈRE, N. – GUILMETTE, C. – BOUVIER, A. – PERROUTY, S. – PILOTE, P. – GAILLARD, N. – LYPACZEWSKI, P. – LINNEN, R.L. – OLIVO, G.R., 2019 – The timing of prograde metamorphism in the Pontiac Subprovince, Superior craton; implications for Archean geodynamics and gold mineralization. Precambrian Research, 320, pages 111-136.

POLAT, A. – KERRICH, R. – WYMAN, D.A., 1998 – The late Archean Schreiber–Hemlo and White River–Dayohessarah greenstone belts, Superior Province: collages of oceanic plateaus, oceanic arcs, and subduction–accretion complexes. Tectonophysics, 289 (4), pages 295-326.

POULSEN, K. – CARD, K. – FRANKLIN, J., 1992 – Archean tectonic and metallogenic evolution of the Superior Province of the Canadian Shield. Precambrian Research, 58 (1), pages 25–54.

RAVENELLE, J. F. – DUBÉ, B. – MALO, M. – MCNICOLL, V. – NADEAU, L. – SIMONEAU, J., 2010 – Insights on the geology of the world-class Roberto gold deposit, Éléonore property, Baie-James area, Quebec. Geological Survey of Canada, Current Research 2010-1, 26 pp.

SALEM, A. – WILLIAMS, S. – FAIRHEAD, D. – SMITH, R. – RAVAT, D., 2007 – Interpretation of magnetic data using tilt-angle derivatives. Geophysics, 78 (1), pages 1-10.

SAPPIN, A. A. – GUILMETTE, C. – GOUTIER, J. – BEAUDOIN, G., 2018 – Geochemistry of Mesoarchean felsic to ultramafic volcanic rocks of the Lac Guyer area, La Grande Subprovince (Canada): Evidence for plume-related magmatism in a rift setting. Precambrian Research, 316, pages 83-102.

SCHULMANN, K. – LEXA, O. – ŠTÍPSKÁ, P. – RACEK, M. – TAJČMANOVÁ, L. – KONOPÁSEK, J. – EDEL, J.B. – PESCHLER, A. – LEHMANN, J., 2008 – Vertical extrusion and horizontal channel flow of orogenic lower crust: key exhumation mechanisms in large hot orogens? Journal of metamorphic Geology, 26 (2), pages 273-297.

SIGÉOM, 2018: Système d'information géominière du québec, carte interactive. Ministère de l'Énergie et des Ressources naturelles du Québec, http://sigeom.mines.gouv.qc.ca.

SIMARD, M. – PARENT, M. – DAVID, J. – SHARMA, K.N.M., 2003 – Géologie de la région de la rivière Innuksuac (34K et 34 L). Ministère des Ressources naturelles, Québec, RG 2002-10, 43 pp.

SPECTOR, A. – F. GRANT, 1970 – Statistical models for interpreting aeromagnetic data. Geophysics, 35 (2), pages 293–302.

STOTT, G.M. – CORKERY, M.T. – PERCIVAL, J.A. – SIMARD, M. – GOUTIER, J., 2010 – A revised terrane subdivision of the Superior Province. Ontario Geological Survey, Open File Report 6260, pages 20-1 to 20-10.

TAYLOR, M. – YIN, A. – RYERSON, F.J. – KAPP, P. – DING, L., 2003 – Conjugate strike slip faulting along the Bangong Nujiang suture zone accommodates coeval east west extension and north south shortening in the interior of the Tibetan Plateau. Tectonics, 22 (4), 16 pp.

TIKOFF, B. – GREENE, D., 1997 – Stretching lineations in transpressional shear zones: an example from the Sierra Nevada Batholith, California. Journal of Structural Geology, 19 (1), pages 29-39.

WHITNEY, D.L. – TEYSSIER, C. – VANDERHAEGHE, O., 2004 – Gneiss domes and crustal flow, in Whitney, D.L, Teyssier, C., and Siddoway, C.S., Gneiss domes in orogeny: Boulder, Colorado, Geological Society of America Special Paper 380, pages 1-19.

WIJNS, C. – PEREZ, C. – KOWALCZYK, P., 2005 – Theta map: Edge detection in magnetic data. Geophysics, 70 (4), L39-L43.

Figures

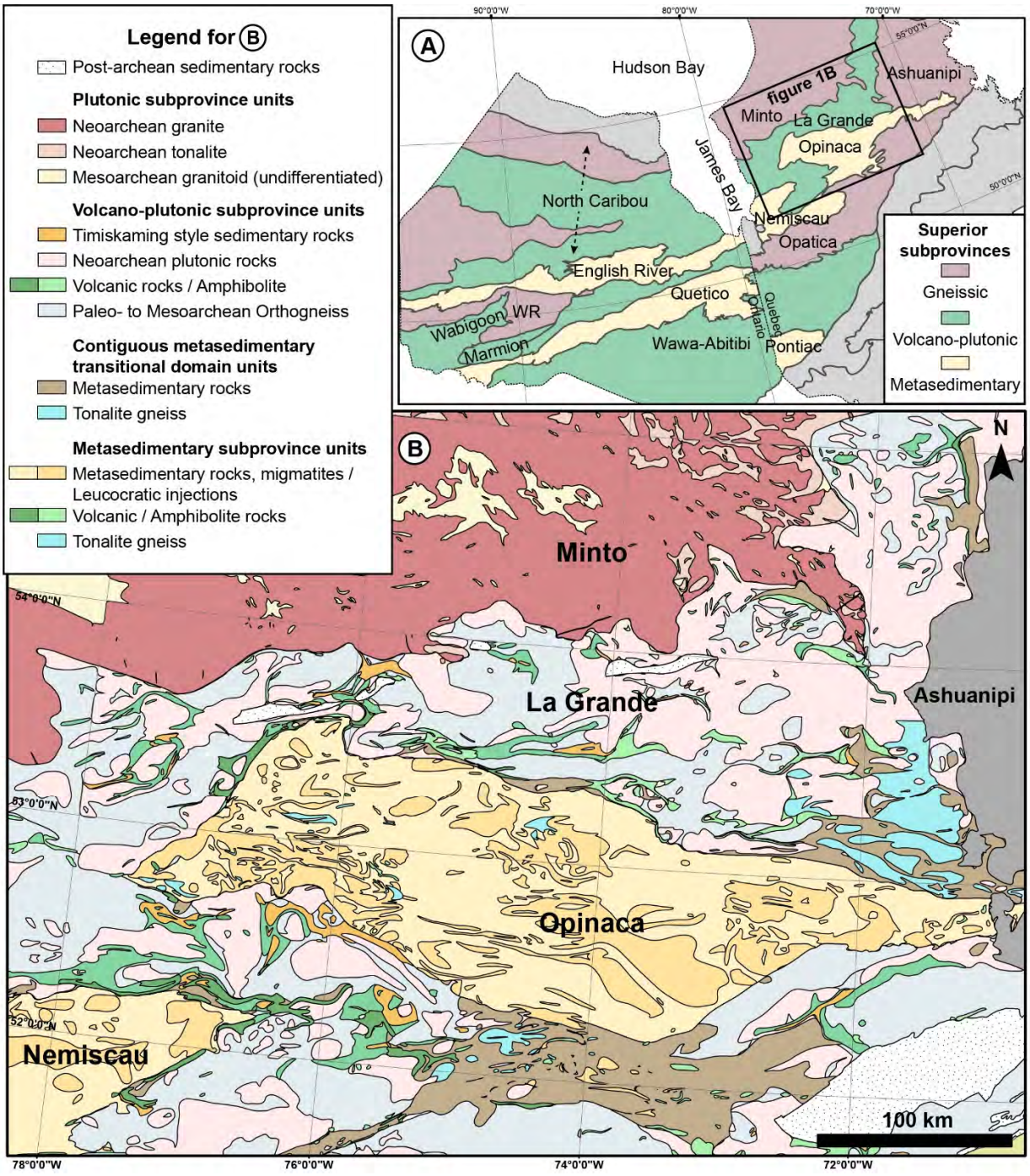

Figure 1: A) Subprovinces of the Superior province. WR – Winnipeg River B) Lithotectonic map of the Eeyou Istchee Baie-James region of the Québec Superior province.

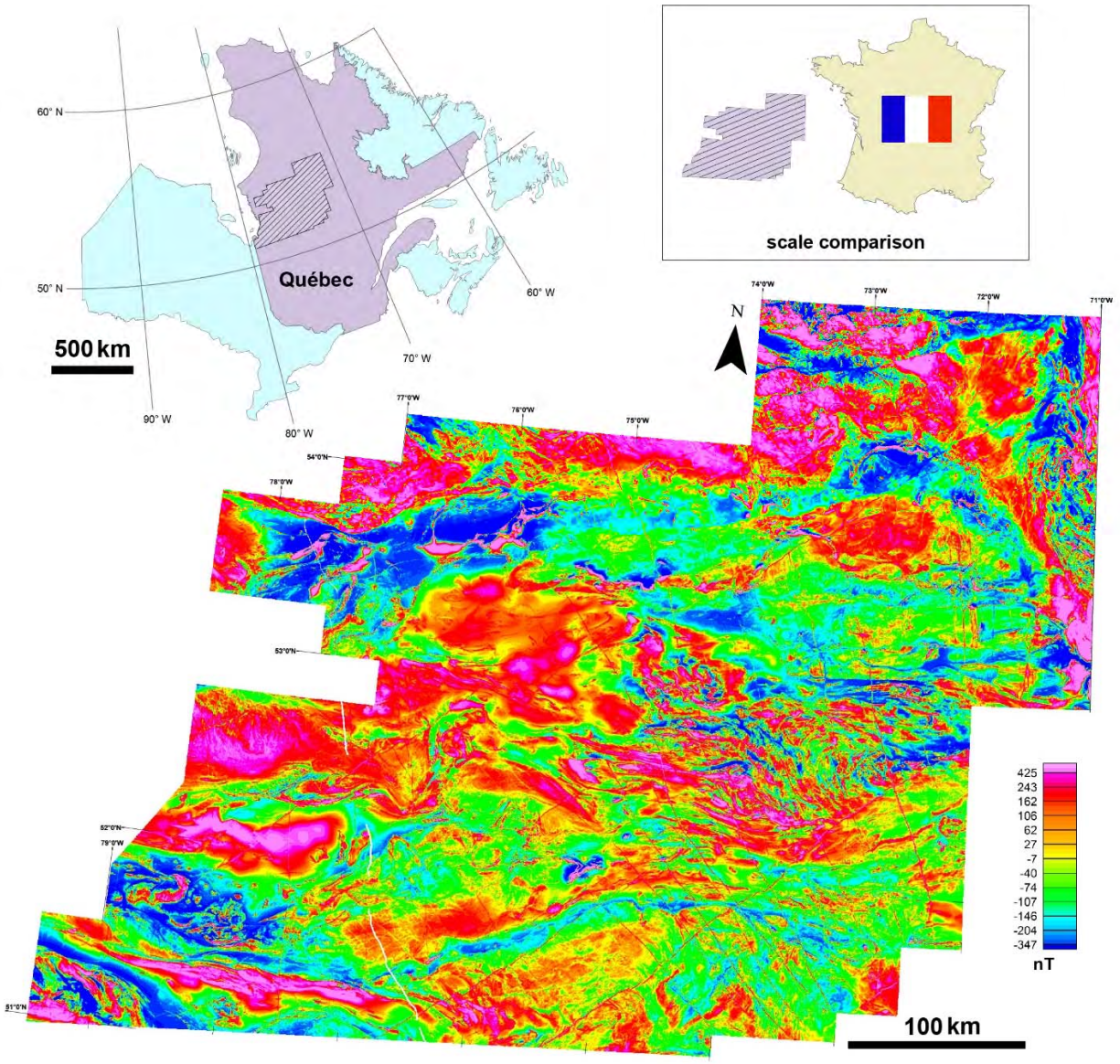

Figure 2: Total magnetic intensity image of the high-resolution aeromagnetic survey used in this study. The data set is a compilation of surveys completed from 2007-2011 (D'amours, 2011) Inset: Location of the compiled survey within the province of Québec, Canada. A scale comparison is made between the size of the survey region and the size of France.

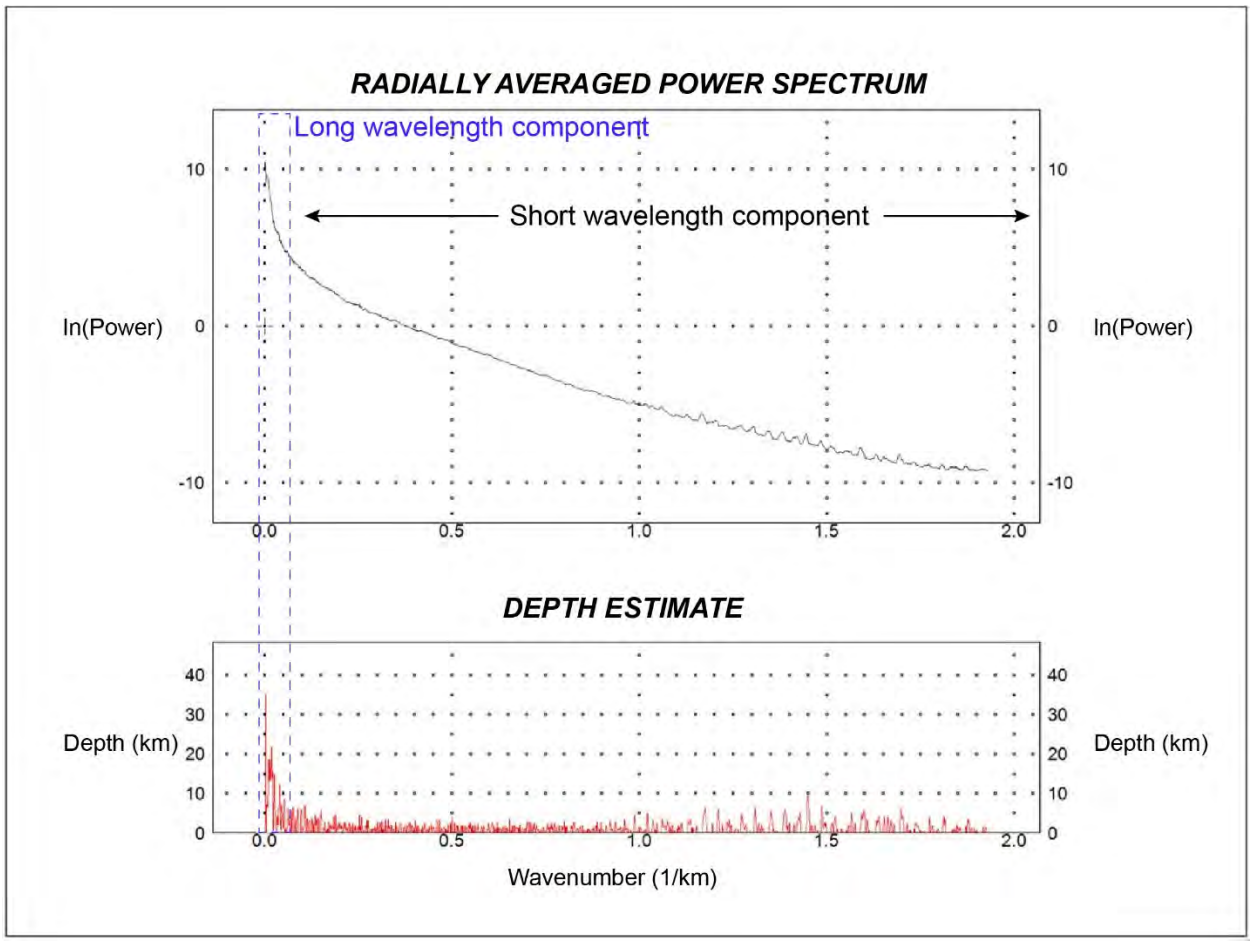

Figure 3: The change in slope within the radially averaged power spectrum (top) identifies the long wavelength component of the aeromagnetic data. This correlates to a signal source between estimated 8-35 km of depth (bottom). The remainder of the signal is the short wavelength component, or "residuals" (top), and correlate to a signal source estimated to be less than 8 km of depth (bottom). This figure was produced in Geosoft's Oasis Montaj.

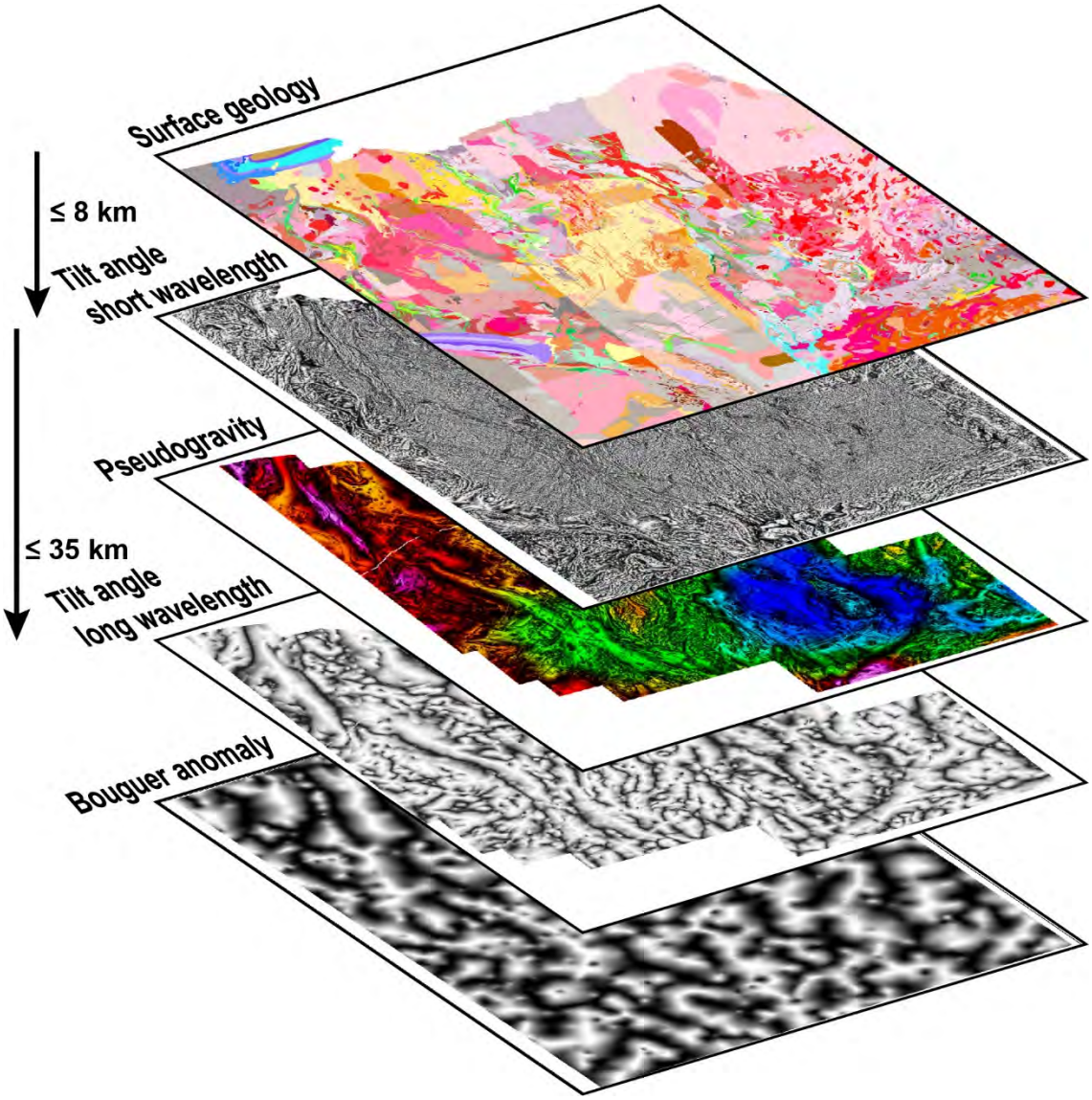

Figure 4: Schematic relationships of different datasets to depth. Surface geology from SIGÉOM (2018). Tilt angle short and long wavelength, and pseudogravity, are images based on the geophysical survey in this report. The Bouguer anomaly map is from Natural Resources Canada gravity data. The depths indicated are approximate and relative to the short and long wavelength maps only.

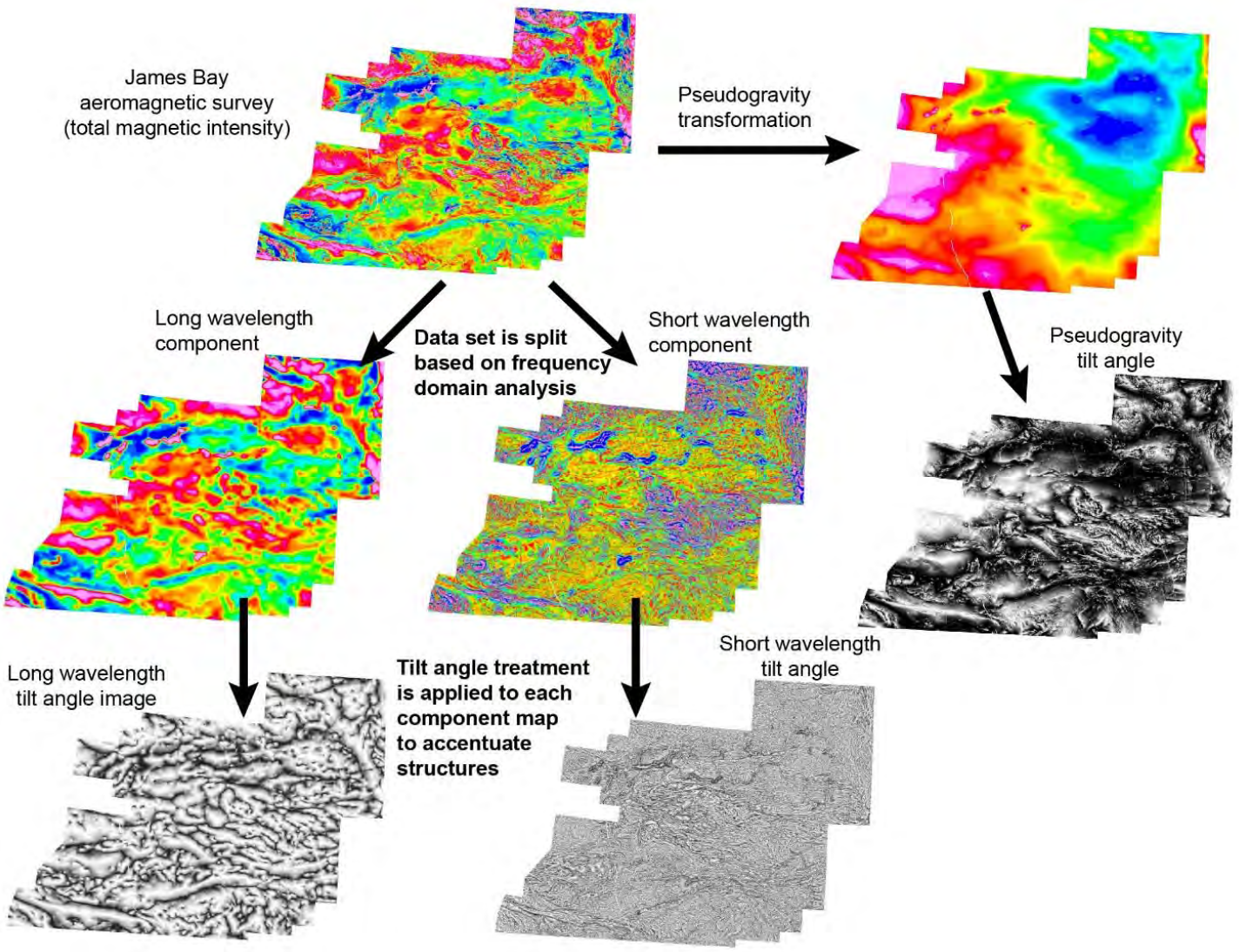

Figure 5: Workflow of frequency domain analysis and treatments applied to the Baie-James aeromagnetic survey data showing the respective images they produce.

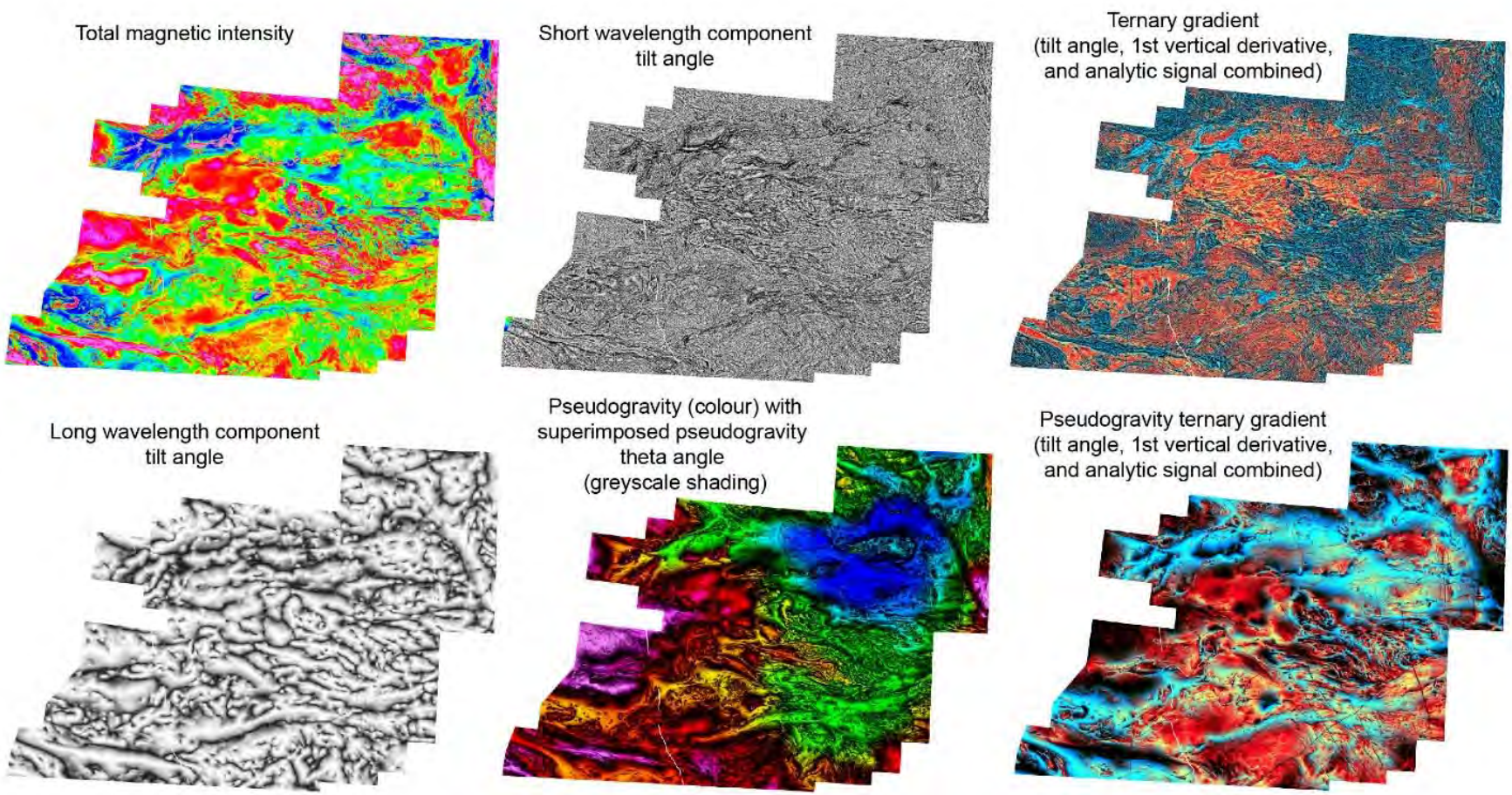

Figure 6: All base treated geophysical images used for figures in this report. Some figures use overlain composite images of these treatments.

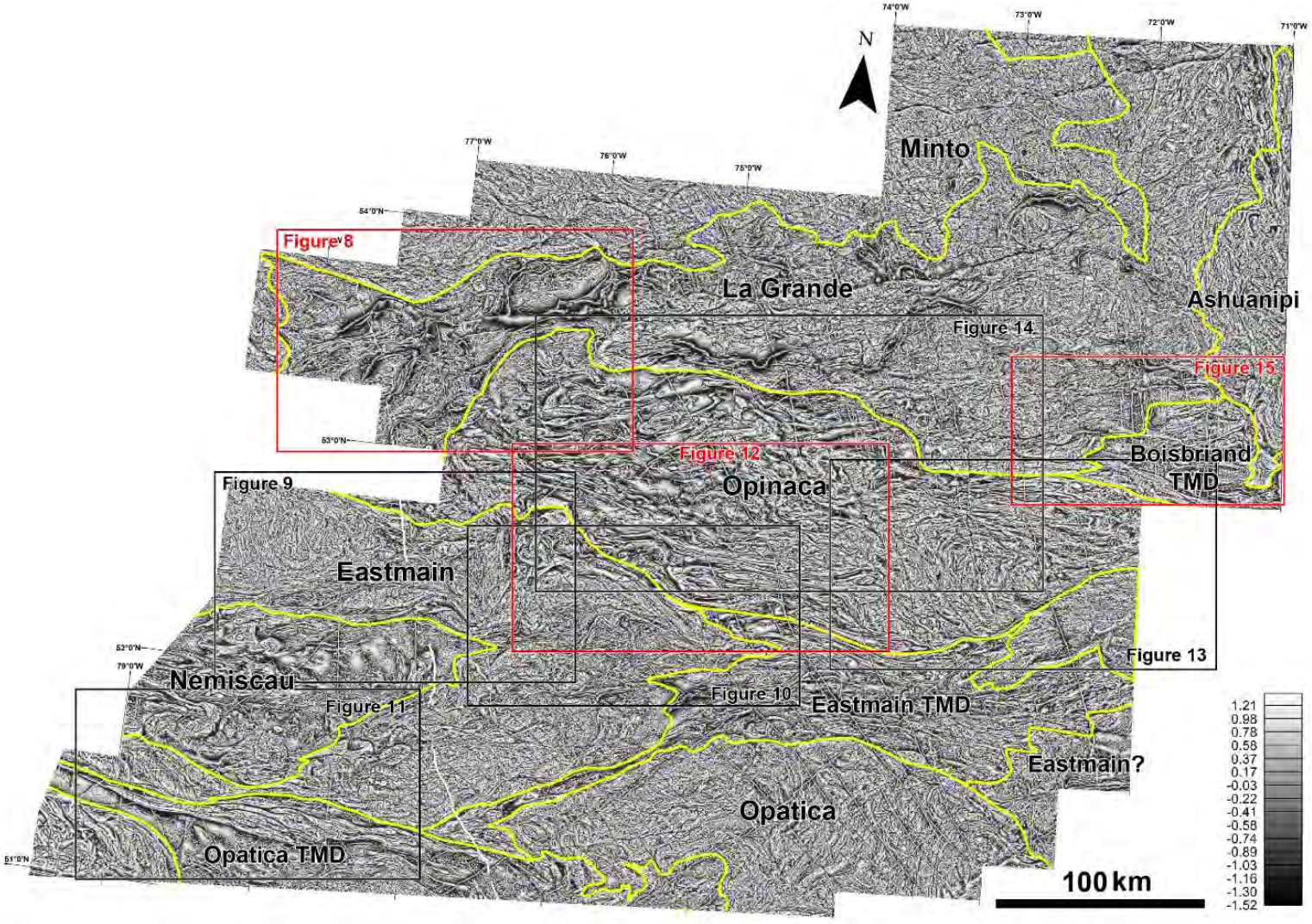

Figure 7: Short wavelength component tilt angle image provides excellent visual textures for defining megascopic penetrative ductile deformation structures, such as folds, boudinage, σ- and δ-type shear structures, and C-S shear fabrics. Examples are detailed in Figures 8-15, for which locations are indicated. Modified subprovince boundaries, including newly defined transitional metasedimentary domains (TMDs) are provided in yellow. The Eastmain domain, defined here, is part of the La Grande subprovince.

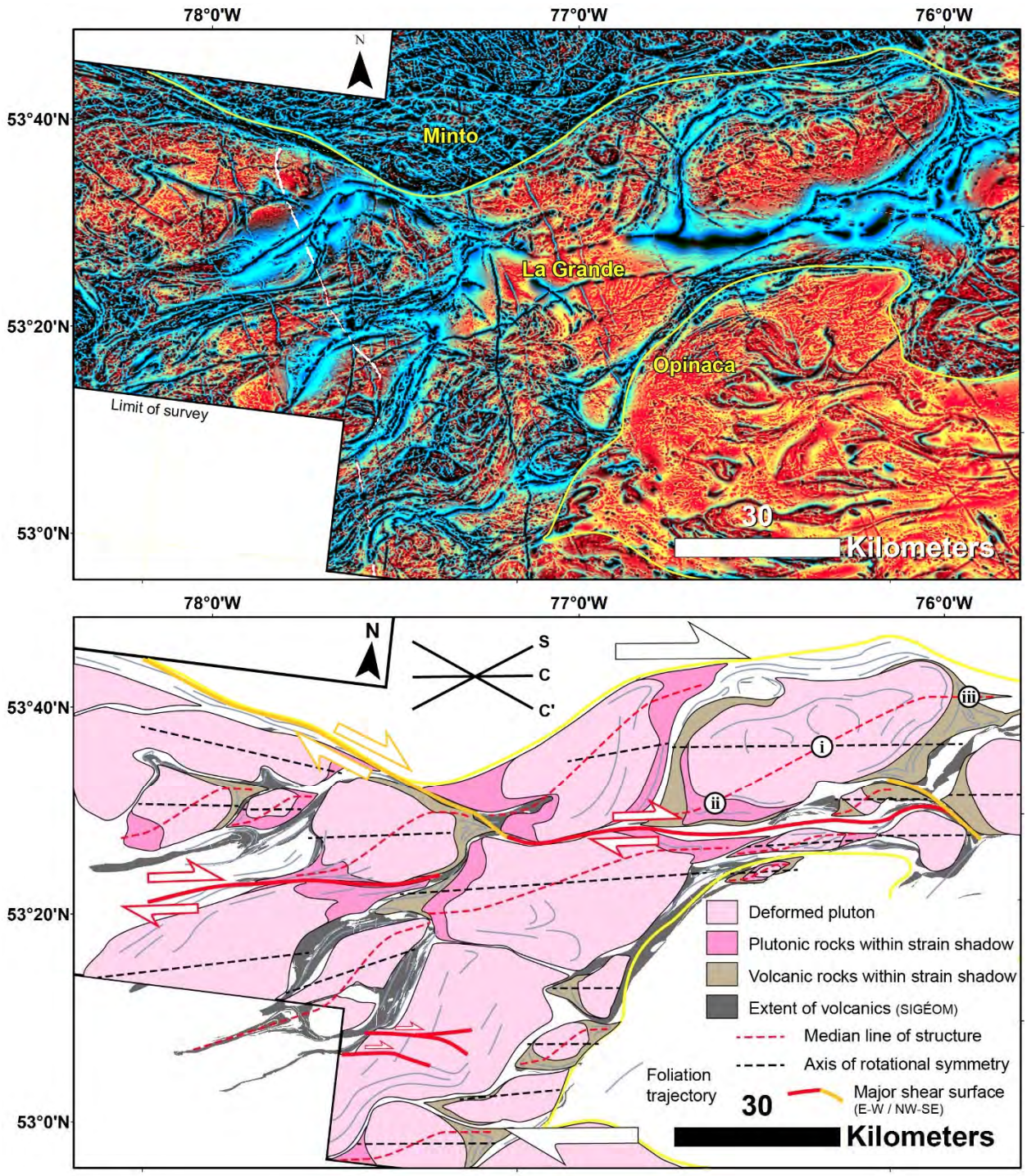

Figure 8: Schematic diagram of σ-type shear structures in volcano-plutonic assemblages in the western La Grande subprovince, interpreted from the ternary gradient image at top. The approximate 30° inclination of the median lines for each structure to their respective axis of rotational symmetry indicate E-W dextral shearing. This is consistent with where foliation trajectories are sheared along major shear surfaces. Markers i-iii indicate structures referred to in the text. Units irrelevant to the structural interpretation have been left blank in the schematic diagram.

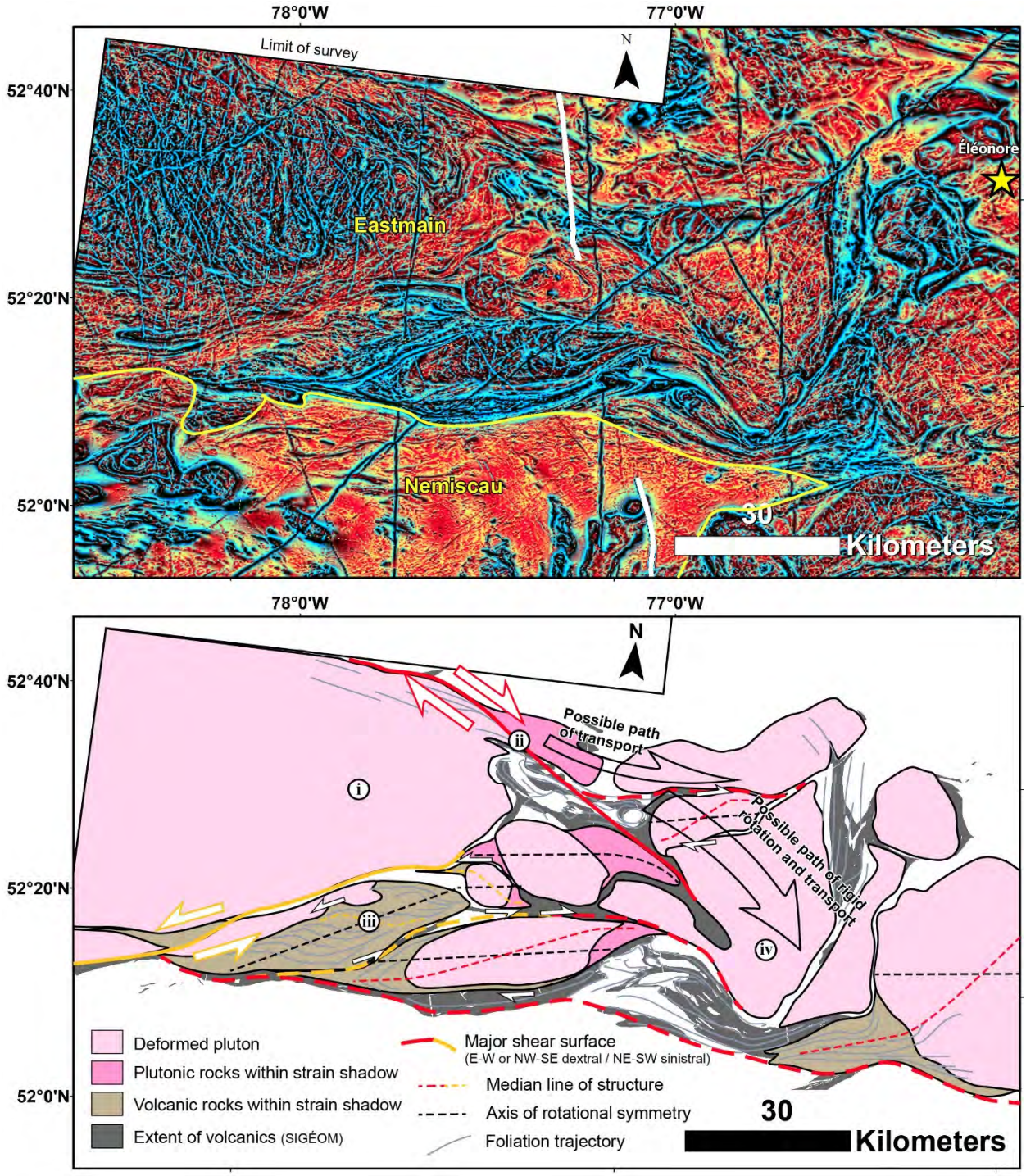

Figure 9: Schematic diagram of large-scale crustal block disaggregation and σ-type and S-C shear structures in volcano-plutonic assemblages in the western Eastmain domain, interpreted from the ternary gradient image at top. The approximate 30° inclination of the median lines for each structure to their respective axis of rotational symmetry indicate E-W dextral shearing, with synthetic NW-SE dextral and antithetic NE-SW sinistral conjugate shearing along the margins of the western boudinaged crustal block. Markers i-iv indicate structures referred to in the text. Units irrelevant to the structural interpretation have been left blank in the schematic diagram.

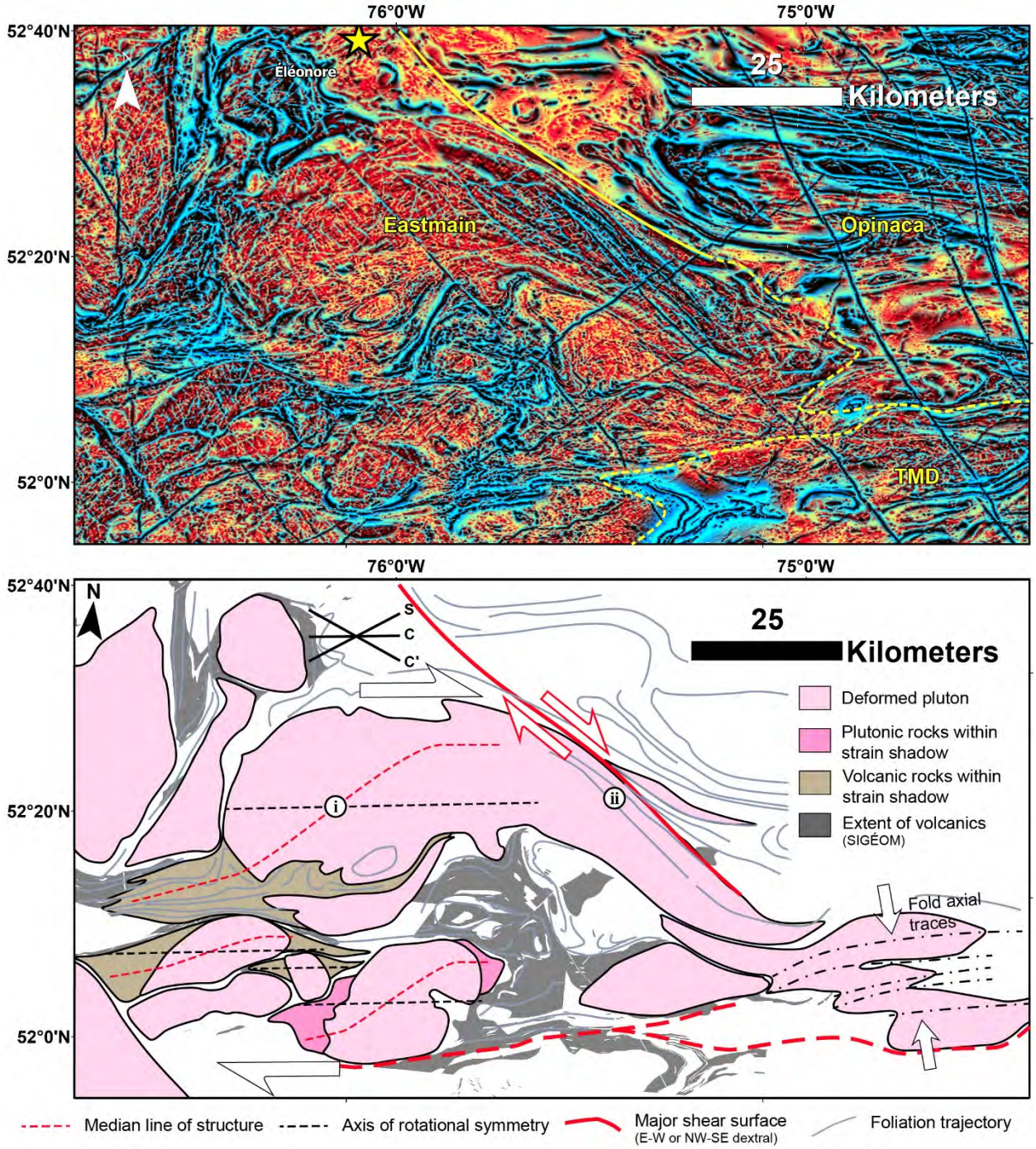

Figure 10: Schematic diagram of σ- and δ-type shear structures in volcano-plutonic assemblages in the central Eastmain domain, interpreted from the ternary gradient image at top. The approximate 30° inclination of the median lines for each structure to their respective axis of rotational symmetry indicate E-W dextral shearing. A deformed pluton abutting the subprovince-bounding NW-SE shear zone forms a δ-type dextral shear structure. Markers i and ii indicate structures referred to in the text. Units irrelevant to the structural interpretation have been left blank in the schematic diagram.

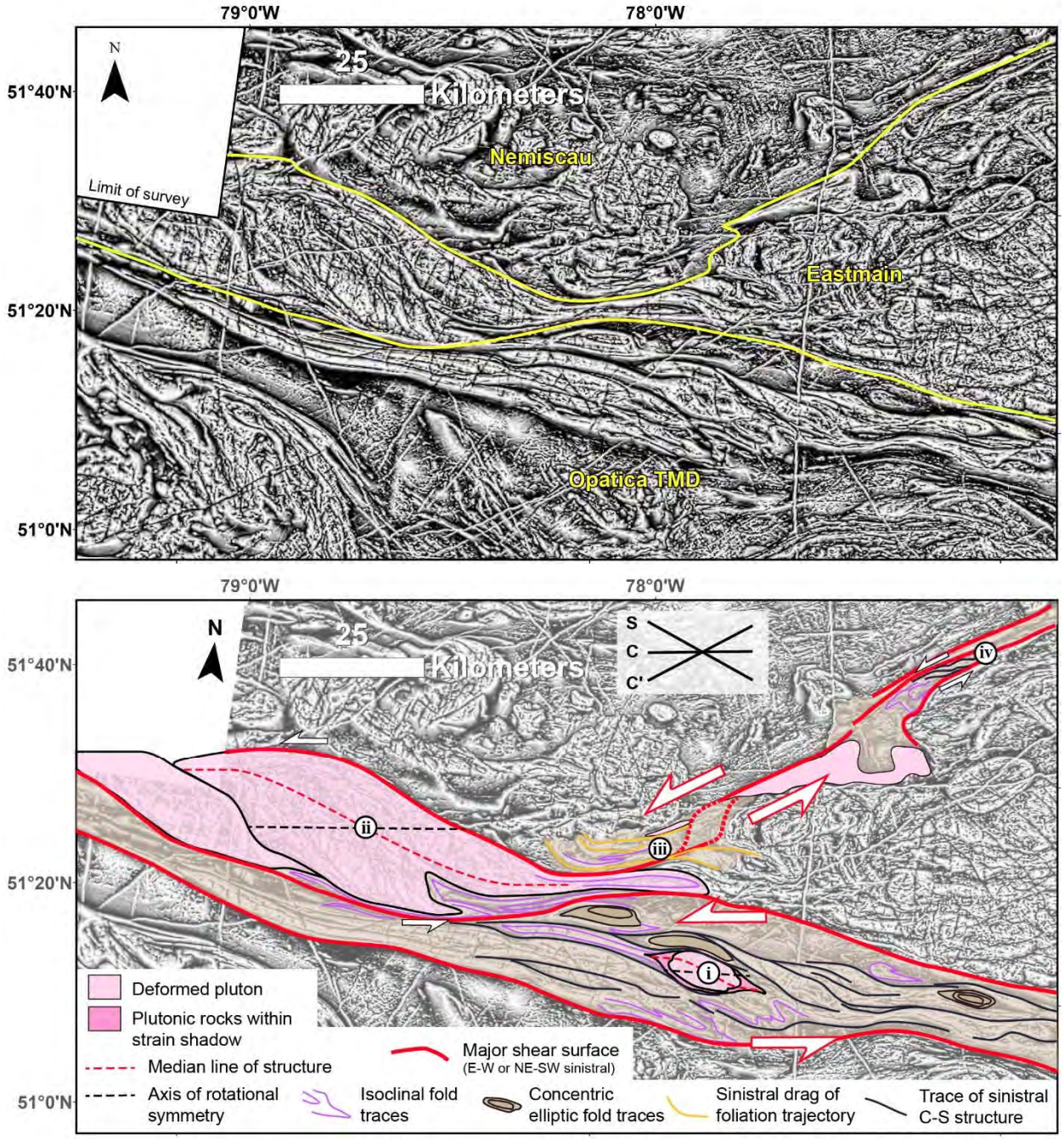

Figure 11: Schematic diagram of σ-type and S-C shear structures in metasedimentary and plutonic units in the Nemiscau, Eastmain domain, and Opatica TMD boundary, interpreted from the tilt angle short wavelength image at top. The approximate 30° inclination of the median lines for σ-type structures to their respective axis of rotational symmetry indicate E-W sinistral shearing. Synthetic NE-SW sinistral shearing of the foliation trajectory suggests shearing and boudinage of the Eastmain domain termination along the boundary with the Nemiscau. Markers i-iv indicate structures referred to in the text..

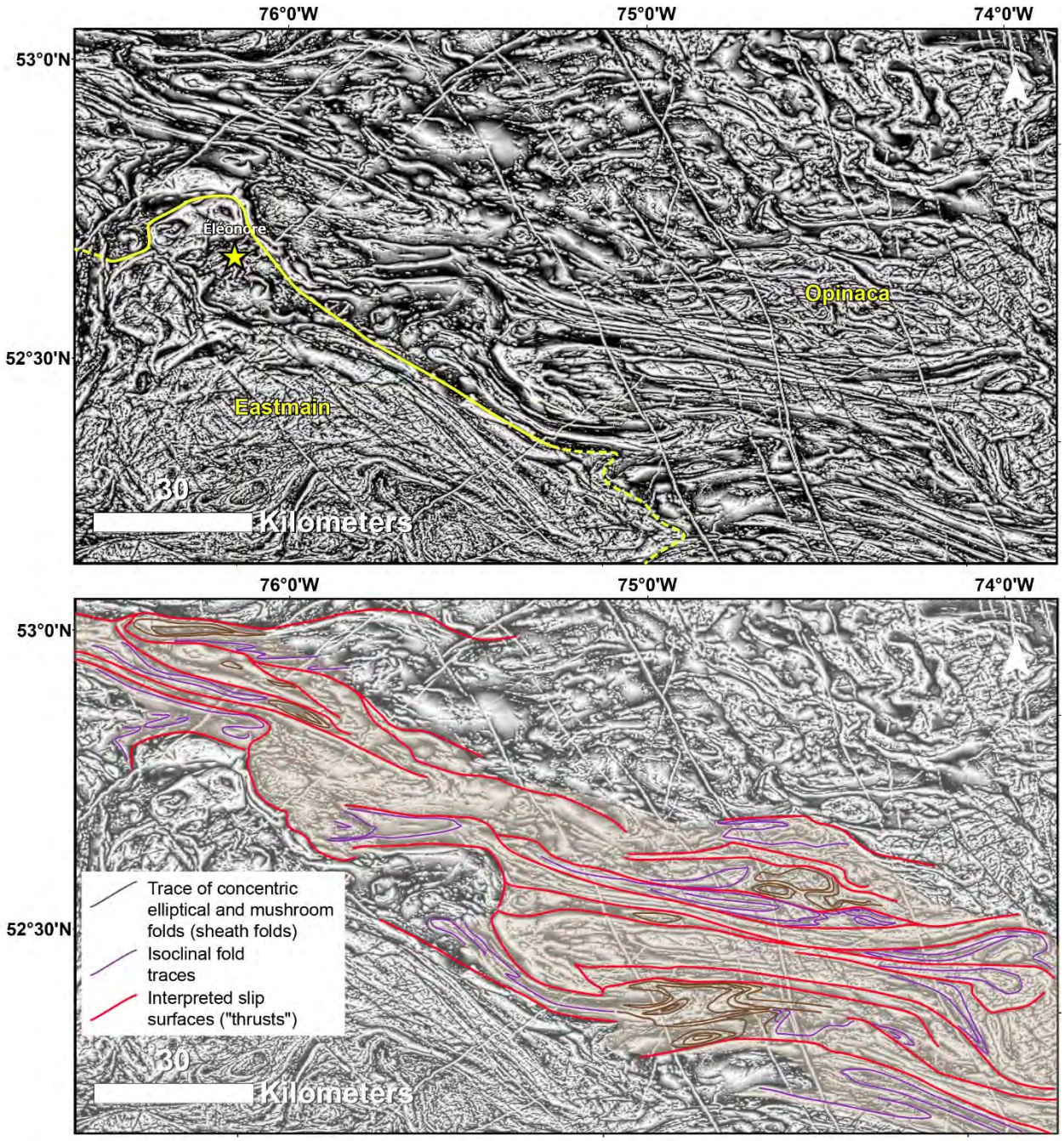

Figure 12: Schematic diagram of cascading folds of slip or shear surfaces, likely thrusts, within the Opinaca subprovince, interpreted from the tilt angle short wavelength image at top. Rootless isoclinal folds, concentric elliptical folds, and mushroom folds abutting or sandwiched between slip surfaces are shear zone structures. The lack of kinematic indicators visible in plan view, and the high aspect ratio of the elliptical folds, are indicative of shear in a thrust sense, hence this is a zone of localized convergent deformation.

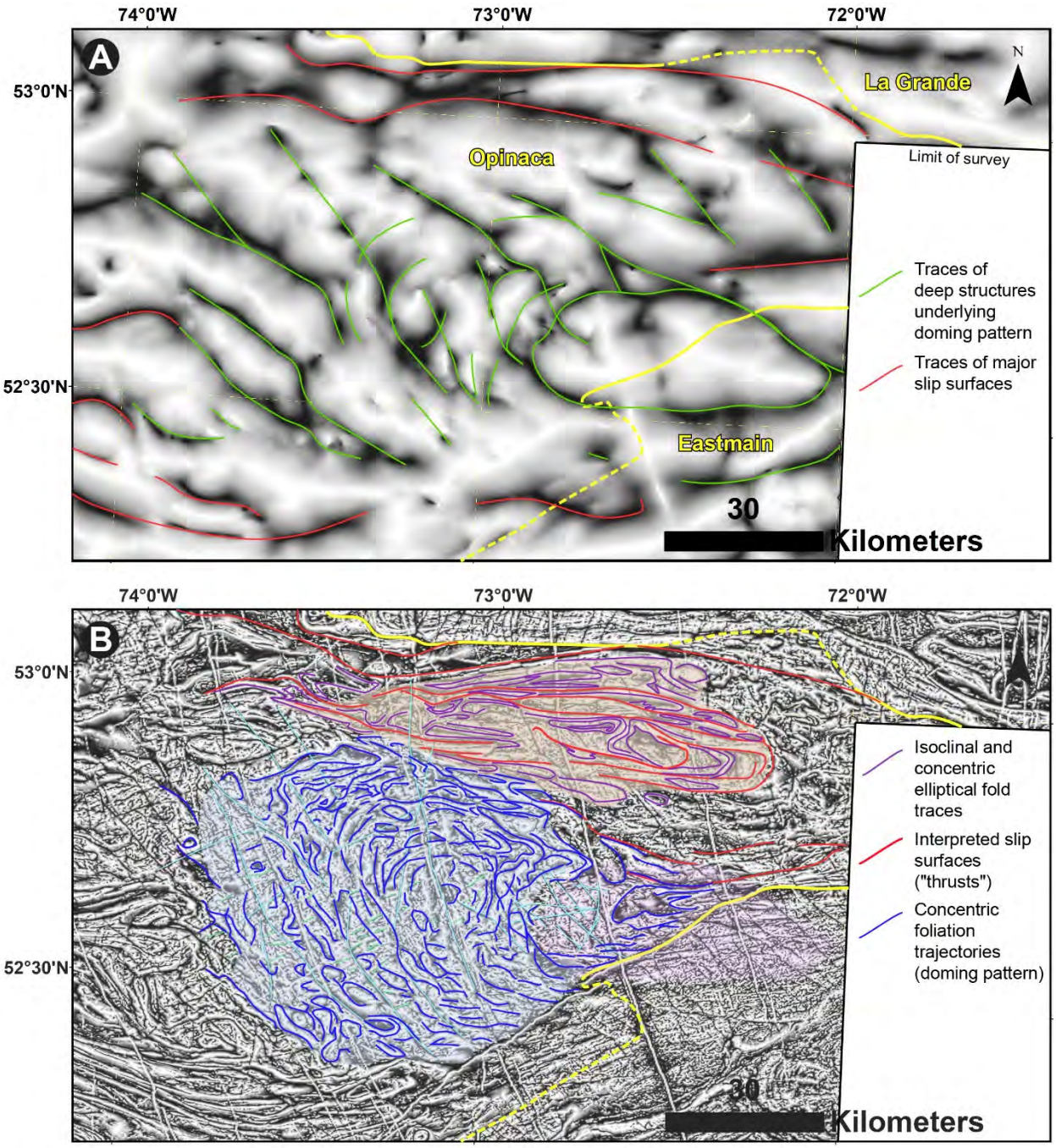

Figure 13: A) Schematic diagram of linear, regularly spaced, parallel to slightly fanned out, deep structures in the Opinaca, interpreted from the underlying tilt angle short wavelength image. These structures may indicate the basement of the Opinaca underwent extension during creation of structures in the overlying paragneiss. B) Schematic diagram of concentric foliation trajectories in the Opinaca are near circular at the centre of the structure, interpreted from the underlying tilt angle short wavelength image. The even aspect ratio of its ellipticity is consistent with a gneissic dome structure. The structure borders a zone of convergent deformation to its north that hosts structures similar to those in Figure 12.

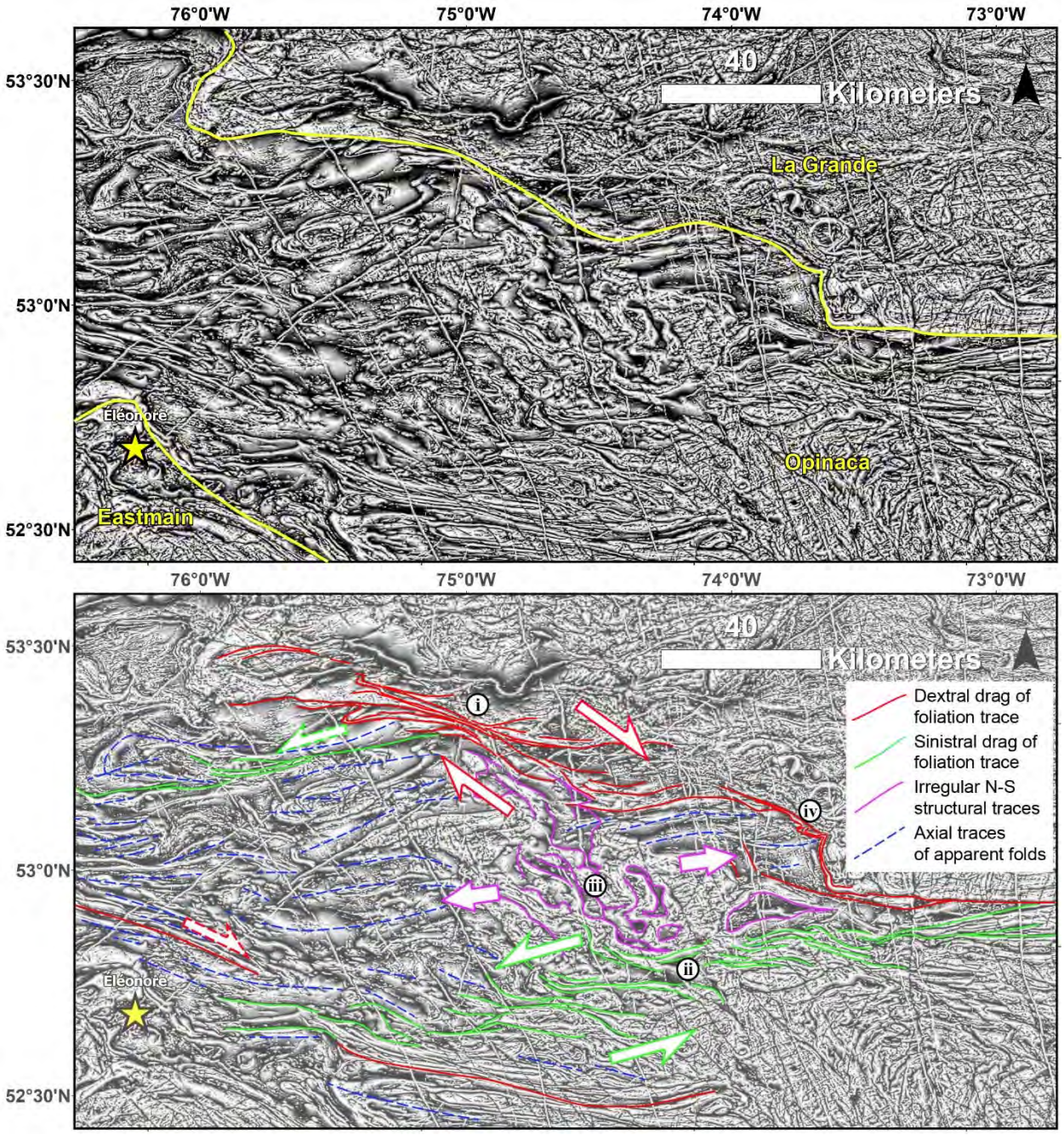

Figure 14: Schematic diagram of conjugate shear zones bounding a zone of E-W extension within the Opinaca subprovince, interpreted from the tilt angle short wavelength image at top. A NW-SE dextral shear zone, and NE-SW sinistral shear zone intersect without cross-cutting, indicating they formed contemporaneously. An irregular N-S oriented foliation marks cuts NE-SW oriented fold axial surface traces where the shear zones converge and is interpreted as an extensional zone exposing a horst of deep Opinaca material. Markers i-iv indicate structures referred to in the text.

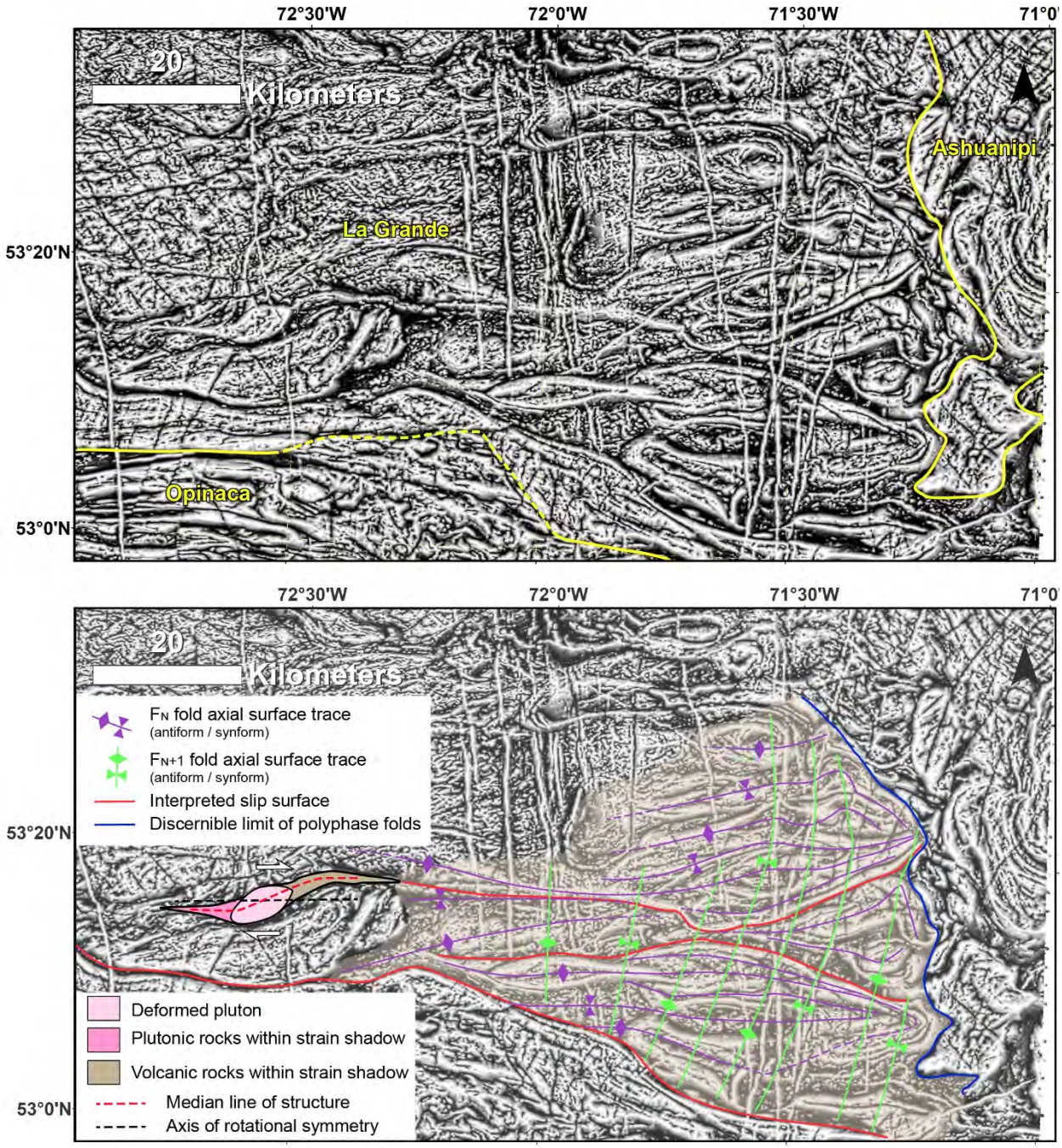

Figure 15: Schematic diagram of superposed fold structures in the Boisbriand TMD (eastern La Grande), interpreted from the tilt angle short wavelength image at top. The repetition of the elliptical fold traces throughout the shaded region, the lack of kinematic indicators, and the lack of intersection between slip surfaces and foliations suggest that this is a dome-and-basin fold superposition pattern, abutting the boundary with the Ashuanipi subprovince. Antiform and synform axial surface traces for each generation were estimated from the visible gradation patterns seen within the tilt angle image.

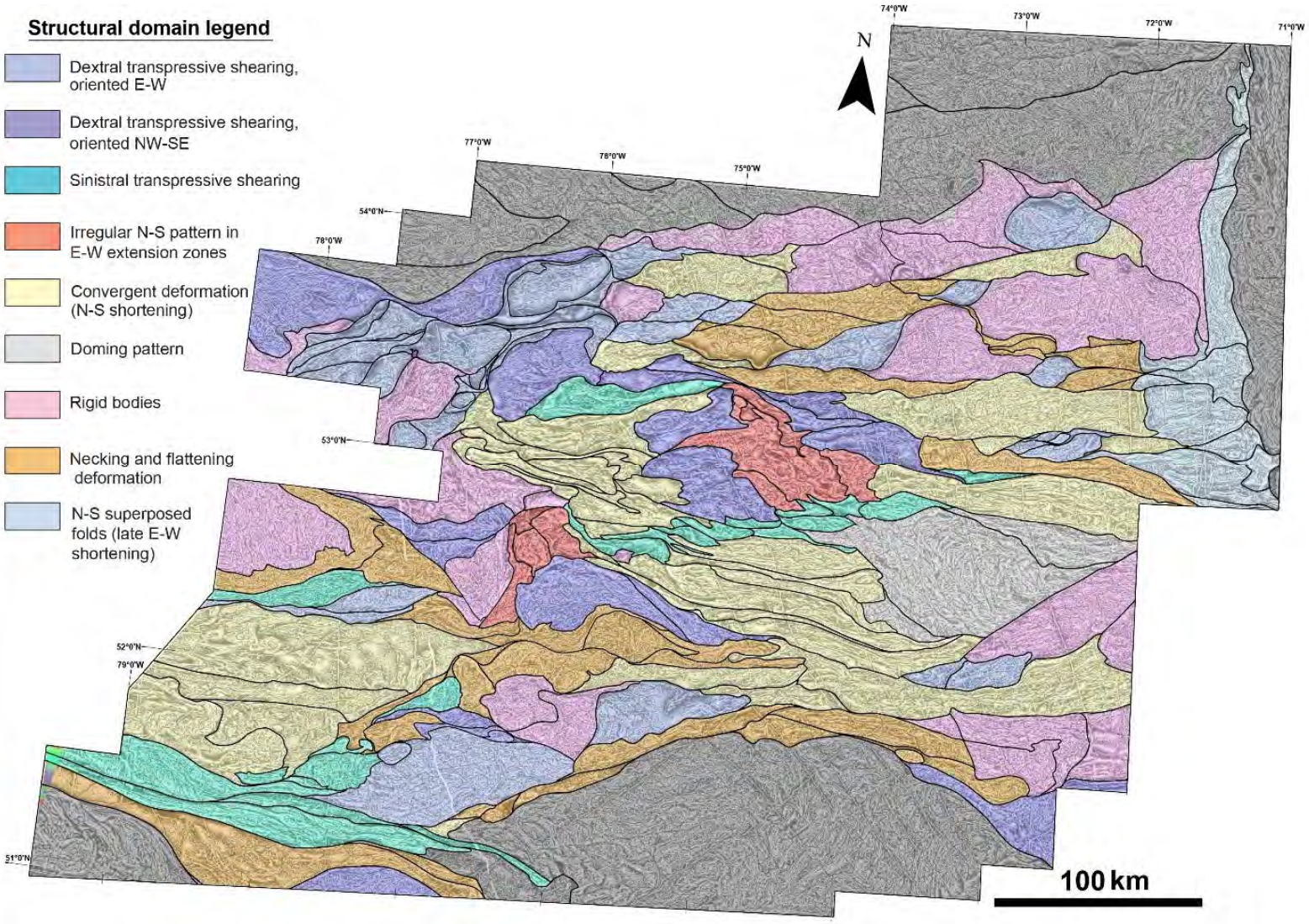

Figure 16: Structural domains interpreted from the short wavelength component tilt angle treated aeromagnetic map (underlying image). The Minto, Ashuanipi, and Opatica subprovinces (dark grey along edges) were not substantially covered by the aeromagnetic survey and were not analyzed for this report.

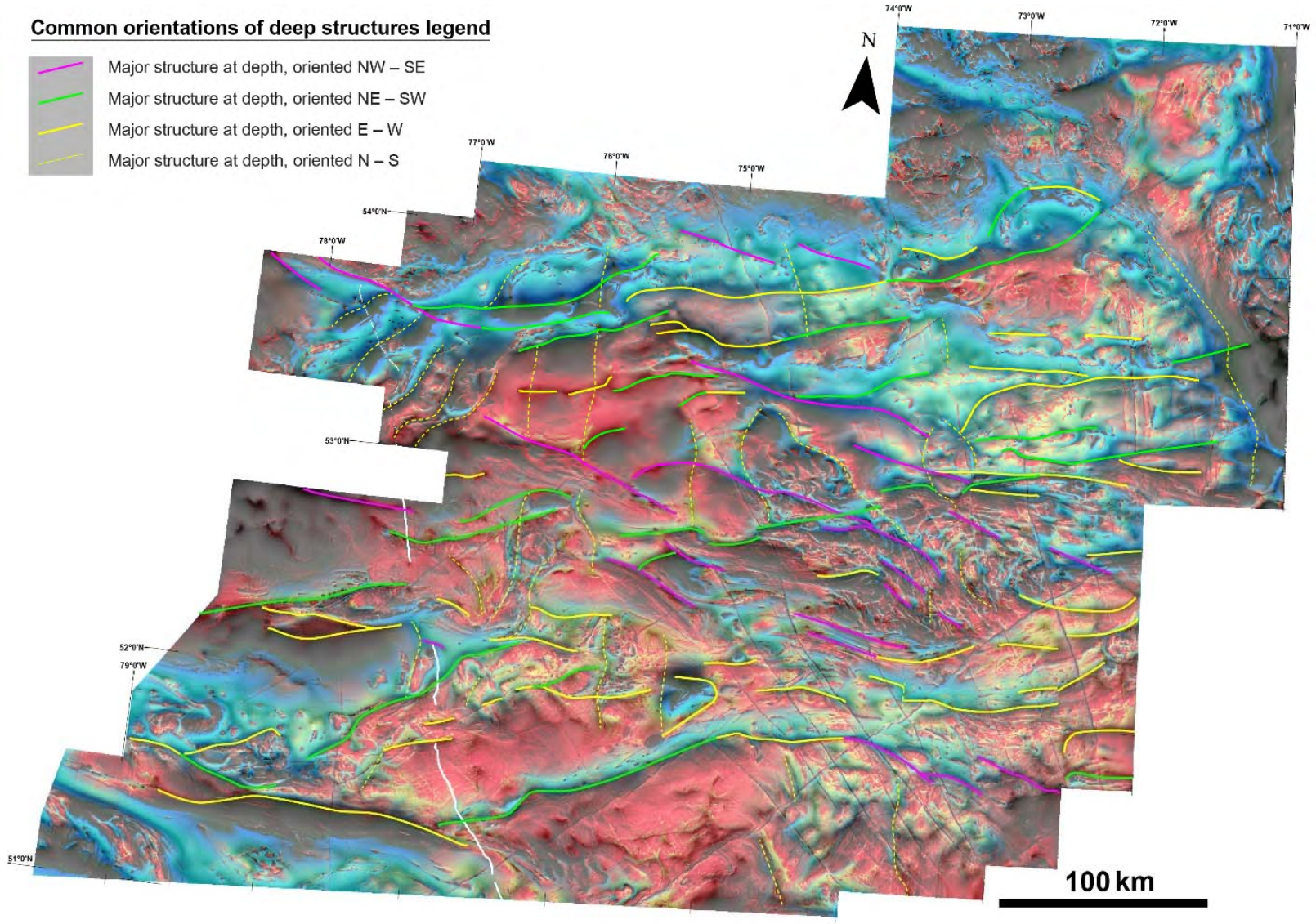

Figure 17: Significant structural orientations revealed from analysis of the deep components of the aeromagnetic survey. The underlying image is a composite of the pseudogravity ternary and the long wavelength component tilt angle images.

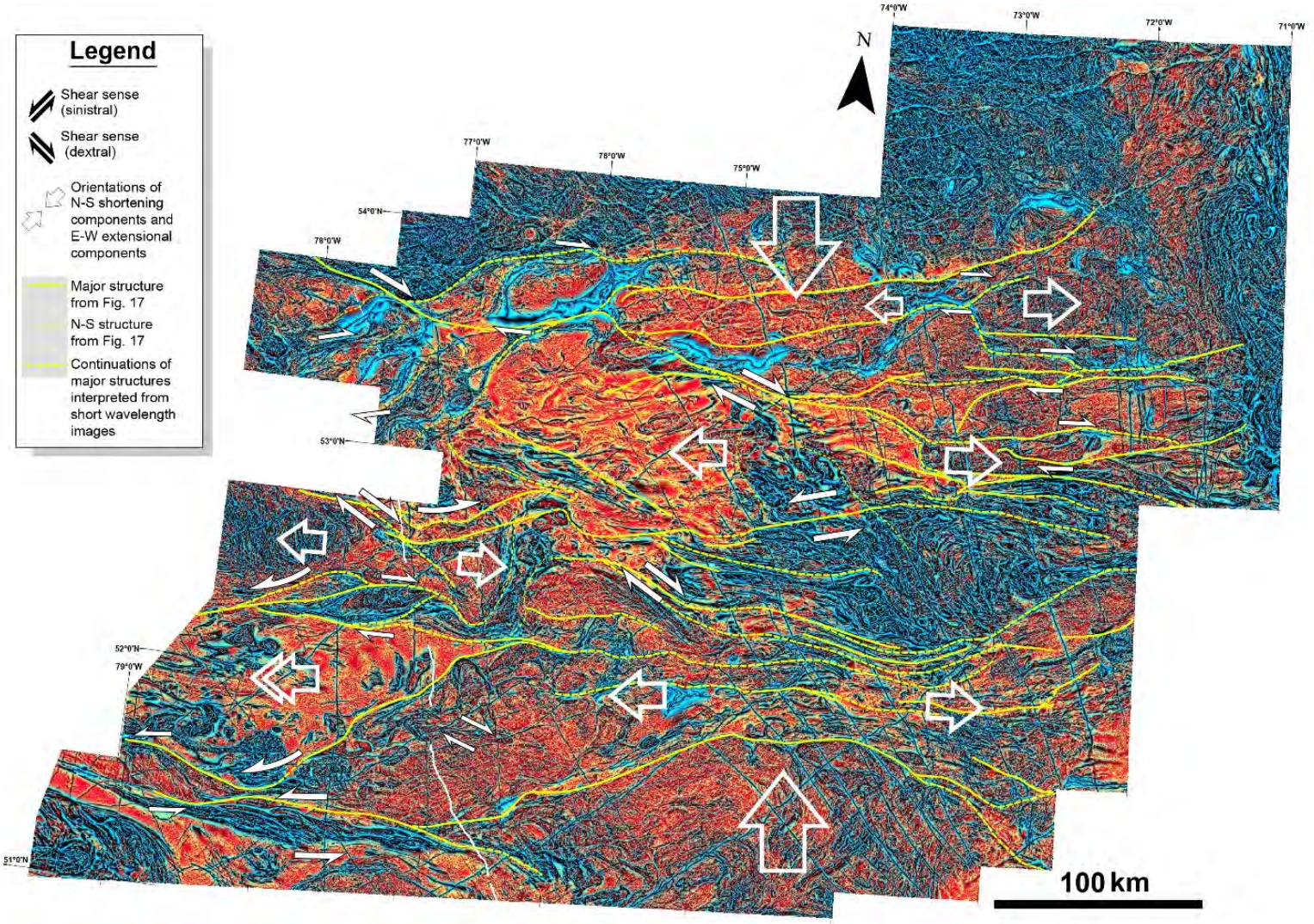

Figure 18: Summary of kinematic indicators found throughout the map, with interpreted orientations of regional shortening and extension components. Major deep structures from Fig. 17 are shown, with additional detail interpreted from the short wavelength component images. The underlying image is the ternary gradient image of the short wavelength component.

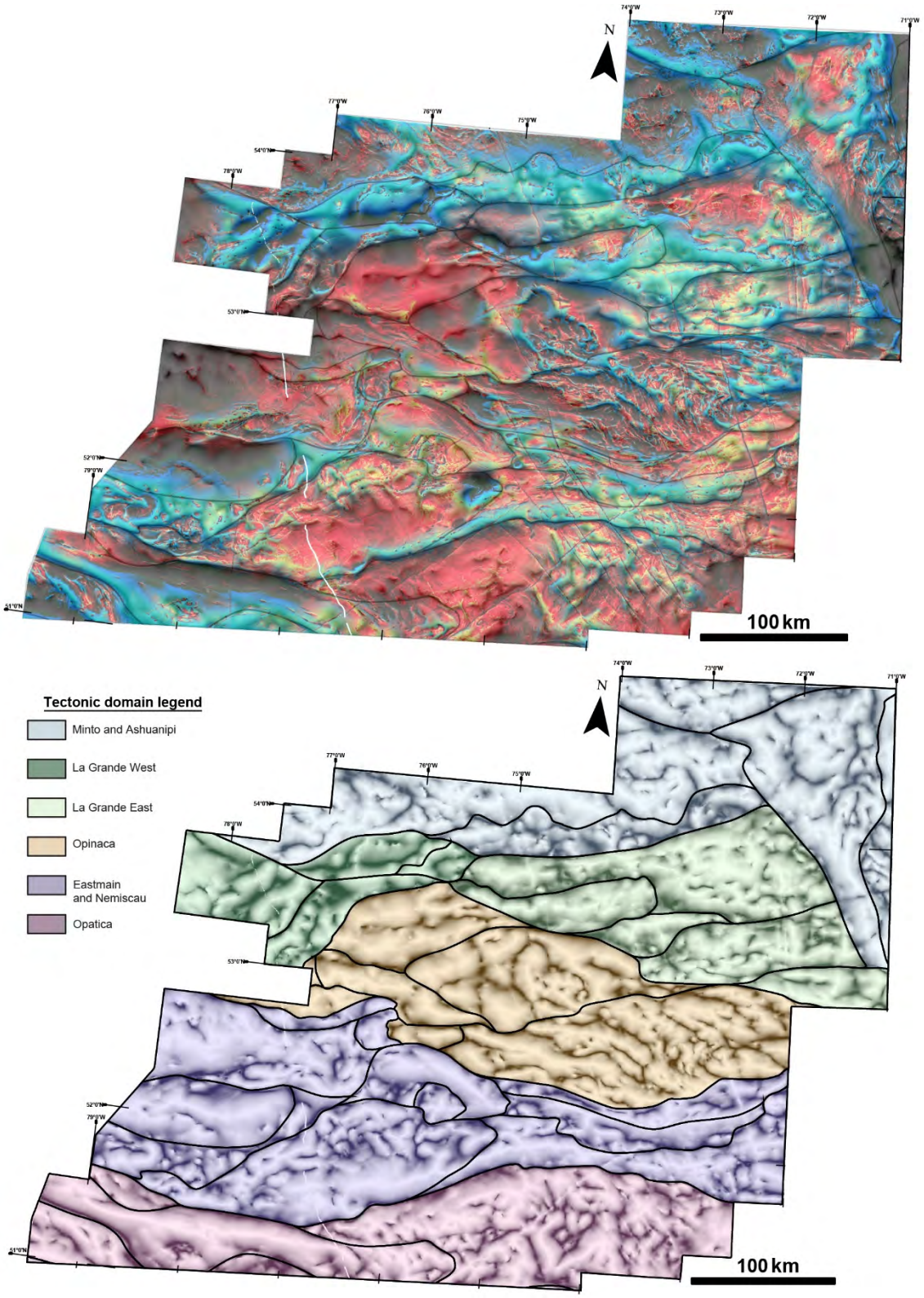

Figure 19: Top: Composite image of the pseudogravity ternary and the long wavelength component tilt angle maps. Bottom: Deep crustal domains interpreted from the above map, with the long wavelength component tilt angle map underlain.

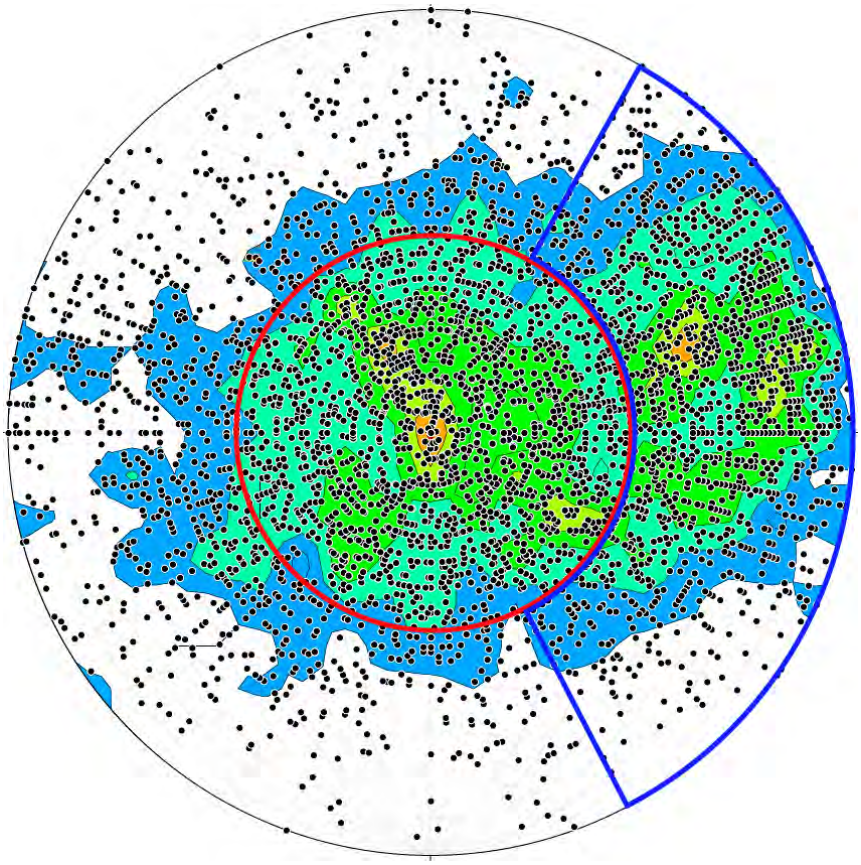

Figure 20: Lower hemisphere equal area stereographic projection of approximately 5000 lineation measurements compiled from SIGÉOM (2018) data for the Eeyou Istchee Baie-James region. The data points within the red domain form a concentration of steeply plunging lineations, and they appear as red dots in Figure 21. Data points within the blue domain form the second concentration of moderate to shallowly eastward plunging lineations, which appear as blue dots in Figure 21. Kamb contours are shown with an interval of 2 and a significance level of 3.

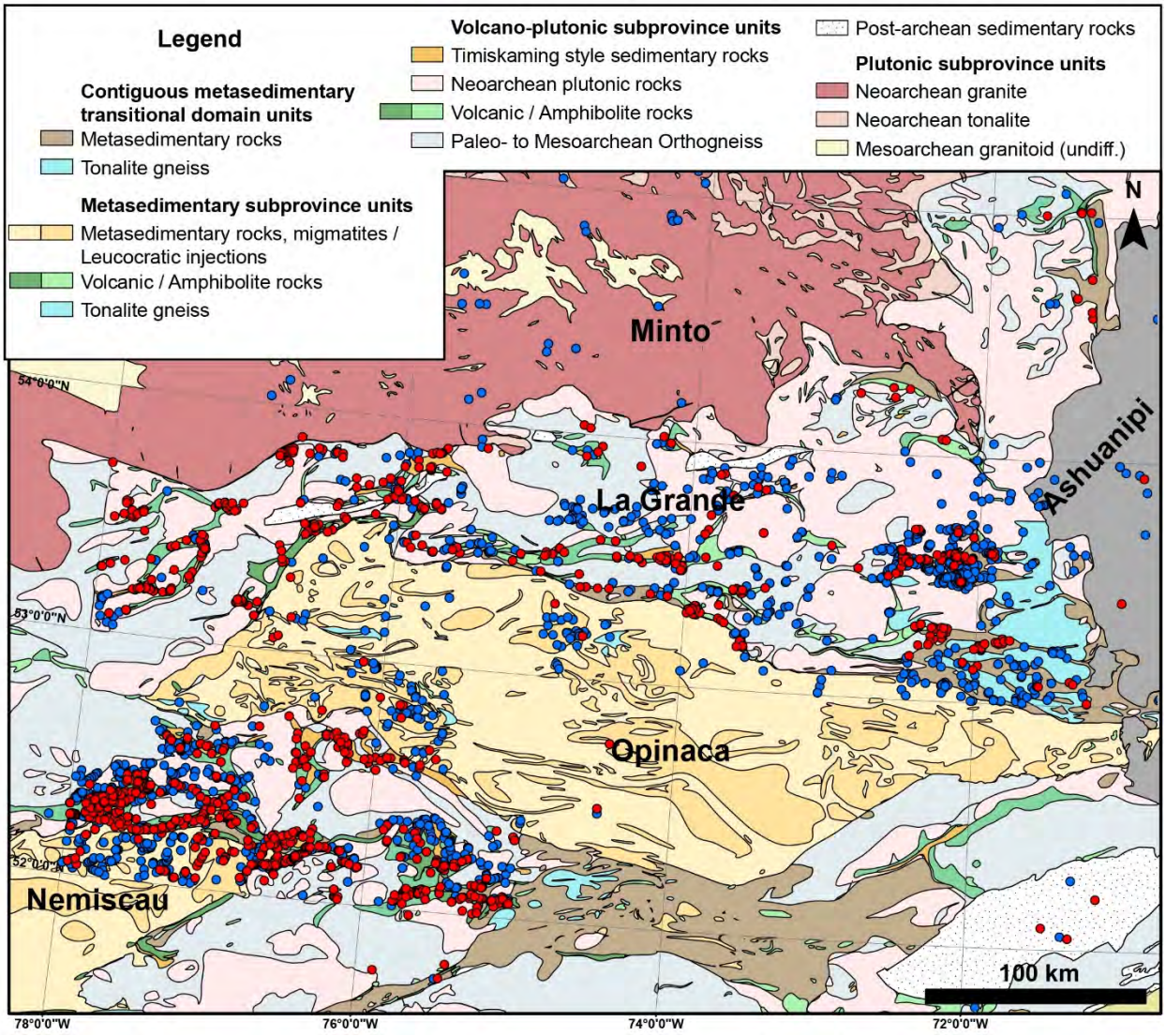

Figure 21: Lithotectonic map of the Eeyou Istchee Baie-James region, showing the two distinct concentrations of ductile stretching lineation measurements defined in Figure 20. Metasedimentary subprovinces exhibit dominantly shallowly eastward plunging lineations, indicating a partitioning of strain by lithotectonic assemblage within the region. Many mixed volcano-plutonic domains exhibit a mix of both subvertical and shallowly eastward plunging lineations, which may have resulted from transpressive deformation. Many purely volcanic domains exhibit concentrations of steeply plunging lineations, another indication of strain partitioning.

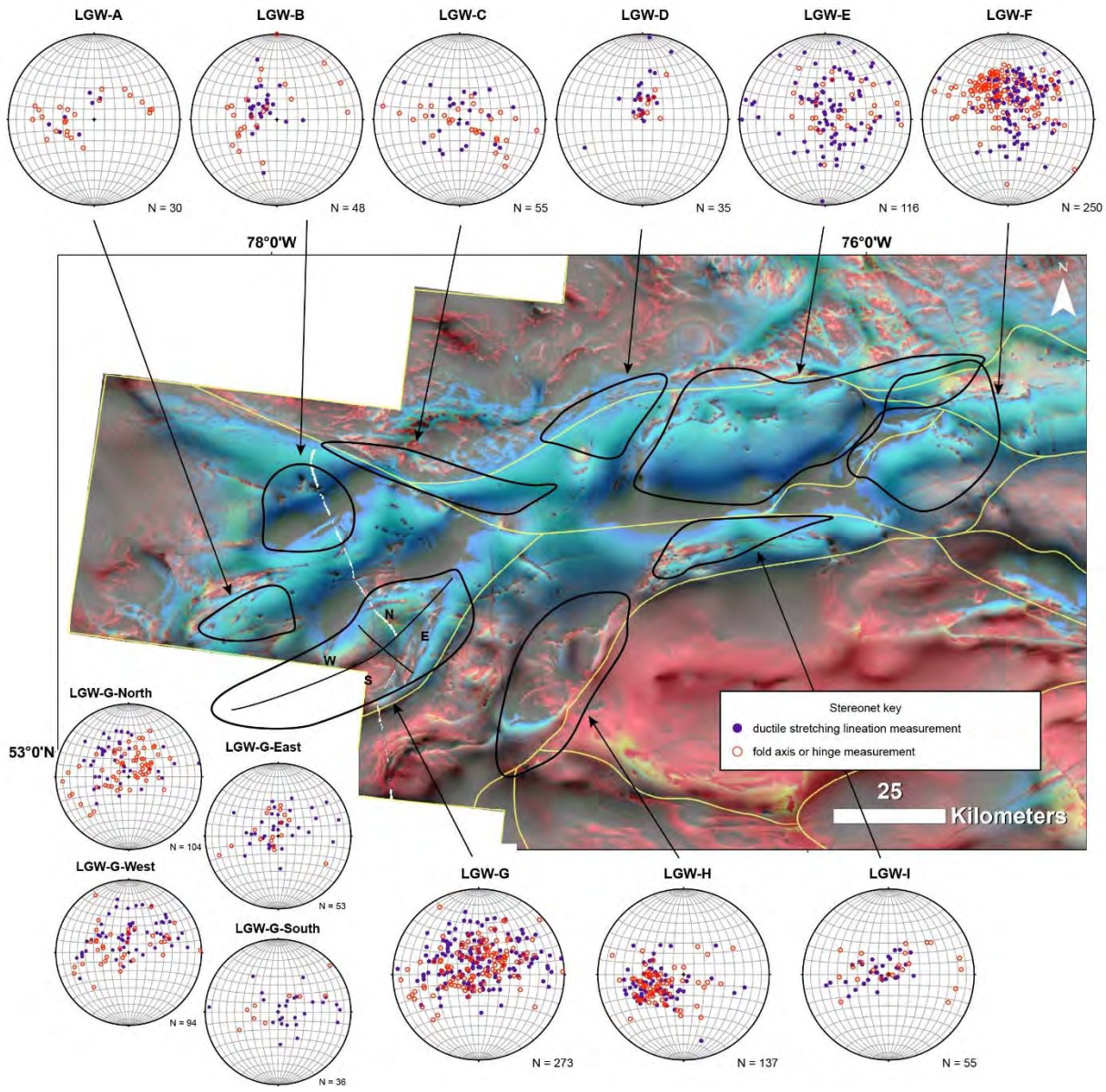

Figure 22: Stretching lineation and fold axis structural data from outcrop (SIGÉOM, 2018) from the western La Grande displayed in equal area, lower hemisphere stereonet plots. The black fields represent the spatial extent of data points compiled. Deep crustal domains from Fig. 19 are shown in yellow. The background image is a composite of the pseudogravity ternary and the long wavelength component tilt angle images.

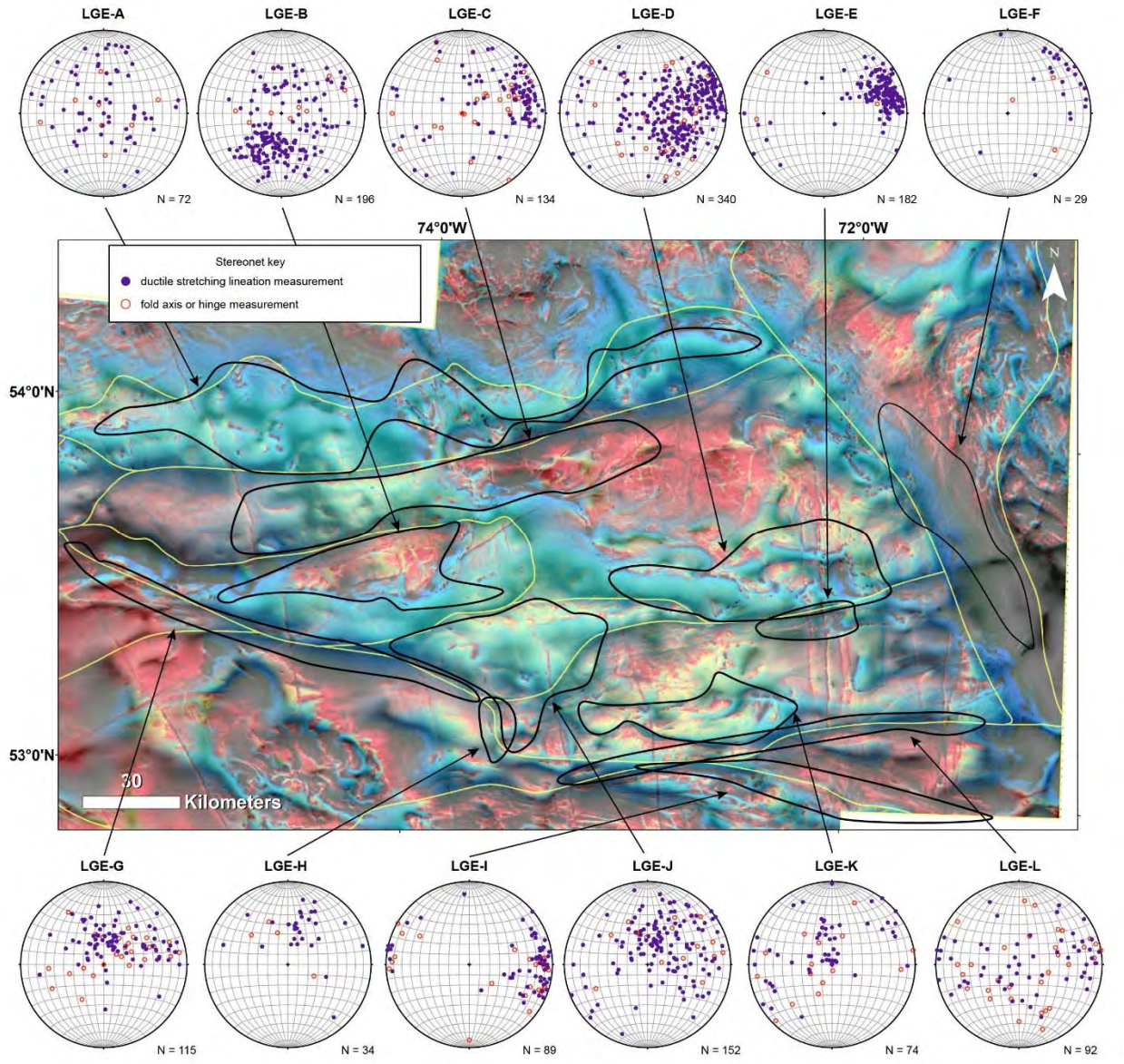

Figure 23: Stretching lineation and fold axis structural data from outcrop (SIGÉOM, 2018) from the eastern La Grande displayed in equal area, lower hemisphere stereonet plots. The black fields represent the spatial extent of data points compiled. Deep crustal domains from Fig. 19 are shown in yellow. The background image is a composite of the pseudogravity ternary and the long wavelength component tilt angle images.

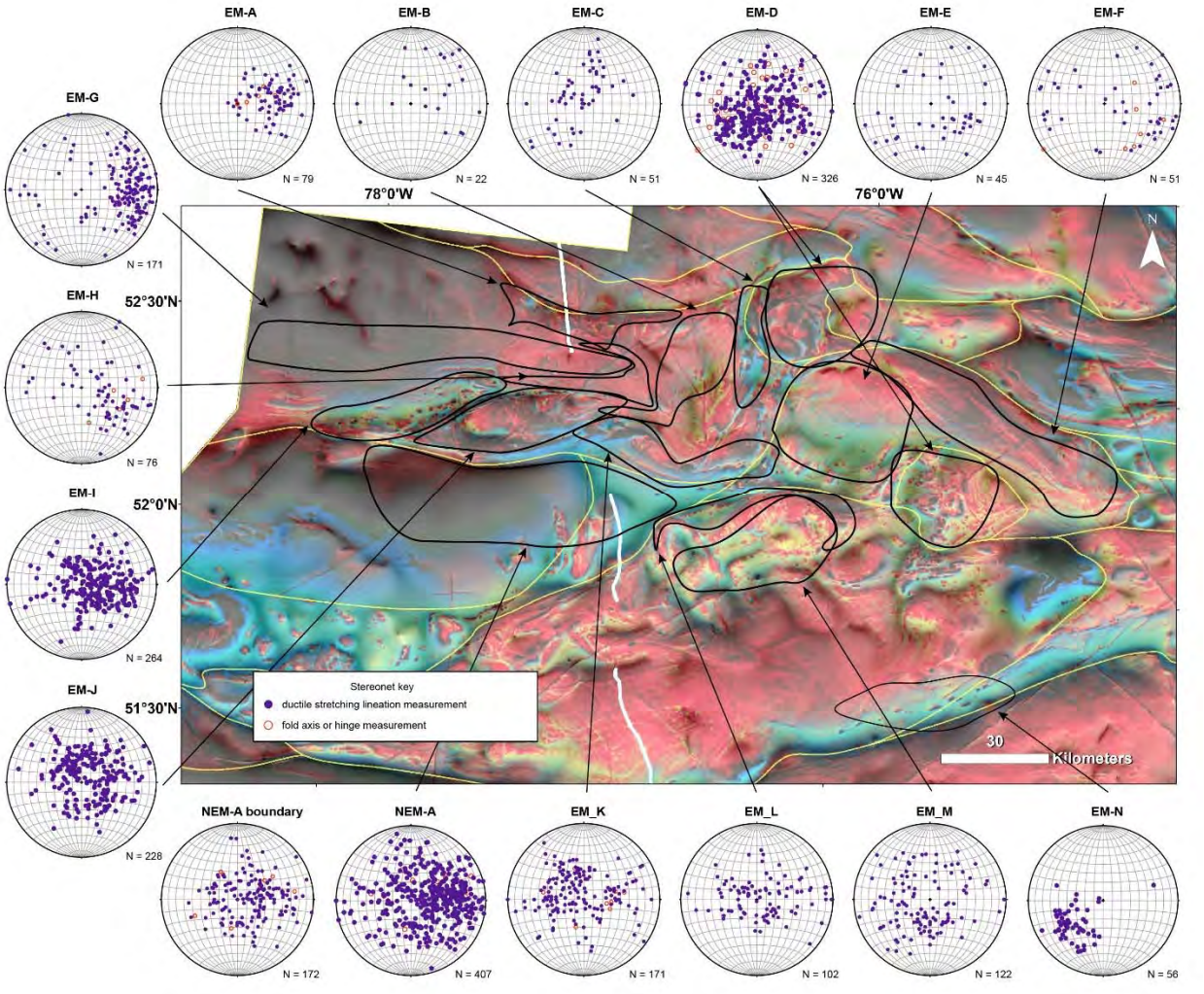

Figure 24: Stretching lineation and fold axis structural data from outcrop (SIGÉOM, 2018) from the Eastmain domain and the Nemiscau subprovince displayed in equal area, lower hemisphere stereonet plots. The black fields represent the spatial extent of data points compiled. Deep crustal domains from Fig. 19 are shown in yellow. The background image is a composite of the pseudogravity ternary and the long wavelength component tilt angle images.

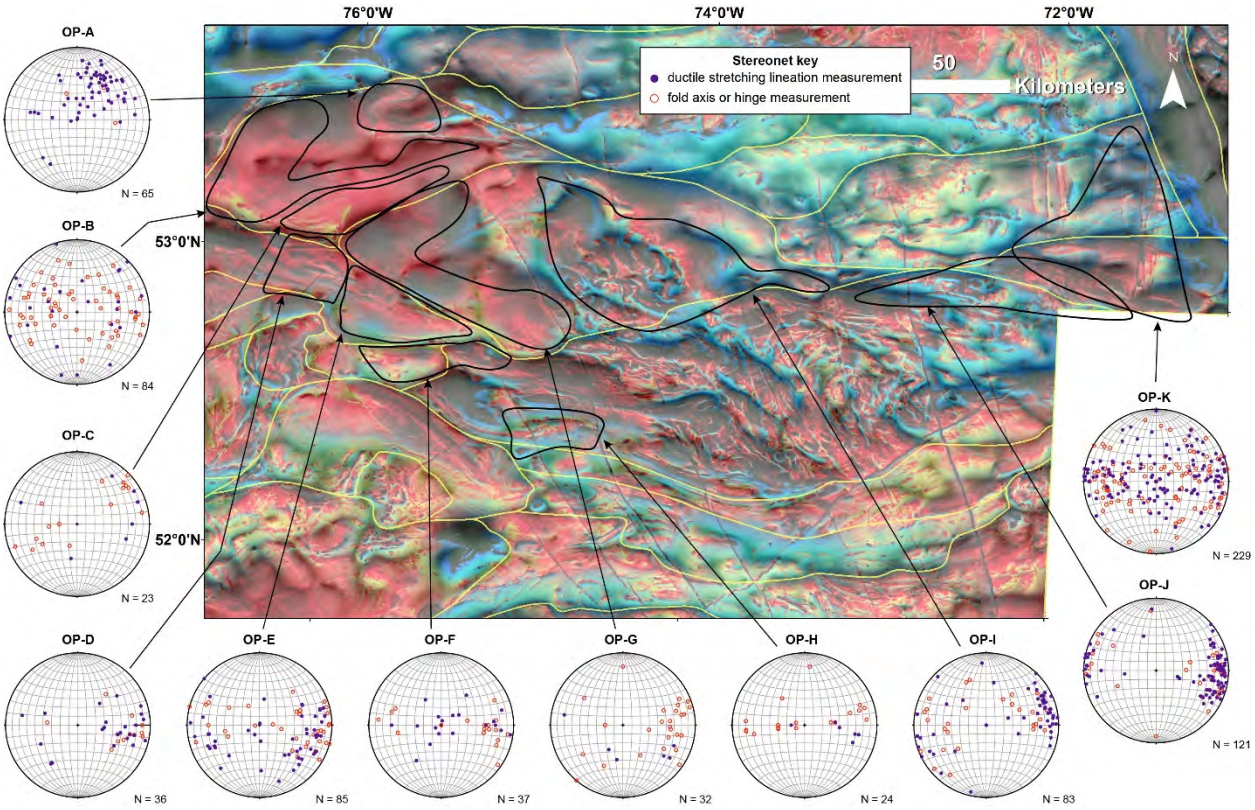

Figure 25: Stretching lineation and fold axis structural data from outcrop (SIGÉOM, 2018) from the Opinaca subprovince displayed in equal area, lower hemisphere stereonet plots. The black fields represent the spatial extent of data points compiled. Deep crustal domains from Fig. 19 are shown in yellow. The background image is a composite of the pseudogravity ternary and the long wavelength component tilt angle images.

with structural domains

77°0'W
76°0'W
75°0'W
54°0'N
78°0'W
53°0'N

100 km

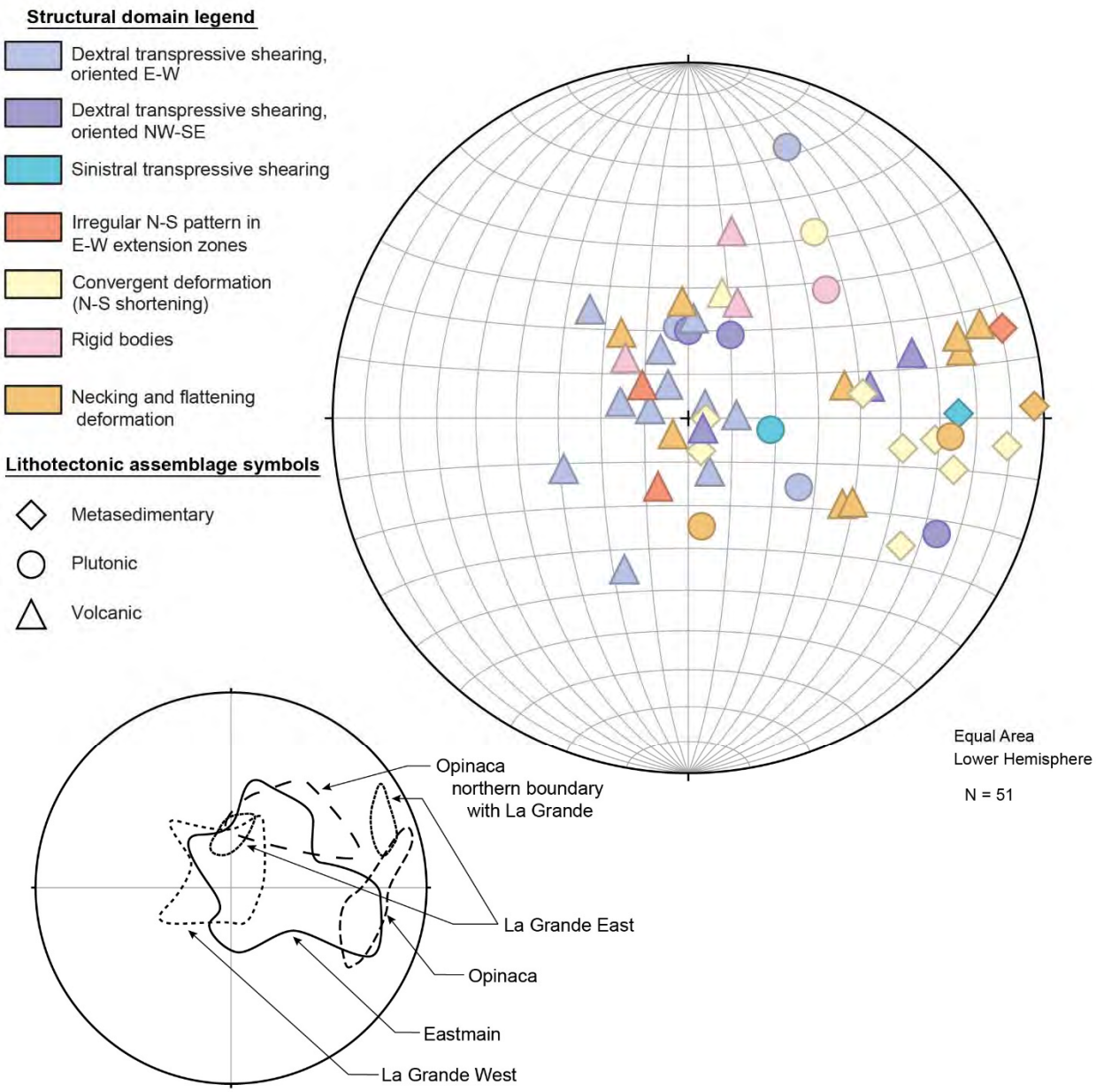

Figure 27: Averaged structural data (maxima from Figs. 22-25) plotted on an equal area, lower hemisphere stereonet, by structural domain and lithotectonic assemblage type. Inset schematic shows a breakdown of the stereonet data according to region.

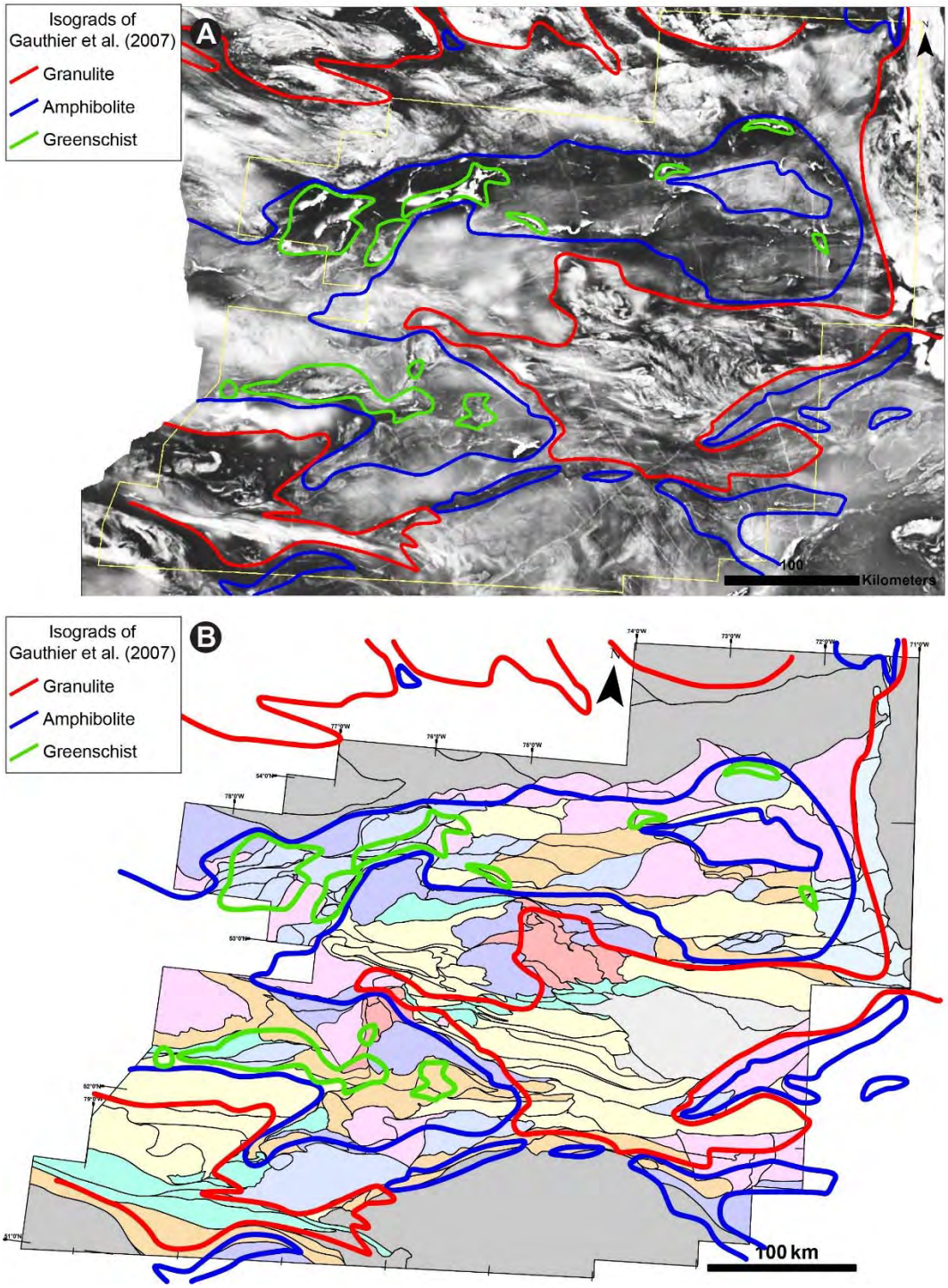

Figure 28: A) Map of metamorphic facies based on Gauthier et al. (2007). Visual textures within the aeromagnetic image were interpreted as associated with each metamorphic facies, based on extrapolations from known study regions. The aeromagnetic image is NRCAN 200m spacing residual total field. The extent of the MERN aeromagnetic survey analyzed in this report is shown in yellow. B) A comparison of the Gauthier et al. (2007) metamorphic isograds and our structural domains shows that granulite facies regions are associated with convergent, sinistral shear, E-W extension and doming domains within the Opinaca and Nemiscau. Greenschist facies regions are associated with E-W dextral transpression regions.

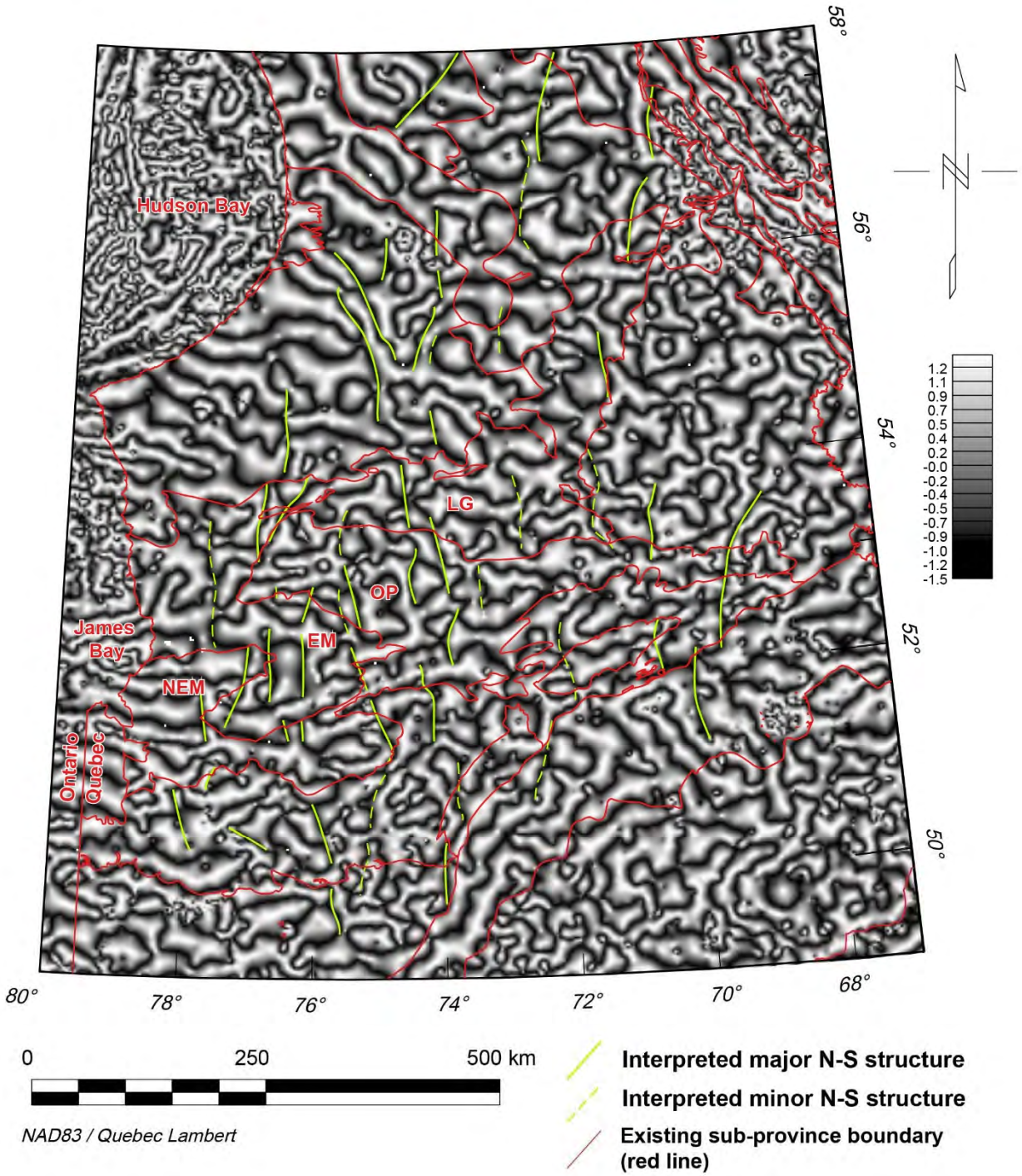

Figure 29: Bouguer anomaly short wavelength component theta angle map, using gravity data from NRCAN. Trend lines of an array of N-S deep structures are shown. From Cleven (2017). OP: Opinaca. EM: Eastmain. LG: La Grande. NEM: Nemiscau.

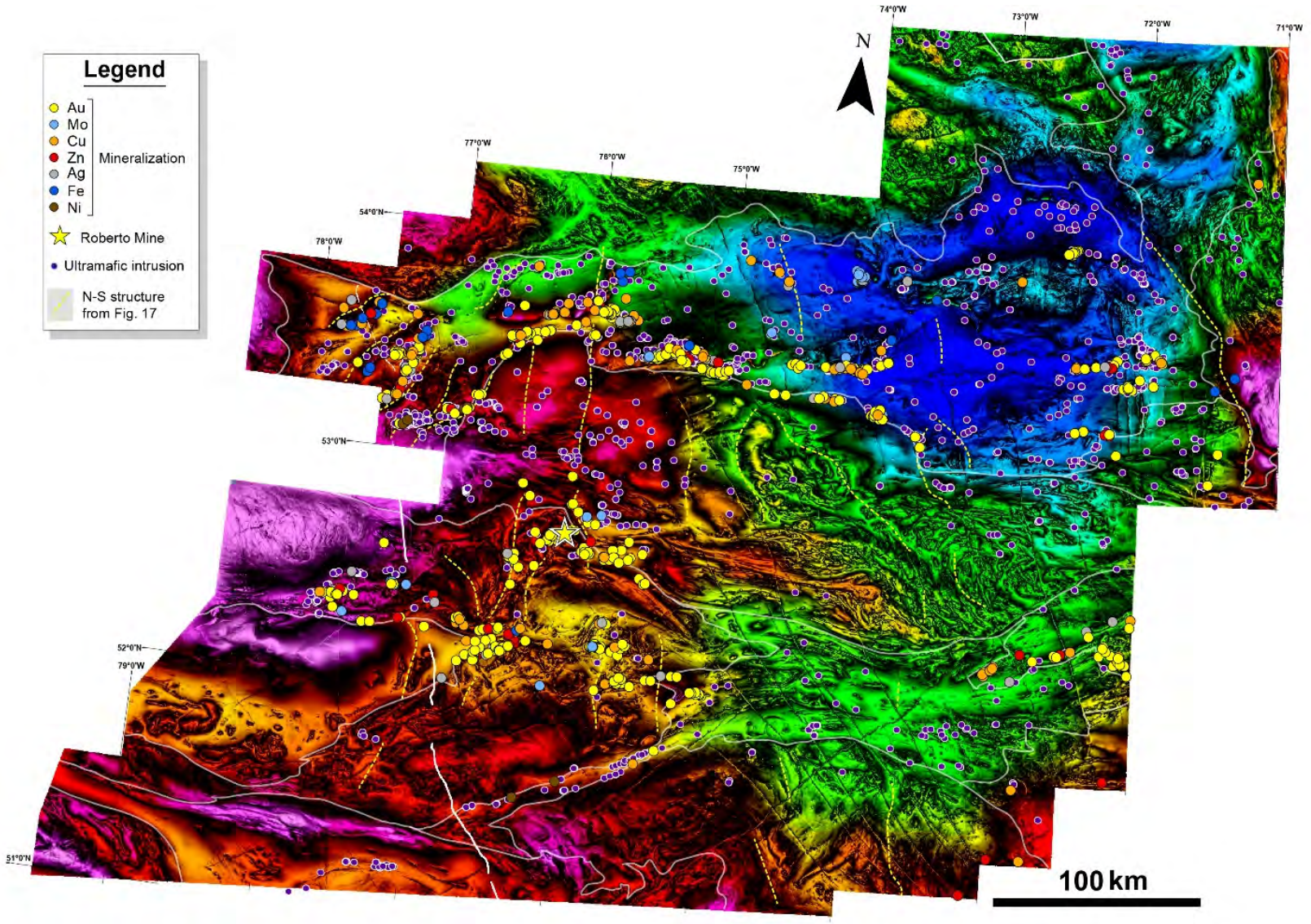

Figure 30: Relationships between mineralization, ultramafic intrusions, and north-south structures at the La Grande/Eastmain and Opinaca boundary. Composite image of pseudogravity (colour scale) with theta angle treatment of short wavelength component (greyscale shading).

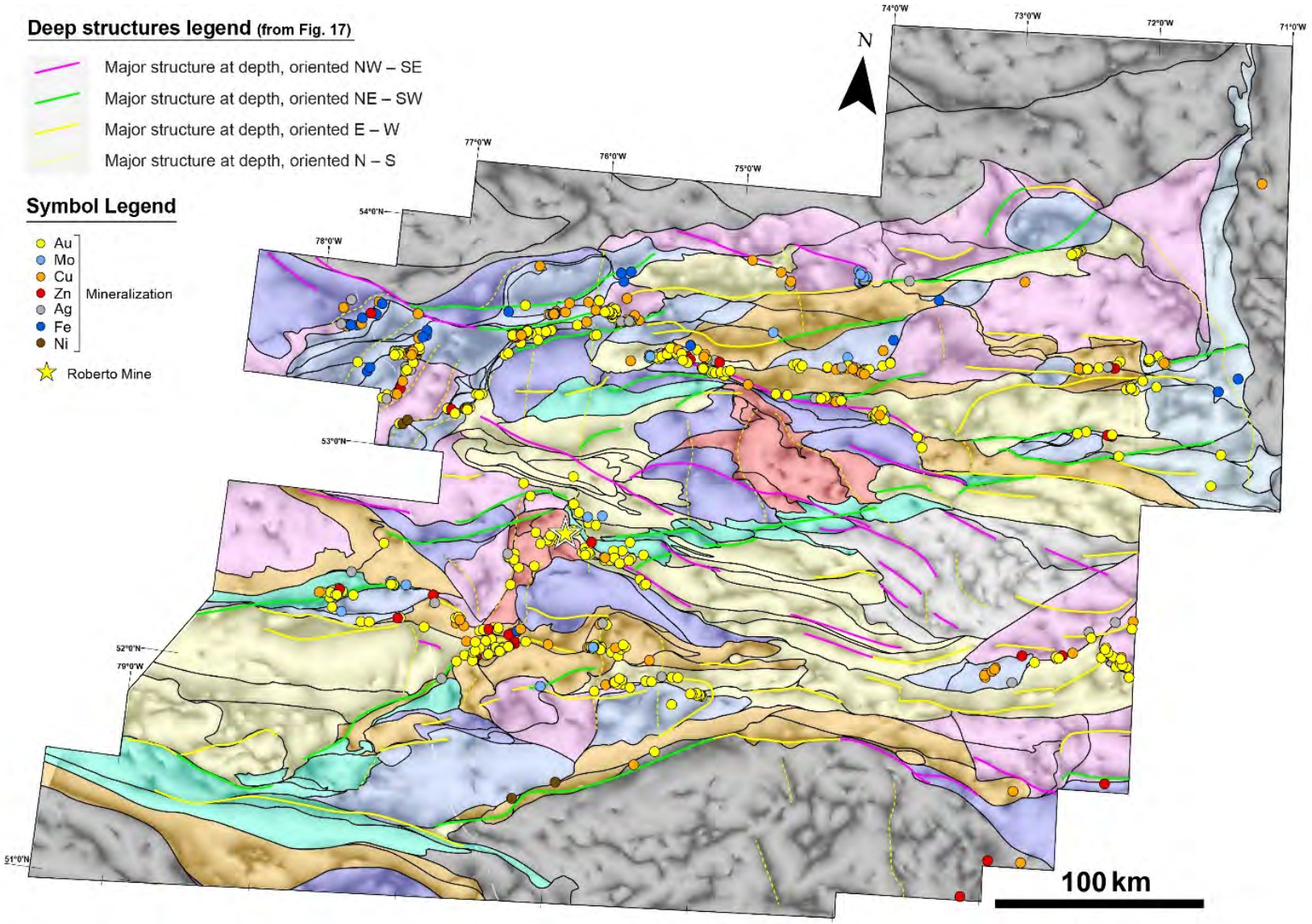

Figure 31: Relationships between mineralization, significant deep structures (Fig. 17) and structural domains (Fig. 16). Underlying image is the long wavelength component tilt angle map.

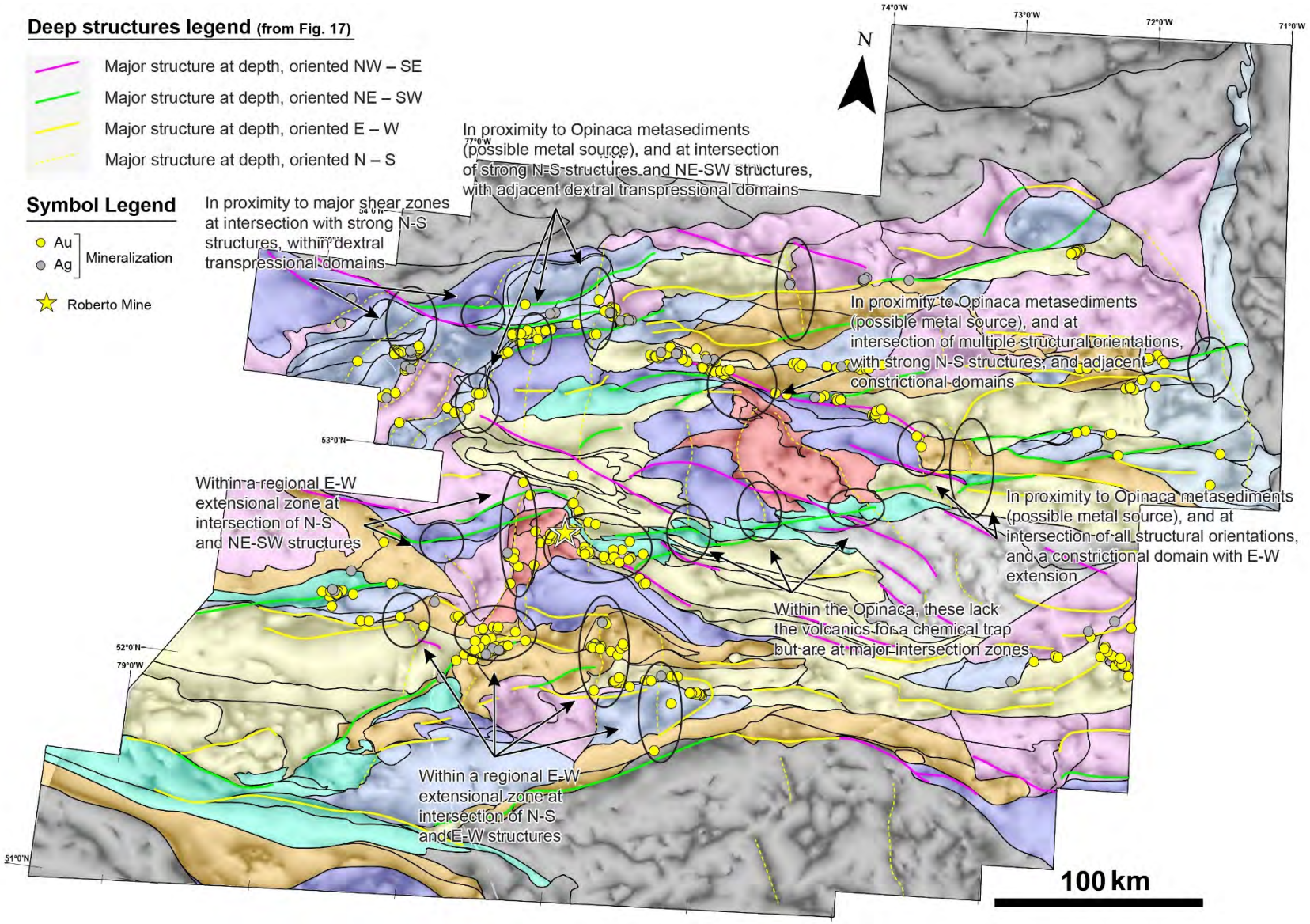

Figure 32: Gold and silver occurrences (epigenetic mineralization), with exploration target regions based on intersections of major structures interpreted from geophysics.

Appendix

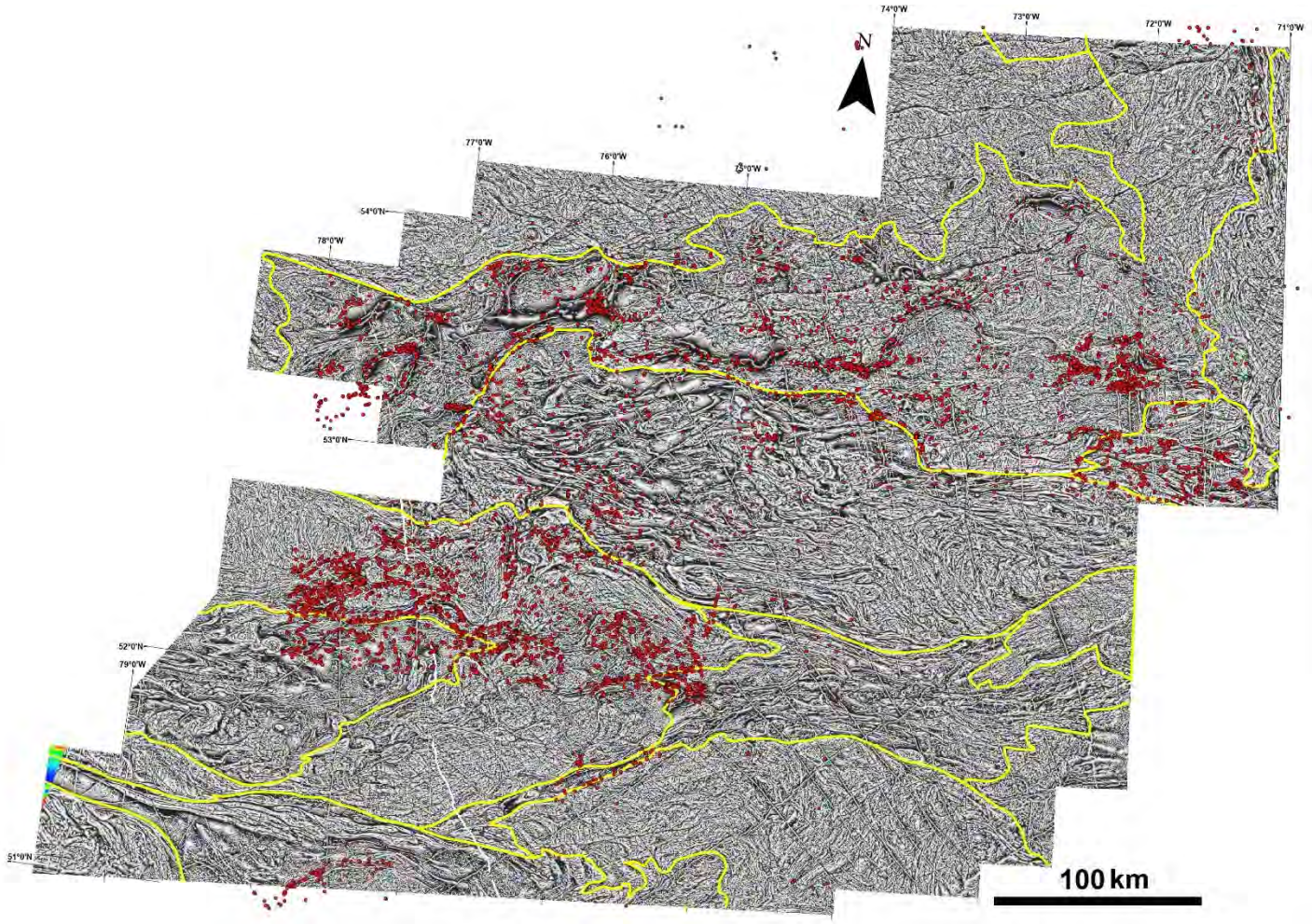

Figure 33: Locations of existing lineation measurements from SIGÉOM (2018). SIGÉOM structure codes for compiled measurements include, for fold axis and hinges: L, 1, 2, 3, 5, 6, C. For ductile stretching lineations: A, B, E, N, Q, Y.

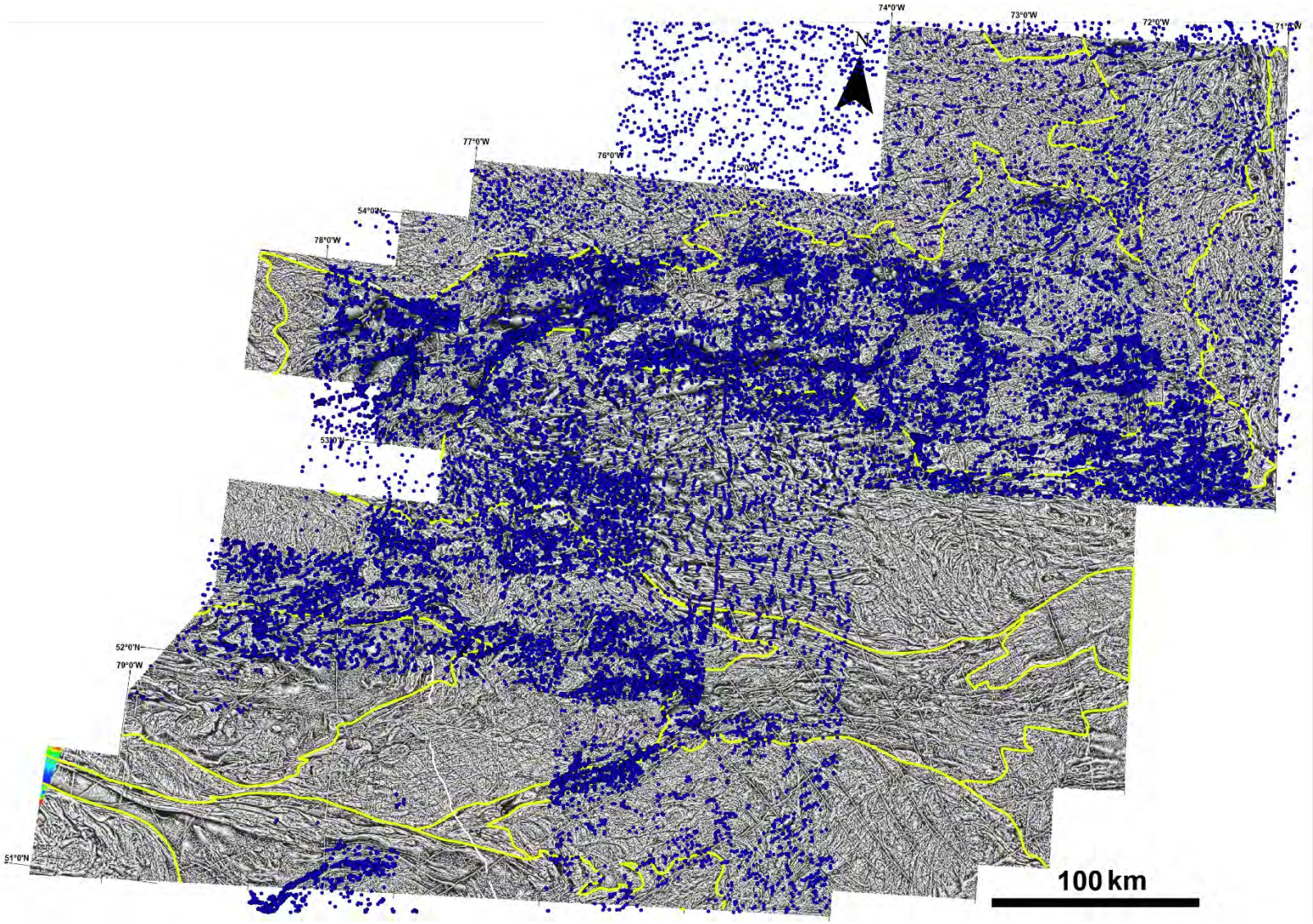

Figure 34: Locations of existing foliation measurements from SIGÉOM (2018). SIGÉOM structure codes for compiled foliation measurements include: C, G, H, L, M, O, P, Q, S, T, W.

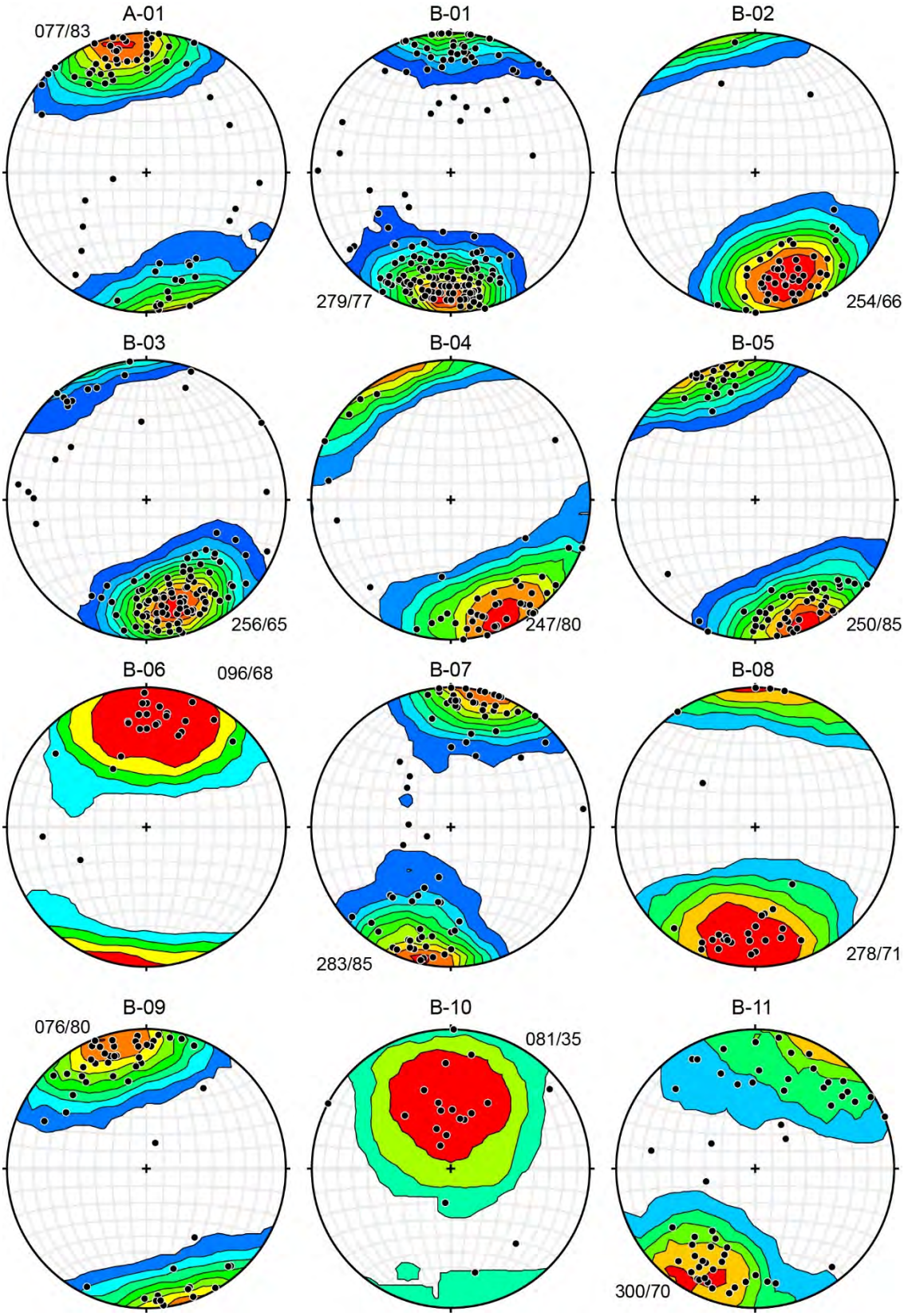

Figure 35: Foliation data used to determine average foliation measurements in Fig. 26.

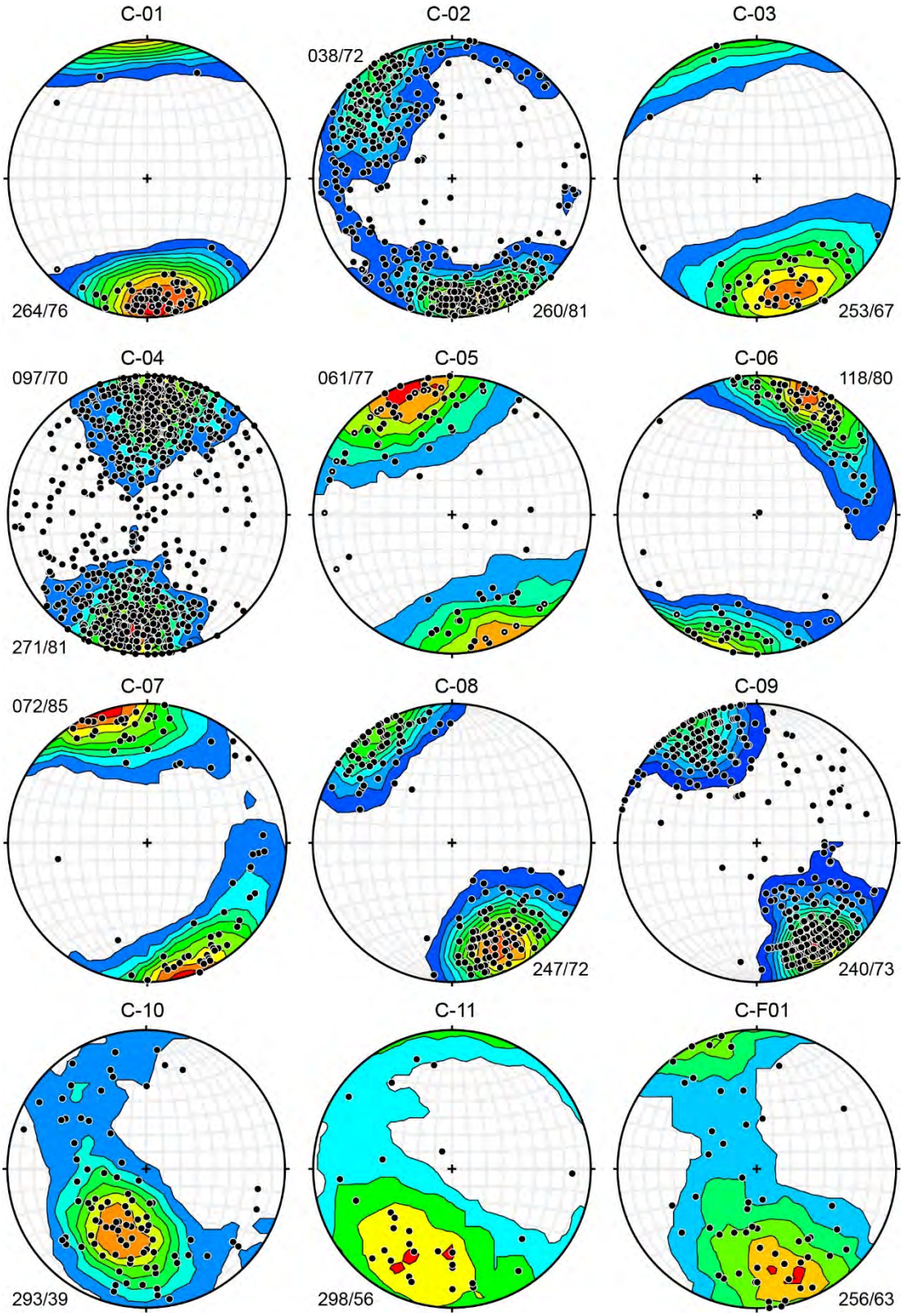

Figure 36: Foliation data used to determine average foliation measurements in Fig. 26.

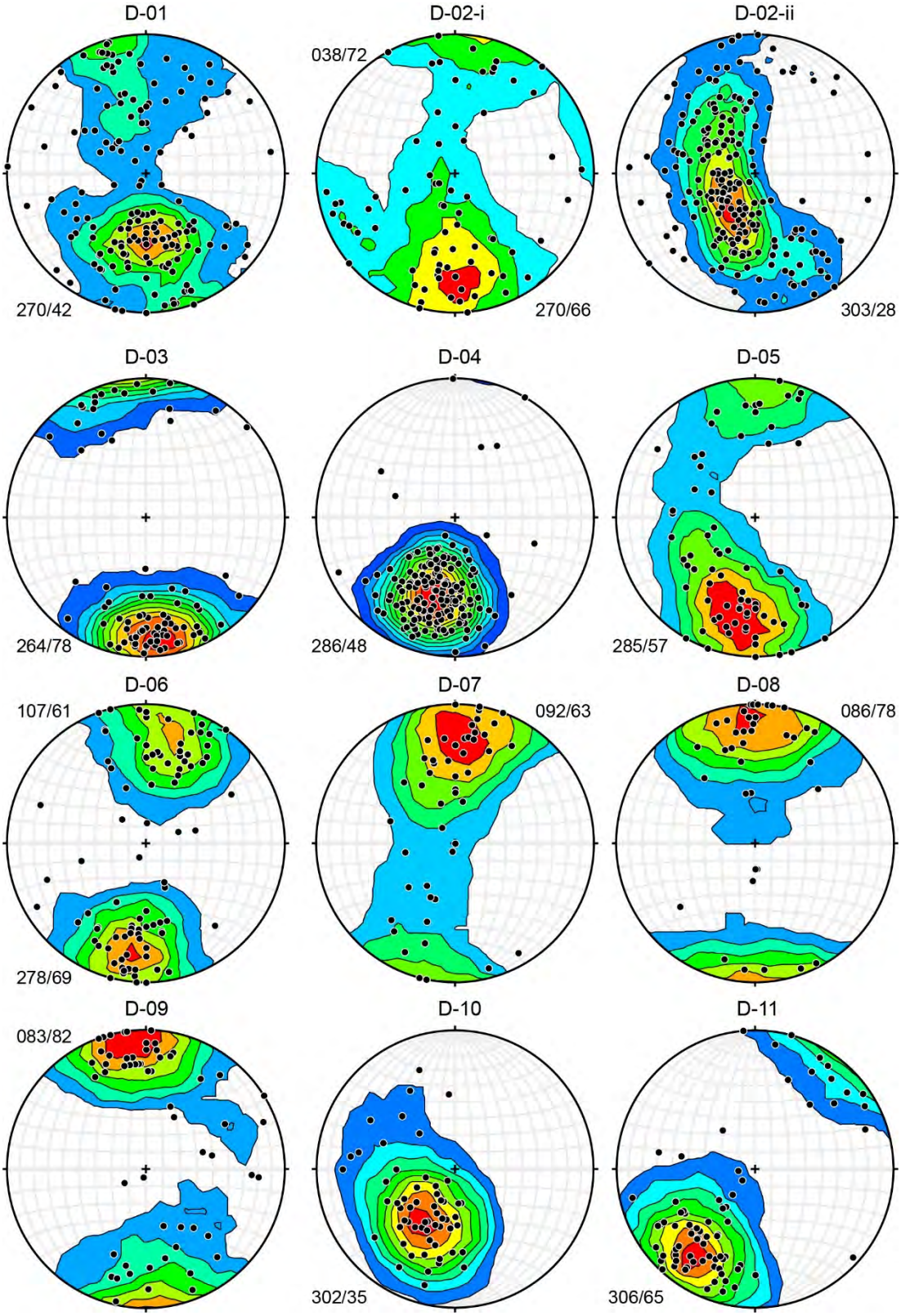

Figure 37: Foliation data used to determine average foliation measurements in Fig. 26.

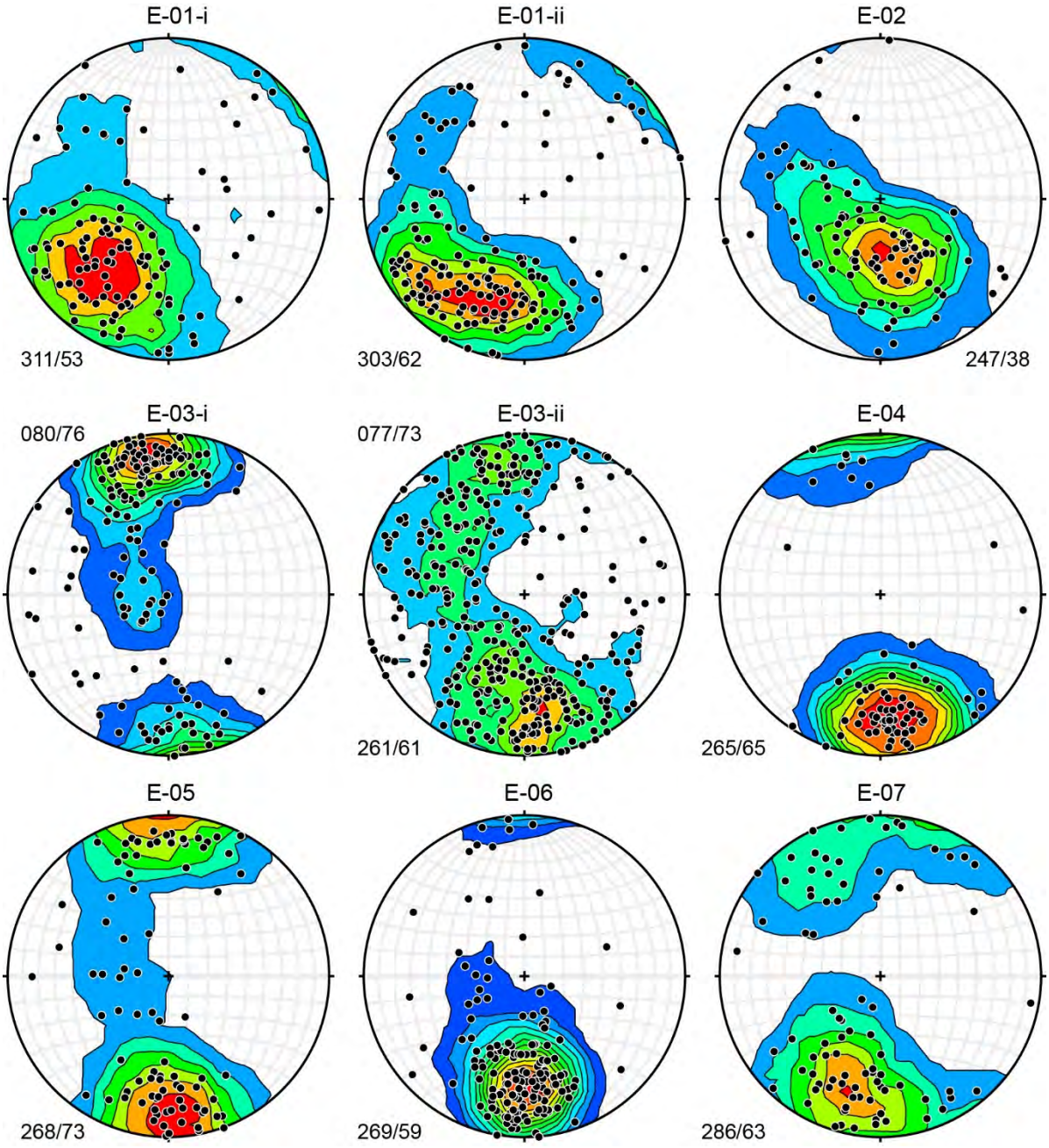

Figure 386: Foliation data used to determine average foliation measurements in Fig. 26.